Numerical and Experimental Study of Glass in the Blow and Blow Forming Process for the Prediction of Thickness Distributions in Glass Perfume Containers

Adrià Biosca Mecías

DOCTORAL THESIS

Title	NUMERICAL AND EXPERIMENTAL STUDY OF GLASS IN THE BLOW AND BLOW FORMING PROCESS FOR THE PREDICTION OF THICKNESS DISTRIBUTIONS IN GLASS PERFUME CONTAINERS
Presented by	Adrià Biosca Mecías
Centre	IQS School of Engineering
Department	Industrial Engineering
Directed by	Dr. Salvador Borrós Gómez Dr. Andrés-Amador García Granada

Als meus pares

“La inspiración existe, pero tiene que encontrarte trabajando”
Pablo Picasso (1881 - 1973)

ACKNOWLEDGMENTS

La realització d'una tesi doctoral implica un llarg període de treball i la col·laboració de moltes persones. Voldria fer arribar el meu agraïment a tothom amb qui he tractat i que m'ha ajudat en el desenvolupament d'aquesta investigació. El meu especial agraïment:

Als meus directors, els Professors Dr. Salvador Borrós i Dr. Andrés-Amador García Granada, per la seva dedicació, ensenyances i valuosa ajuda en els moments més necessaris per fixar el rumb de la recerca.

Al Dr. Vicenç Pedret Clemente, director general de Ramon Clemente, per confiar en mi i en el futur d'aquesta tesi des del primer instant. Moltes gràcies pel seu suport i oportunitats oferides. Gràcies per la seva flexibilitat durant els darrers quatre anys en els que he compaginat les meves tasques a Ramon Clemente amb la realització d'aquesta tesi.

Tanmateix, a tots els companys de Ramon Clemente, als que hi treballen actualment i als que ja s'han jubilat. Gràcies per la seva ajuda, ensenyant-me i buscant resposta a tots els dubtes que m'han sorgit. Gràcies per haver-me acompanyat i recolzat durant aquesta llarga etapa.

To Dr. Matthew Hyre, for his guidance and discussions about numerical simulations; and to Emhart Glass for providing useful experimental data.

Finalment, i sobretot, agraeixo als meus pares, la meva germana i la meva família per la seva paciència, ànims, pregàries i suport incondicional.

The main funds to develop this thesis were provided by Ramon Clemente.
Including partial funding with European Regional Development Funds under the Nuclis project RD16-1-0015, granted by ACCIÓ, Generalitat de Catalunya.
"laCaixa" Foundation also provided financial support.

ABSTRACT

Numerical and experimental study of glass in the blow and blow forming process for the prediction of thickness distributions in glass perfume containers

The design of the blank mold cavity is a critical step in the development of new perfume containers as it defines the glass thickness distribution of the manufactured bottles. Despite that, mold cavity design is still based on empirical knowledge and trial and error. Hence, several manufacturing tests may be required, which increase time to market and involve significant downtimes. Ramon Clemente is a glass manufacturing company that wants to bridge the gap between industrial experience in glassmaking and scientific and engineering knowledge present in numerical simulations. The goal is to implement a numerical model to describe the thermo-mechanical behavior of glass during the blow and blow forming process and predict the glass thickness distribution of the manufactured bottles. Therefore, this thesis focuses on a numerical and experimental study of the production of glass perfume containers. Then, thermal analyses were performed using an infrared thermal camera under industrial manufacturing conditions. These included experimental measurements of the glass gob, parison and final container throughout the forming process. In addition, forming operations and glass properties defined a framework to numerically model the blow and blow forming process using ANSYS Polyflow. Subsequently, two numerical models were implemented. First, a gob drop test to provide a description of the glass flow over time to validate the characterized viscosity and the Newtonian non-isothermal flow predicted by the simulations. Later, a numerical model of the blow and blow forming process to predict the glass thickness distribution of the manufactured containers. Numerical results were correlated with experimental glass temperatures and thickness distributions of sectioned containers. Results lead to gain a better understanding of the thermo-mechanical behavior of glass inside the mold cavities. Moreover, simulations successfully predicted the thickness distribution after the container forming process, showing the influence of the blank mold cavity and process conditions in both axisymmetric and three-dimensional models. Validation of the 3D model has strong implications for Ramon Clemente, as it paves the way for numerically predicting the glass thicknesses of complex perfume containers instead of being limited to axisymmetric bottles. Therefore, allowing to develop new glass containers faster and of better quality.

RESUM

Numerical and experimental study of glass in the blow and blow forming process for the prediction of thickness distributions in glass perfume containers

El disseny del motlle preparador és un punt crític en el desenvolupament de nous flascons ja que defineix la distribució d'espessors de vidre en les ampolles fabricades. Tot i això, el disseny d'aquestes cavitats encara es basa en el coneixement empíric i la metodologia d'assaig i error. Per aquestes raons, diverses proves de fabricació poden ser necessàries, les quals impliquen temps no productius i allarguen el temps de desenvolupament. Ramon Clemente és un fabricant de flascons de vidre que vol escurçar el buit actual entre l'experiència dels vidriers i el coneixement científic de les simulacions numèriques. L'objectiu és implementar un model que descrigui numèricament el comportament termomecànic del vidre en el procés de fabricació per bufat-bufat per predir la distribució d'espessors en els flascons. Així doncs, aquesta tesi es centra en un estudi numèric i experimental de la producció d'ampolles de vidre. Emprant una càmera termogràfica es van realitzar anàlisis tèrmiques sota condicions reals de fabricació. Aquestes inclogueren mesures experimentals de la gota de vidre, *parison* i flascons acabats en tot el procés productiu. A més, les operacions de conformat i les propietats del vidre definiren un marc teòric per modelar numèricament el procés de bufat-bufat amb ANSYS Polyflow. Posteriorment, es varen implementar dos models numèrics. Primer, un assaig de caiguda de la gota proporcionà una descripció del flux de vidre al llarg del temps per validar la caracterització de la viscositat i el flux no isotèrmic i newtonià previst per les simulacions. Després, un model numèric del procés de bufat-bufat per predir el repartiment d'espessors de vidre en els envasos fabricats. Els resultats numèrics es van correlacionar amb temperatures experimentals del vidre i amb els gruixos dels flascons tallats. Els resultats obtinguts permeten tenir una millor comprensió del comportament termomecànic del vidre dins de les cavitats dels motlles. A més, les simulacions predigueren correctament la distribució d'espessors al final del procés, en funció del disseny del motlle preparador i de les condicions de fabricació, tant en el model axisimètric com tridimensional. La validació del model numèric en tres dimensions és molt important per a Ramon Clemente, ja que obre la porta a predir numèricament els gruixos de flascons amb geometries complexes en lloc de limitar-se a ampolles axisimètriques. Per tant, permetent desenvolupar nous flascons de vidre pel sector de la perfumeria de forma més ràpida i de millor qualitat.

RESUMEN

Numerical and experimental study of glass in the blow and blow forming process for the prediction of thickness distributions in glass perfume containers

El diseño del molde preparador es un punto crítico en el desarrollo de nuevos frascos ya que define la distribución de espesores de vidrio en las botellas fabricadas. Todo y eso, el diseño de estas cavidades aún se basa en el conocimiento empírico y la metodología de ensayo y error. Por estas razones, pueden ser necesarias varias pruebas de fabricación, las cuales implican tiempo no productivo y alargan el tiempo de desarrollo. Ramon Clemente es un fabricante de frascos de vidrio que quiere reducir el vacio actual entre la experiencia de los vidrieros y el conocimiento científico de las simulaciones numéricas. El objetivo es implementar un modelo que describa numéricamente el comportamiento termo-mecánico del vidrio en el proceso de fabricación por soplado-soplado para predecir la distribución de grosores en los frascos. Así pues, esta tesis se centra en un estudio numérico y experimental de la producción de botellas de vidrio. Usando una cámara termográfica se realizaron análisis térmicos bajo condiciones reales de fabricación. Éstas incluyeron medidas experimentales de la gota de vidrio, *parison* y frascos acabados durante el proceso productivo. Además, las operaciones de conformado y las propiedades del vidrio definieron un marco teórico para modelar numéricamente el proceso de soplado-soplado con ANSYS Polyflow. Posteriormente, se implementaron dos modelos numéricos. Primero, un ensayo de caída de la gota proporcionó una descripción del flujo de vidrio a lo largo del tiempo para validar la caracterización de la viscosidad y el flujo no isotérmico y newtoniano previsto por las simulaciones. Después, un modelo numérico del proceso de soplado-soplado para predecir el reparto de espesores de vidrio en los envases fabricados. Los resultados numéricos se correlacionaron con temperaturas experimentales del vidrio y con los grosores de los frascos cortados. Los resultados obtenidos permiten tener una mejor comprensión del comportamiento termo-mecánico del vidrio dentro de las cavidades de los moldes. Además, las simulaciones predijeron correctamente la distribución de espesores al final del proceso, en función del diseño del molde preparador y de las condiciones de fabricación, tanto en el modelo axisimétrico cómo tridimensional. La validación del modelo numérico en tres dimensiones es muy importante para Ramon Clemente, ya que abre las puertas a predecir numéricamente los grosores de los frascos con geometrías complejas en lugar de limitarse a botellas axisimétricas. Por lo tanto, permitiendo desarrollar nuevos frascos de vidrio para el sector de la perfumería de forma más rápida y de mejor calidad.

TABLE OF CONTENTS

LIST OF FIGURES

Figures from Chapter 1

Figures from Chapter 2

Figures from Chapter 3

Figures from Chapter 4

LIST OF TABLES

Tables from Chapter 1

Tables from Chapter 3

Tables from Chapter 4

LIST OF ABBREVIATIONS

ANFEVI	Asociación Nacional de Fabricantes de Envases de Vidrio
BB	Blow and Blow
CAD	Computer Aided Design
CIMNE	International Centre for Numerical Methods in Engineering
CNC	Computer Numerical Control
DG	Double Gob
DO	Discrete Ordinates
FAOVI	Fabricantes de Otros tipos de Vidrio
FEM	Finite Element Method
FEVE	the European Container Glass Federation
HVG	Research Association of the German Glass Industry
IPGR	International Partners in Glass Research
IR	Infrared
IS	Individial Section
LWIR	Long-Wavelenght Infrared
MIS	IS machine
NNPB	Narrow Neck Press and Blow
PB	Press and Blow
PFEM	Particle Finite Element Method
RC	Ramon Clemente
RTD	Resistance Temperature Detectors
TG	Triple Gob
TNO	Netherlands Organization for Applied Scientific Research
UDF	User-Defined Function
VFT	Vogel-Fulcher-Tamman equation

CHAPTER 1
MOTIVATION AND AIMS

1.1 INTRODUCTION

In the origins of civilization, glass was considered one of the most precious materials. It possessed unique qualities of brightness, transparency and translucency with functional and aesthetic uses. In addition to personal adornment or jewelry, glass was also used to store and preserve food, medicines and ointments. Glass was an innocuous and non-porous material with a very low chemical interaction rate, being an effective barrier against external elements and ensuring that the products stored inside would maintain all their properties, aroma and flavor. Therefore, glass was one of the preferred materials due to its unique properties of impermeability, cleanliness and because in contrast to metals or ceramics, glass did not leave any trace of flavors or odors.

Small beads and arrowheads made of carved and polished glass have been found in Mesopotamia that date back to the Bronze Age, around 3000 BC. Towards 1650 BC, the production of small hollow glass containers began with the core-forming technique. Initially, a core made of clay was used to generate the internal shape and then it was covered with softened glass rods or submerged in a crucible with molten glass. Finally, it was reheated and rotated on a flat surface to smooth its external surface. Casting was also used to create complex forms of containers by introducing molten glass into an open mold and pressing the glass to obtain the shape of the mold cavity. It was not until 1000 BC in the Roman Empire, that the revolutionary technique of glass blowing was born, involving blowing air through a metal pipe inside a molten glass core. This new technique allowed the artisans to produce larger objects, but also to produce them faster, with the possibility of serializing and economizing the production process with the use of molds. For the first time, glass could compete with cheaper materials such as ceramics, but bringing its unique qualities. In this way, pots and other daily use tools made of glass could be acquired by a wide sector of society. With the division of the Roman Empire in the fifth century, Byzantine culture continued to develop the Roman techniques for glass production. After the fall of the Eastern Roman Empire in the 15th century, Venice took the limelight during the Renaissance, which was shared in the following centuries with France, Germany and other European countries.

During the history of mankind, there has always been secrecy surrounding the glass making techniques. As glass was considered a highly valued material along with gold and precious stones, the ability of the artisans to produce this precious material from the fusion of sand was considered sorcery in ancient times. Later, many families of glassmakers settled near forests to obtain the natural resources required for glass production. This fact allowed them to remain isolated during centuries from political conflicts and to protect their knowledge and activities. On the other hand, the Venetian artisans were moved to the island of Murano and a guild was created to protect their secret compositions and work systems. Glass workers could not work outside the region or disclose their knowledge by law under the death penalty.

It was not until the 17th century when the glass knowledge and its manufacturing methodologies began to spread with the publication of a state-of-the-art treaty on glass technology [1] that gained great recognition at that time. This marked the beginning of many improvements in glass technology. The raw materials were purified in Murano and a new formula was elaborated with magnesium, to obtain a glass of better quality called *crystallo*, which was perfectly colorless and crystalline. In England, coal started to be used as furnace combustible and higher temperatures were obtained, improving the quality of the glass. English glassmakers also added lead oxide to the glass composition to obtain glass with great brightness. In Bohemia, the use of lead was initially replaced by potassium fluxing agents and later by sodium carbonate to also improve the glass quality.

Noticing the interest in glass and other artistic expressions in Europe after the Middle Ages, it is easy to understand the high social level of these artisans. The Republic of Venice and the French monarchy granted privileges and titles of nobility to their master glassmakers to support their activities [2], [3]. The Spanish monarchy also granted special privileges to establish the *Real Fábrica de Cristales de La Granja* in 1720 [4], [5] to provide its own glass products instead of relying on expensive imports. A glass container production plant is still emplaced there, currently owned by Verescence [6]. In fact, the origins of some of the oldest glassmaking companies date back to those times as Heinz Glas (Germany) in 1622 [7] or Pochet du Corval (Bresle Valley, France) in 1623 [8], [9].

The many improvements in the glass production process developed during the industrial revolution and the growing demand for containers for the food and drink industry led to the mechanical production of glass containers at the very end of the 19th century. Furthermore, in Paris, the most influential and revolutionary fashion designers redefined the image of the twentieth-century society: not only they designed their clothes, but also the aromas and glass bottles of their perfume brands. These fashion designers merged the fashion and perfumery industries to conceive the actual industry of the glass perfume packaging. All these social changes and technological innovations made evolve the manual glass workshops to fully automated factories that are used to produce millions of glass containers for the packaging industry.

Glass is an essential material for the packaging industry. Glass is specially chosen to make bottles for the perfumery industry, but also containers for many high-end products for the food and drink industries. Its aesthetic properties make glass containers to be used as an exceptional marketing and product differentiation tools. In this sense, the transparency and brilliance of the glass add value to the packaging and to the product itself. Moreover, glass is not only a beautiful

material with unique conservation properties but it is also environmentally-friendly. Glass containers can be reused many times. But in addition, glass is a 100% recyclable material, so it can be recycled indefinitely without losing any of its fantastic properties. Therefore, for many reasons, glass is a very common and desired material for the packaging industry when the sense of taste or smell becomes a key element.

The total revenues of the European market for cosmetics and perfume glass bottles were estimated to be worth USD 632.17 million in the last 2017 [10]. Glass packaging for the fragrance and perfumery sector represented approximately 38.7% of the total volume and the skincare products (oils and serums) another 17.8%. Based on a study [11] conducted by FEVE (the European Container Glass Federation), glass packaging in Europe grew by 1.6% in volume (tons) in 2014. This means that more than 22 million tons or about 50 billion glass containers were sold to customers inside and outside the EU markets (see **Table 1**). In 2014, the production of glass containers in Spain accounted for 2.1 million tons.

Table 1. *Total production in tons of bottles and jars for the food and drink industry and flacons for perfumery, cosmetics and pharmaceutical industries in Europe and by country between 2010 and 2014* [11].

Country / Area	**2010**	**2011**	**2012**	**2013**	**2014**
Germany	3,787,750	4,065,452	3,934,844	3,933,641	3,973,786
Italy	3,506,532	3,568,710	3,391,637	3,445,302	3,467,462
France	3,152,023	3,310,186	3,146,755	3,030,949	3,097,473
United Kingdom	2,316,604	2,310,667	2,226,321	2,240,759	2,245,986
Spain	1,979,957	2,067,016	2,012,381	2,087,000	2,099,236
Portugal	1,312,909	1,351,919	1,441,962	1,439,429	1,451,735
Other North and Central	1,950,400	2,041,404	2,096,753	2,093,984	2,138,703
Other EU South-East	1,068,659	1,186,726	1,198,207	1,364,601	1,403,563
Turkey	779,462	822,502	950,000	1,021,000	1,172,313
Poland	986,347	986,750	996,660	1,003,551	1,078,071
Total Europe	**20,840,643**	**21,711,331**	**21,395,520**	**21,660,216**	**22,128,328**

The previous data in **Table 1** is referred to the production of glass containers for the food and drink industry, as well as to flacons for perfumery, cosmetics and pharmaceutical industries. In another FEVE communication, a production of 20.1 million tons can be attributed to the food and drink industry in Europe in 2014 [12], resulting in a total production of 1.9 million tons of glass flacons manufactured for the perfumery, cosmetics and pharmaceutical industries.

According to another study [13] conducted by Vidrio España, the market for glass packaging in Spain grew by 0.9% in volume (tons) in 2016. More than 2.6 million tons of glass were produced in Spain in 2016 (see **Table 2**). The figures are divided between two associations, ANFEVI and FAOVI. ANFEVI contains the results of companies that produce glass bottles for the food and drink industry. FAOVI includes three companies: Ramon Clemente, Bormioli Rocco and Verescence La Granja; this includes glass containers for perfumery, cosmetics and pharmaceutical industries, but also tableware and electrical insulators. In 2016, the total revenue of the ANFEVI companies was 944.3 million Euros and 180.6 million Euros for the FAOVI companies.

Table 2. *Total production in tons of bottles for the food and drink industry (ANFEVI) and flacons and other glasses (FAOVI) in Spain between 2014 and 2016 [13].*

Industry	**2014**	**2015**	**2016**
ANFEVI	2,429,749	2,487,338	2,506,699
FAOVI	157,394	155,386	176,218
Total	**2,587,143**	**2,642,724**	**2,665,486**

Ramon Clemente [14] (henceforth also referred to as RC) is a company that develops, manufactures and sells glass bottles for the perfumery industry. The headquarters of the company is located in El Masnou (Barcelona, Spain) and in its facilities there is a glass plant in operation since 1931 [15]. RC has more than 85 years of experience working with glass and its production process has been evolving over the years: initially, glass perfume bottles were handmade or produced with semiautomatic tools, it was not until 1968 when the first automatic IS machine was installed [15]. Today, the glass factory has two furnaces with a capacity of 45 and 32 tons that provide glass to five single gob IS machines. The glassmaking plant has a production capacity of 54 tons or around 250,000 containers per day. Each year, Ramon Clemente produces more than 11,600 tons or 70 million of containers for the perfumery industry. RC also has two other facilities where manufactured glass containers can be painted and decorated to supply a finished glass product.

Figure 1. *Example of some of the glass containers developed by Ramon Clemente for the glass perfumery packaging industry.*

Ramon Clemente is a family business that has found its place in a very large industry; it is a small player, which produces less than 1% of the European volume of glass containers for the perfumery, cosmetic and pharmaceutical industries. Many competitors are multinationals with large investments, enormous furnaces and double and triple gob IS machines where it is almost impossible to compete on price. Therefore, Ramon Clemente competes on service, offering exclusive and standard glass bottles and focusing on fast developments of their new bottles. Despite the small market share, RC develops more than 50 new glass perfume bottles every year. Therefore, the capability to manufacture a good product, the improvement of its quality and the reduction of the time to market for the new developments are key issues for Ramon Clemente to keep enhancing its strengths. The production planning of RC is also very flexible and customer demand-oriented, which allows for short series and tailored productions that many competitors cannot offer. Almost every day there is a job change in each of its five production lines. Ramon Clemente has adapted its infrastructure to make its weaknesses its strengths.

To continue enhancing its strengths, to develop new containers faster and with better quality, Ramon Clemente has the purpose to bridge the gap between the industrial experience in glassmaking acquired over many decades and the scientific knowledge embedded in the computer-aided engineering simulation tools developed in recent years. But in turn, the complexity of the industrial process makes this proposal a very ambitious goal. The actual development of a new glass perfume bottle and its manufacture will be presented briefly. Here, the most relevant stages of the glass forming process will be defined and how they relate to the design of the glass container and its mold equipment during the development process. This will help the reader to have an idea of the necessary steps to develop and manufacture a new glass bottle for the perfumery industry, highlight the most relevant difficulties that Ramon Clemente faces and then define goals to solve them.

When it comes to the industrial production of a new glass perfume bottle, the development of the new product is divided into two stages: the definition of the bottle design and its specifications and, subsequently, the design of the mold equipment used to manufacture that container. Typically, the initial customer requirements for a new perfume bottle are an aesthetic design (i.e. an external geometry and a glass thickness distribution) and its nominal capacity. With these premises starts the development of the glass container at Ramon Clemente. The initial design defined by the customer may be adapted when necessary to ensure that it can be manufactured (e.g. definition of mold partition lines, demolding angles, container stability, minimum dimensions of the funnel, etc.).

In the past, there was a tendency to design lightweight containers to cut back manufacturing and transportation costs. The objective was to optimize the glass thickness distribution to reduce the amount of glass used, but still, be able to pass the required load tests [16]. Nowadays, the new developments in the perfumery industry follow the opposite principle: the tendency is to obtain bottles with an overweighed aspect, with a thick glass base [17]. This is used to enhance the aesthetic properties of the glass packaging and increase the perceived value of the final product. One of the most important aspects during the evaluation of the container design is the definition of the external volume and the container weight to obtain a bottle design with the specified internal capacity and the desired glass thickness distribution. These evaluations cannot be taken lightly; the definition of a bottle with a feasible design and a reasonable internal thickness distribution to ensure that it can be manufactured correctly is not trivial. Moreover, once the dimensions and specifications of the bottle are defined, the rest of the packaging elements (e.g. valve, cap, decoration, box, etc.) and, obviously, the mold equipment used to manufacture the glass bottle will be defined according to the validated bottle design. Therefore, if after manufacturing the first glass samples, the container design needs to be modified, this may involve significant delays in the development of the glass perfume bottle.

After specifying the design of the glass perfume bottle, the development of the mold equipment can be started. The mold equipment used for the manufacture of glass bottles by the blow and blow glass forming process is divided into three different molds, which are subdivided again into smaller parts (see **Figure 2**): the neck ring mold consists of two neck ring halves, the guide, plunger and the blow head; the blank mold is formed by two blank mold halves, the funnel and the baffle; finally, the blow mold is defined again by two blow mold halves and the bottom plate. Mold equipment parts are commonly made of cast iron. Bronze can also be used if a higher thermal conductivity is needed between the glass and the mold cavities.

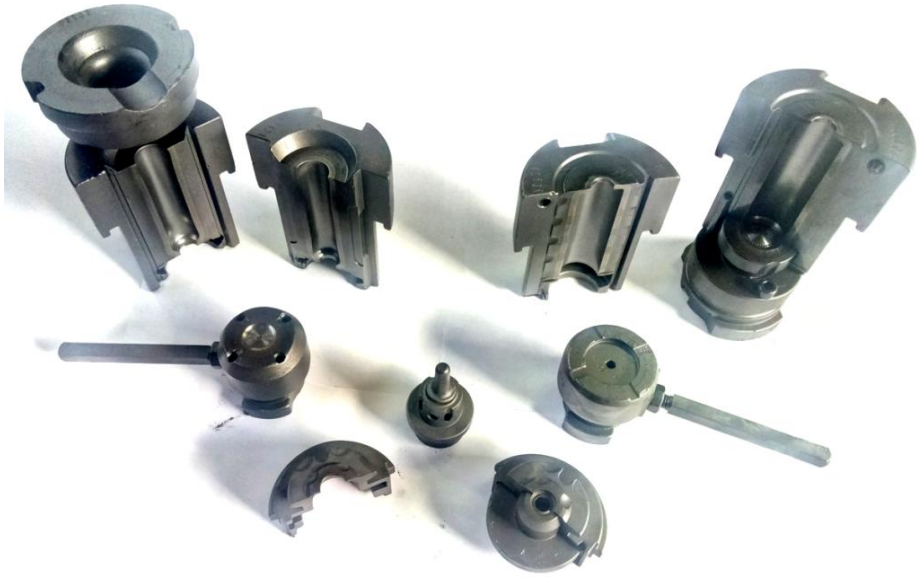

Figure 2. *Mold equipment used for the manufacture of glass bottles through the blow and blow glass forming process: blank mold (left), neck ring mold (bottom) and blow mold (right).*

The development process of the mold equipment is commonly divided into the following stages:

1. All the external parts of the mold equipment and the mold cavities are designed and a prototype of each piece is CNC machined in cast iron.
2. The operation times of the machine and the process temperatures are defined to test the mold prototypes on an individual section of the production line to manufacture the first units of the new glass container.
3. During the manufacturing tests, the quality of the formed glass bottles is controlled and adjustments are made to solve production problems and container defects.
4. If necessary, production tests are repeated with new designs of the mold cavities and/or new configurations of the production process until the desired quality is achieved in the manufactured glass bottles.
5. Finally, eight pieces of each mold equipment part are machined with the final designs to be able to manufacture the glass containers in a six-section IS machine.

The design of all the mold cavities is tailor-made for each new development, as a function of the design and final shape of the container. The neck ring forms the finish of the bottle, the blank mold cavity is used to define the parison and the blow mold cavity describes the external geometry of the final container. The design of the neck ring mold and the blow mold cavity is not obvious, but it is mainly based on the specifications and geometry of the glass bottle design. However, the development of the blank mold cavity, which defines the internal distribution of glass in the final container, is based solely on empirical knowledge and trial and error methodology. The design of the blank mold cavity and the glass parison formation are key issues to define the thickness distribution of the final glass container. In spite of that, there is no way to predict this glass thickness distribution before manufacturing the container. Therefore, to validate the mold design there is not any other possibility than perform manufacturing tests on the production line.

A scheme of the industrial process for glass production is presented in **Figure 3**. It begins with the mixing of the raw materials and the melting in the furnace. The melt is refined in the working end and conditioned in the forehearth. Afterward, the molten glass stream flows through the feeder and the orifice ring and it is cut with shear blades, forming discrete glass gobs. The delivery equipment distributes these gobs to each section of the IS machine where the container forming process takes place. The stages in the blow and blow container forming process are: gob loading inside the blank mold, plunger insertion and settle blow, counter blow and parison formation, transfer from the blank to the blow mold, glass reheat and stretch, final blow and take out (see **Figure 4**). Finally, the manufactured containers are sent through an annealing lehr, where the cooling rate is controlled to release the internal stresses of the glass bottles. Afterward, a quality control inspection is carried out and the containers are packed in boxes and pallets.

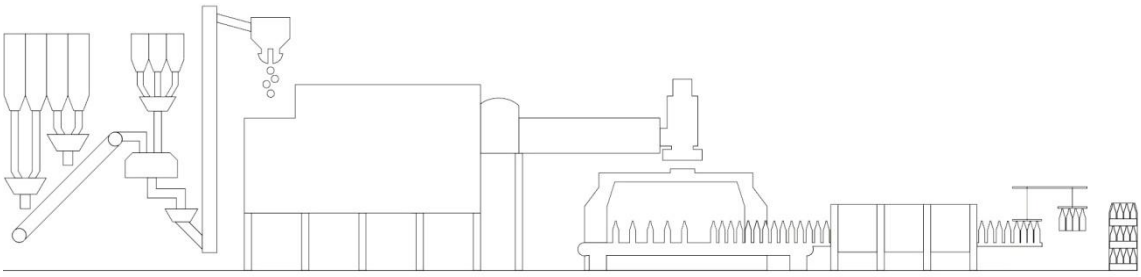

Figure 3. *Stages of the glass production process from start to end. Mixing of the raw materials (**i**); melting in the furnace (**ii**); refining (**iii**) and conditioning (**iv**) of the molten glass; gob forming and delivery (**v**); container forming (**vi**); annealing (**vii**), quality inspection (**viii**) and packing (**ix**) of the finished containers.*

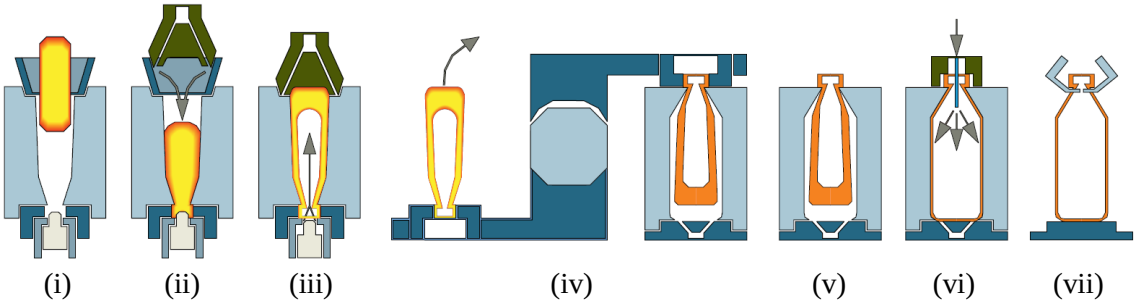

Figure 4. *Container forming IS machine stages of the blow and blow container forming process. Gob loading (**i**), settle blow (**ii**), counter blow (**iii**), inversion (**iv**), reheat and stretch (**v**), final blow (**vi**), and take out (**vii**).*

The industrial glass forming process takes place inside two different molds. The glass gob is initially transformed into a parison in the blank mold and becomes the final container inside the blow mold. When the forming process in both molds is carried out by blowing the glass against the walls of the mold cavity, this is known as the blow and blow (BB) forming process. As an alternative, instead of blown, the glass can be pressed with a plunger in the first mold, then the forming process is called press and blow (PB) or narrow neck press and blow (NNPB). These two other processes are used either to produce jars and lightweight containers [18]–[20]

respectively, which are generally used for the food and drink industry.

During the development of a new container, the designed mold equipment is tested in the production line and containers are manufactured. Blank mold cavities of previously developed containers with similar shapes (if any) can be taken as reference, but commonly, during the development of the mold equipment, few iterations may be necessary until the desired glass container is manufactured. When undesired glass distributions or other defects are obtained in the production tests, hypotheses are assumed based on empirical results about how blown glass expands inside the mold cavities. These aim to understand the results and obtain clues to improve the manufactured glass containers. This approach works many times, but unfortunately, in others, the empirical hypotheses may not be correct, then the defects of the glass bottle must be solved by pulling strings until the desired results can be obtained. A complete understanding of the industrial process for the manufacture of glass containers has not yet been reached. There is no accurate way to predict the glass flow inside the molds and only very little information can be obtained from the forming process.

Viscosity is the most important property in glassmaking, not only because it defines the resistance of glass to flow, but also because it has a strong dependence on temperature. The viscosity together with the temperature distribution strongly influences the glass flow in the forming process, especially during the blowing stages. Both properties vary rapid and continuously during the container forming process: initially, gobs are around 1,200 ºC where the glass behaves like a fluid; after forming, the temperature distribution in the final containers is around 650 ºC and the glass almost loses the ability to flow. The heat is transferred from the glass to the walls of the mold cavities at the contact interfaces. Due to the contact, a temperature distribution is defined in the glass domain; creating, in turn, a viscosity distribution. Therefore, when the blowing stages start, the temperature and viscosity distributions govern the mechanical behavior and the expansion of the glass inside the mold cavities. These thermo-mechanical phenomena, in addition to the design of the mold cavities, machine operation times and process temperatures completely define the glass thickness distribution and the external dimensions of the manufactured containers.

Information as the glass thickness distribution and other quality parameters can be obtained from glass containers once they are manufactured. But very little information can be obtained from the glass forming process itself. Most stages of the manufacturing process take place inside the closed molds. Thus, the glass can only be seen in the stages of gob loading and parison inversion. On top of that, in these two stages glass moves very fast: either loading into the blank mold or being transferred from the blank to the blow mold. Obtaining accurate information on glass is very challenging due to the high temperatures, the corrosive environment and the fast-paced forming process. Knowledge about the blowing stages and glass expansion would be very helpful for the design of the blank mold cavities.

Therefore, the glass forming process has been conceived as a black box system so far: from a specific input a corresponding output is obtained, but there is not much knowledge about its internal operation. In the blank mold, the gob is the input and the parison is the output. In the blow mold, the parison is the input and the final container is the output. As it is very difficult to obtain information about that intermediate step called parison, one can approximate the entire glass forming process as a black box system. Then, from a defined set of mold cavities and production parameters (e.g. machine operation times and production rate, process temperatures,

orifice ring and gob dimensions, etc.) a container with a specific glass thickness distribution is obtained.

To summarize, the glass perfume bottles developed and manufactured by Ramon Clemente are very demanding. The perfumery industry is very close to the fashion industry and designers always seek to differentiate their products from the others with new fancy container designs. Glass perfume containers tend to have difficult shapes, which are generally non-axisymmetric, with complex glass thickness distributions and high-quality requirements with a low tolerance to defects. Therefore, many times, containers with new shapes are challenging to be developed following empirical strategies due to the lack of previous containers with similar shapes. In addition to that, the blow and blow forming process used to manufacture glass perfume containers is complex and it is still not well understood. This is partly because only very little information can be obtained from the mold cavities under industrial manufacturing conditions, which historically has been conceived as a black box system. Therefore, there is no accurate way to predict the glass flow inside the molds.

In conclusion, the development process of the mold equipment to manufacture very demanding glass perfume bottles generally requires several iterations and production tests. The design of the mold cavity is a critical step for the development of each new container and its mold equipment as completely defines the thickness distribution of the manufactured container. In spite of that, in many aspects, it is based on empirical knowledge. But still, in the end, most of it is reduced to trial and error. The use of heuristic problem-solving techniques to solve container defects does not guarantee an optimal solution when only a specific amount of time and resources are available. The iterations necessary to develop a new container and mold equipment are expensive, increase the time to market and involve huge downtimes in the production line. In addition, suboptimal production conditions can cause defects in manufactured containers and a decrease in the production rate.

This thesis will not be a mere transfer of knowledge between the university and Ramon Clemente: scientific and engineering knowledge will be added to the valuable industrial experience acquired over the years of manufacturing glass containers. At the same time, the use of numerical simulations as a tool to guide the design of the mold equipment for the development of new glass perfume bottles will be very beneficial for Ramon Clemente. The quality of the manufactured containers will be improved, while the amount of expensive experimental iterations will be reduced.

As stated before, Ramon Clemente must bridge the gap between industrial experience in glassmaking acquired over many decades and scientific knowledge embedded in the computer-aided engineering simulation tools present in recent years to develop new glass perfume containers faster and of better quality. The objective of this thesis is to **implement a numerical model to describe the thermo-mechanical behavior of glass during the blow and blow forming process to numerically predict the glass thickness distribution of the manufactured containers.** This thesis focuses on a numerical and experimental study of the blow and blow forming process used to manufacture glass perfume bottles.

To achieve this goal, a work plan has been proposed for this thesis with the development of the following key aspects:

- Study the glass properties and the blow and blow container forming process based on Ramon Clemente's production lines and define a framework to describe the container forming process (**Chapter 2**).

- Carry out experimental analyses to define the conditions of the glass gobs under manufacturing conditions. This includes performing infrared measurements of the glass gobs during the gob forming, delivery and loading operations (**Chapter 3**).

- Perform different numerical and experimental studies to model and validate the blow and blow container forming process to predict the glass thickness distributions of the manufactured containers (**Chapter 4**).

1.2 CONTENT OF THIS DISSERTATION

Glass forming is a complex industrial process, in which the IS machine performs many operations to manufacture a glass perfume container. The glass properties, the mold equipment and the sequential operations of the IS machine are totally interrelated, defining the heat transfer, temperature and viscosity of the glass inside the molds. Thus, the development of a numerical model to predict the glass thickness distribution of the final container after the blow and blow container forming process is a very ambitious goal to be achieved starting from scratch.

The container forming process is conceived as a black box system, with very little information available on the thermo-mechanical behavior of the glass during the blowing stages of the process. For this reason, the first step before starting to model is to gather as much information as possible. **Chapter 2** presents a description of the glass production operations. In addition, the glass material properties necessary to describe the glass domain in the numerical model are defined and described. Glass viscosity is the most relevant property for glassmaking. It is very sensitive to the glass composition and its temperature. The viscosity of Ramon Clemente's glass was characterized in an external laboratory. Finally, the heat transfer phenomena present during the container forming process make it difficult to define the temperatures of the glass domain under industrial manufacturing conditions; a methodology was therefore defined to measure the glass temperatures using an infrared thermal camera.

Experimental measurements to define the conditions of the glass gobs under manufacturing conditions were performed using an infrared thermal camera; these measurements are discussed in **Chapter 3**. In the first part of the chapter, the thermal properties of the glass gob, analyzed during the gob forming process, are described. This analysis led to a better understanding of the thermal phenomena that occur in the glass during the gob forming process. In addition, several experimental tests were performed to measure the temperatures on the surface of the glass gob with the infrared thermal camera, validating the temperature distributions described in the literature. The delivery and loading operations of the gob are also studied later in **Chapter 3**. Infrared measurements were performed to determine the deviations of the delivery conditions present in the glass gobs as a function of the position of the individual sections in a six-section IS machine.

After gaining confidence with the infrared thermal camera and being able to properly define the glass temperatures, experimental and numerical studies were performed and are discussed in **Chapter 4**. First, a glass gob drop test on a cast iron plate was carried out. Validation of the glass temperatures, material properties and non-isothermal formulations was successfully established by comparing the numerical and experimental deformation of the glass gobs after the impact with the plate. Once the non-isothermal formulations had been used to validate the dependence of the glass viscosity on the temperature and other material properties of the glass, numerical and experimental studies of the blow and blow container forming process were carried out. In this case, two glass perfume bottles, representative of the wide range of the most common containers manufactured by Ramon Clemente, were used to validate the numerical simulations of the container forming process. The numerical results show that the model predicts the final thickness distribution as a function of the blank mold cavity and the forming

process conditions. These simulations were performed using an axisymmetric model but also compared with the results of a three-dimensional model.

A numerical simulation that describes the glass flow inside the mold cavities during the blow and blow forming process is a very powerful tool. Until now, the black box system transformed an input into an output. However, being able to describe, predict, and therefore understand the phenomena that occur during the container forming process will help to improve the quality of the manufactured containers and reduce the time required to develop new glass perfume containers.

1.3 REFERENCES

[1] A. Neri, *De arte vitraria. Libri VII*. Amsterdam: Henrico Wetstenium, 1686.

[2] J. M. Fernández Navarro, *El Vidrio, Textos Universitarios*. Madrid: Consejo Superior de Investigaciones Científicas y Sociedad Española de Cerámica y Vidrio, 2003.

[3] "La Glass Vallée - History." [Online]. Available: http://www.la-glass-vallee.com/en/the-glass-valley/historical/history. [Accessed: 30-May-2019].

[4] L. Pérez Bueno, "Real Fábrica de Cristales de S. Ildefonso (La Granja); antecedentes y apuntes para su historia," *Arte Español*, vol. 15, pp. 9–15, 1926.

[5] M. T. Ruiz Alcón, *Vidrio y cristal de La Granja*. Madrid: Instituto Diego Velazquez del Consejo Superior de Investigaciones Científicas, 1969.

[6] "SGD La Granja se convierte en Verescence La Granja," 2016. [Online]. Available: https://www.lagranja-valsain.com/sgd-la-granja-se-convierte-en-verescence-la-granja/. [Accessed: 12-Sep-2016].

[7] "Heinz Glas - Our Family Tradition." [Online]. Available: https://heinz-glas.com/en/thats-us/family-tradition/. [Accessed: 30-May-2019].

[8] P. Gillet, *Les maîtres du verre et du feu - Quatre siècles d'excellence*. Pochet - Le Courval: Perrin, 1998.

[9] "Groupe Pochet - History." [Online]. Available: http://www.groupe-pochet.fr/group/#!/history. [Accessed: 30-May-2019].

[10] Mordor_Intelligence, "Global Cosmetics and Perfumery Glass Bottles Market (2017-2023)," Hyderabad, India, 2018.

[11] M. Delle Selve, "EU Container Glass Production Growth Shows Industry Resilence," Brussels, 2015.

[12] M. Delle Selve, "Glass Packaging Demand Growth: The Market Trusts Glass," Brussels, 2017.

[13] Vidrio_España, "Contribución Económica, Ambiental y Social del Sector del Vidrio en España (2014/1016)," Madrid, 2017.

[14] "Ramon Clemente." [Online]. Available: http://www.rclemente.net/.

[15] M. Torrentó Boix, *Multinacionals de butxaca: Explicades pels seus Capitans*. Barcelona: Mobil Books, 2017.

[16] S. Tamura and R. W. Marek, "Evaluation about Drinking Bottle's Reduce and Reuse Effectiveness: Super Light Returnable Glass Bottles and Life Cycle Assessment," *Int. J. Environ. Prot. Policy*, vol. 2, no. 5, pp. 153–160, 2014.

[17] M. Redding, "Transforming glass for fragrances and skincare; glass bottles and jars always look elegant," *Beauty Packaging*, 2017.

[18] H. Griffel, "Lightweighting in the Glass Container Industry," in *Conference on Glass Problems*, 1987, vol. 8, no. 3–4, pp. 156–170.

[19] A. Fenton, O. Wiegand, and K. H. Mann, "Light weighting containers," *Glass International*.

[20] S. Balan Mendoza Jaime, S. Alves Ortiz, T. Bassani Dantas, and C. Ferreira Damasceno, "A Comparison of the Performance of Lightweight Glass Containers Manufactured by the P&B and B&B Processes," *Packag. Technol. Sci.*, vol. 15, no. 4, pp. 225–230, 2002.

CHAPTER 2
FRAMEWORK TO MODEL THE CONTAINER FORMING PROCESS

2.1 INTRODUCTION

As introduced in the previous chapter, the manufacture of a glass perfume container is a complex industrial process. The glass properties, mold equipment and the sequential operations of the IS machine are completely interrelated, defining the heat transfer, temperature and viscosity of the glass inside the mold cavities. The coupling of these thermo-mechanical phenomena complicates the development of new glass perfume containers, usually requiring several production tests. However, modeling the industrial process to manufacture glass containers is also a very complex task due to these very same reasons. Numerical simulations cannot be done from scratch. To succeed in modeling the blow and blow container forming process and numerically predict reliable numerical results, a previous understanding of that black box system is required.

For many years plant operators have run the IS machine to successfully manufacture glass perfume containers. Experience helps to understand the container forming process and the phenomena that occur between the glass, the molds and the IS machine. In this way, they are able to configure the IS machine to produce a new glass container, to solve production defects, to maintain the process stable, etc. However, most of the knowledge acquired by the machine operators is empirical or based on trial and error. In addition, very little information can be obtained during the forming process since glass remains inside the mold cavities. Especially about the thermal conditions at the glass-mold contact interface, that define the heat transfer between both domains or about the mechanical behavior of the glass during the blowing stages of the process. A better understanding of the industrial manufacture of glass containers is needed to model the problem, as empirical or partial knowledge is not enough. It will be necessary to define machine parameters, material properties and physical, thermal and mechanical phenomena to describe the forming process using mathematical equations required in the numerical model. In conclusion, craftsmanship and experience in glassmaking have to be translated into scientific knowledge.

Therefore, the first step in **Chapter 2** will be to gather as much information as possible and transfer all the practical knowledge acquired over many years of experience working with glass, into defined process stages, material properties and boundary conditions that can be described by the numerical model. First of all, a detailed description of the glass manufacturing operations based in the Ramon Clemente production lines will be presented. It is important to describe the blow and blow container forming, as it is the process to model. But also the previous stages are necessary, including the gob forming, delivery and loading operations. These previous operations define the thermal conditions present in the glass gob when it is loaded into the blank mold, just before starting the container forming process.

Relevant material properties are necessary to describe the glass domain in the numerical model. Glass properties are defined by its chemical composition. Ramon Clemente containers are made of soda-lime glass, which is a very common type of glass in the industry. However, each manufacturer has its own chemical composition and, therefore, its material properties. Fortunately, many glass material properties can be obtained from literature, or depending on their importance can be easily characterized in external laboratories following standard procedures. In this sense, glass viscosity is the most important material property for glassmaking. First, because it defines the ability of glass to flow. But above all, because viscosity is very sensitive to the glass temperature.

As detailed in the operation of the blow and blow forming process, glass temperatures rapidly vary from 1,200 ºC to 650 ºC in the few seconds required to manufacture a perfume container. Therefore, to describe the glass flow, viscosity must be characterized. At the same time, as viscosity is strongly influenced by the temperature; thermal conditions in the glass domain are also necessary to couple both thermal and mechanical phenomena. Therefore, the heat transfer, temperature gradients and any thermal phenomena that could define the temperature and viscosity distributions within the glass domain during the forming process will be a matter of study. For this reason, it will be necessary to define the contribution of the different thermal phenomena to the glass thickness distribution obtained in the finished glass containers, to define the level of detail necessary to describe the heat transfer by the numerical model.

However, heat transfer between glass and molds in the forming process is a much more complex phenomenon to describe compared with material properties. Despite its complexity, it is very relevant since it defines the temperature distribution within the glass domain, coupling the thermo-mechanical behavior of glass during the forming process. The heat transfer is defined by the semitransparent thermal radiation within the glass, the glass thermal conductivity and the contact conductance at the glass-mold interfaces. These thermal phenomena depend on the manufacturing conditions present inside the molds during the container forming process, so they must be defined experimentally under industrial manufacturing conditions. The different approximations used to describe, measure and model the heat transfer phenomena in the numerical simulations of the glassmaking operations will be briefly reviewed.

Finally, due to the importance of the heat transfer defining temperature and viscosity distributions within glass, that is, the glass flow; an experimental method is required to obtain information on the glass temperatures and its evolution throughout different stages of the forming process. It will be necessary a device to measure the glass temperatures of the gobs at the gob forming, delivery and loading operations and also during the blow and blow container forming process. For this reason, several methods to measure the glass temperatures under

industrial manufacturing conditions were presented; including contact measurement devices and also non-contact measurement devices based on infrared sensors. From this discussion, it can be concluded that a non-contact infrared thermal sensor is probably the most flexible option to measure the glass temperatures in many stages of industrial glass production. Due to its wide field of view, an infrared thermal camera was chosen to measure the temperatures on the glass surface. The methodology presented in this chapter will be applied in the following chapters to obtain thermal information about the glass conditions in the forming process, to define the initial conditions of the numerical simulations and to validate the predicted results by the numerical model.

To summarize, the glass forming is a complex and not well understood industrial process where many phenomena occur. So, before start modeling the blow and blow process, it is wise to gather as much information as possible. Therefore, the main objective of this chapter is to **study the glass properties and the blow and blow container forming process** based on Ramon Clemente's production lines. This information will be used to **define a framework to describe the container forming process.** Later, this will be modeled in a virtual environment, **based on mathematical equations** to predict the phenomena occurring to glass during the industrial production of the containers.

To achieve this objective, the following tasks were proposed:

- Describe the phenomena occurring in the several operations of the glass forming process that need to be understood to model the container forming process.

- Define which are the relevant material properties, process parameters and thermal phenomena to be described by the numerical model.

- Characterize the glass material properties based on Ramon Clemente glass composition.

- Define a method to experimentally measure the glass temperatures during the glass production under manufacturing conditions.

2.2 DESCRIPTION OF THE GLASS CONTAINER MANUFACTURE

Ramon Clemente manufactures glass containers made of soda-lime glass. A typical composition of soda-lime glass is defined by the following proportions: silica (SiO_2) 73%, sodium oxide (Na_2O) 13.5% and calcium oxide (CaO) 10%. Other minor components can be added to the mixture to define the final chemical composition of the glass. A defined amount of recycled glass or cullet is also added as it lowers the temperatures required to melt the glass, reducing the energy consumption of the furnace. The glass manufacture begins with the weighing and mixing of the raw materials. Then, they are introduced into the furnace and melted, followed by the refining in the working end and conditioning and delivery of the glass melt with the forehearth. This first part of the process is common to many glass manufacturing processes. But, as it remains in a completely different area of knowledge, it is beyond the scope of this thesis. Detailed information about the raw materials, glass compositions and furnace operation can be found in the literature.

Afterward, different glass forming processes can take place, which in this case will be the gob forming, delivery and loading operations and the blow and blow forming process to manufacture glass perfume containers. These will be explained in the following sections.

(A) Glass Melt Delivery and Gob Forming Process

The function of the delivery channel or forehearth is to deliver the glass melt from the furnace to the equipment that will form the glass products, in this case, the IS machine to produce perfume containers. In the forehearth, the molten glass is cooled and conditioned to the required viscosities for the forming stages. The glass melt cools by transferring heat to the refractory walls and by radiative heat transfer through the glass-air surface. At the same time, burners positioned through the entire delivery channel control the glass temperature and the pull rate by adding more or less heat to the glass energy balance. Therefore, the glass is hotter near the surface and colder near the refractory walls and bottom of the forehearth. Refractory pieces of the forehearth in contact with glass are made from very dense material composition to reduce the chemical erosion. There is also an outer layer made from high porosity bricks that acts as a thermal insulator.

The purpose of the feeder is to collect the flow of molten glass from the forehearth and deliver it in the form of gobs to the IS machine. The gob forming process represents the transition from a continuous melting process to a discrete forming operation to manufacture the glass containers. The molten glass is conditioned and glass arrives at the feeder with a uniform temperature and composition; however, spouts and orifice rings are not properly insulated and usually have relatively high local heat losses [1]–[3]. For this reason, the glass in the feeder is frequently heated with burners. The spout and the orifice ring can also be heated with electrical windings.

Since the gob forming process defines the gobs delivered to the IS machine, it is important to accurately control various parameters such as the weight, geometry, viscosity and temperature

of the glass gob to consistently produce glass containers with the desired specifications. The most relevant parameters to define the glass conditions in the gob forming process are: the temperature set point of the last forehearth section, the height of the feeder tube, the diameter of the orifice ring, the oscillating velocity profile of the feeder plunger and the production rate of the IS machine. This last parameter defines also the cadence of the shear blades. In general, these parameters will define the weight, geometry (i.e. diameter/length ratio) and temperature of the formed glass gobs.

The gob is tailor-made for the container to be produced. Depending on the requirements to manufacture a specific container, different configurations of the mentioned parameters can be used to obtain gobs with different aspect ratios and temperatures while maintaining the same weight of glass. Usually, the best gob geometry is the shortest one that will load cleanly into the mold, without dragging excessively on the sides of the funnel or the blank mold. The main task of the gob forming process is to obtain gobs with a uniform diameter, constant weight and reproducible glass conditions throughout the container production.

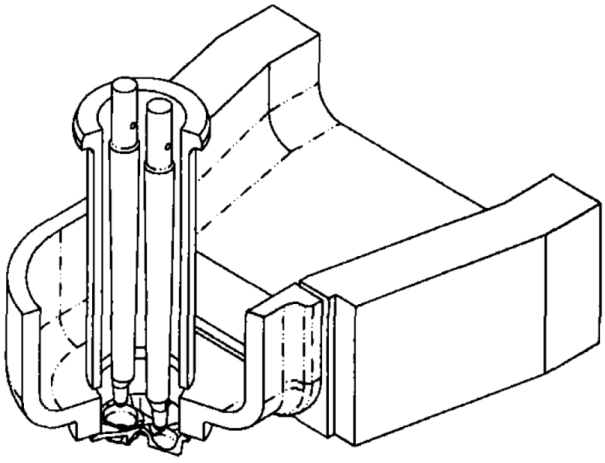

Figure 1. *Feeder assembly located at the end of the delivery channel showing its main elements (spout, feeder plunger, rotating tube and orifice ring) in a double gob configuration.*

The feeder assembly is composed of five main elements: the spout, feeder plunger, rotating tube, orifice ring and the shear blades (see **Figure 1**):

- The spout is the last refractory piece mounted at the end of the forehearth channel. Its geometry along with the movement of the other feeder elements conducts the molten glass flow to the orifice ring to form the gobs. As the other delivery channel parts in contact with glass, it is made from a dense refractory material to reduce the chemical erosion from the molten glass and elongate its lifetime.

- The orifice ring is a circular refractory piece fixed below the spout. In general, the diameter of the hole in the orifice ring defines the diameter of the extruded glass gob. In the manufacture of perfume containers, a wide range of orifice ring diameters is used depending on the weights and geometries required for the glass gobs.

- The rotating tube acts as a flow control valve: it regulates the height between the tube itself and the bottom of the spout to allow more or less glass flow, pull rate and gob

weight. The tube is positioned in the middle of the spout, so glass flow will proceed around both sides and the two streams will meet forming a stagnation point. The tube rotates to stir the glass around the spout and eliminate that stagnation point, otherwise, it would appear as a visible cord defect in the manufactured containers.

- The feeder plunger acts as a piston controlling the extruded flow of molten glass and the weight of the gobs. The extruded glass flow is determined by the plunger vertical motion, glass viscosity and gravity. The oscillating velocity profile of the feeder plunger is driven by a cam. It is defined with three steps: initially, there is a long upward movement, followed with a fast downward stroke and just before the cut of the gob the upward movement starts again. During the upward motion, the plunger ascends, allowing the molten glass to start flowing through the orifice ring due to the low viscosity of glass and gravity. With the downward motion of the plunger, the molten glass is pushed and extruded through the orifice ring to form the gob. When the upward plunger motion starts again, negative pressure can be obtained to suck the glass gob, to allow a better cut and also to minimize the contact of the remaining glass with the cold shear blades.

- The shear blades cut the extruded glass gob to the desired length to produce glass containers with the desired weight. Its cadence is defined by the production rate of the IS machine. Before each cut, a lubricant and cooling oil/water emulsion is sprayed onto the shear blades to obtain a clean cut and avoid shear marks on the tips of the gob and the final container.

A detailed thermal study of the glass temperatures measured with an infrared thermal camera during the glass gob extrusion through the orifice ring at the gob forming process will be presented in the first part of Chapter 3.

(B) Gob Delivery and Loading Operations

The main function of the delivery equipment is to distribute the formed glass gobs to the blank molds of the IS machine at the start of the container forming process. The orifice ring, the shear blades and the scoop are positioned on the centerline of the IS machine. Once the glass gob is cut, it will fall onto the scoop and slide through the delivery equipment to each of the individual sections of the IS machine. The glass gob distributor synchronizes the position of the scoop with the IS machine operation times to be able to deliver glass gobs to the individual sections before starting the container forming process. The troughs and deflectors used in the delivery equipment of each individual section have different lengths. This defines, in turn, the conditions of the glass gobs at the end of the delivery equipment depending on the position of the IS machine where the gob has been delivered. The loading equipment consists of three components:

- The scoop receives the extruded glass gobs after the shear cut and changes its direction from vertical to the angle of the troughs. The inner profile of the scoop has a curved and a straight section to accelerate the gob horizontally. The most common configuration is a single scoop mounted on a gob distributor that turns to deliver the glass gobs to all the individual sections of the IS machine.

- The troughs are linear channels that cover the horizontal distance between the machine centerline and the blank mold of each machine section. Then, the length of the troughs depends on the position of the section in the IS machine, being longer as they move away from the middle sections. The slope of the troughs when assembled on the machine also differs as a function of the position of the section.

- The deflectors change the direction of the gob for a second time. Their inner profile has a curved section to smoothly reduce the radial forces due to the centripetal acceleration of the gob and redirect the glass gobs to obtain a vertical load into the blank mold. To the naked eye, all the deflectors have a similar curvature. However, to improve the gob verticality before loading, a straight section is added to the end of the internal deflectors. So deflectors of the middle sections are longer than the side ones.

The scoop is commonly made of aluminum and it is water-cooled. The material of the troughs and deflectors is cast iron. Maintaining an adequate surface of the inner profiles in the delivery equipment components is very important to reduce the friction coefficient with the glass gobs and to improve the performance of the delivery operation. The surface of the delivery equipment in contact with the glass gobs is coated with graphite-based resin. An oil/water emulsion can be sprayed on the scoop before each gob is delivered, following the same principle used to lubricate the shear blades before each cut. Finally, the machine operator lubricates periodically the troughs and deflectors using also a graphite-based lubricant. This maintenance reduces the friction coefficient with the glass gobs and the erosion of the inner profiles.

The initial properties of the glass gobs when are extruded in the gob forming process will be defined in the first part of **Chapter 3**. The only parameter that needs to be defined in the delivery equipment is the width of the channels as a function of the diameter of the orifice ring and the weight of the formed gobs. A detailed experimental study of the glass gob properties at the end of the delivery and loading operations will be presented in the second part of **Chapter 3**. Finally, in the first part of **Chapter 4,** a numerical and experimental study of a glass gob test will be performed.

(C) Blow and Blow Container Forming Process

The industrial production of glass containers is carried out by the use of the IS machine. The IS machine consists of several individual forming sections. Each of them contains all the parts of the mold equipment, assembled in the blank mold and blow mold sides of the machine, which are coupled together by the inversion arm. Each individual section can be operated independently of each other. So, if there is a problem in one section, that section can be stopped or their parameters modified without affecting the production in the other sections of the IS machine.

Many subsequent operations are necessary to manufacture a container, but the most important parameters to be defined in the container forming process are the machine operation times, the production rate and the process temperatures. Once defined the production rate, the operation times of the IS machine determine how the total amount of time is distributed in each of the

operations. During the forming process, the heat is transferred from the glass to the walls of the mold cavities at the contact interfaces. Therefore, glass temperature varies rapidly: initially the gobs are around 1,200 ºC and, after forming the container, the temperature distribution is around 650 ºC, low enough for the glass container to withstand gravity and low deformations after the blow mold is open. So, the production rate and the machine operation times define the contact time in the different stages and, as a consequence, the total heat transferred to the molds, which defines the temperature distribution within the glass during the forming process. The configuration of the IS machine is complex since there are many parameters and they vary according to the specifications of the container produced. The configuration of the IS machine and other production parameters are tested together with the design of the mold cavities during the manufacturing tests carried on during the development of the mold equipment.

As explained in **Chapter 1**, there are several processes to manufacture glass containers according to their geometry and uses. In the case of glass containers for the perfumery industry, since the diameters of the finish are very small and, in general, the container geometries are non-axisymmetric, plungers cannot be used to define the parison as in PB or NNPB processes. Therefore, once the glass gobs are formed, cut and delivered into the blank molds of the IS machine, the manufacture of the glass perfume containers is performed by the blow and blow forming process, where both glass expansions are the result of blowing the glass against the walls of the mold cavity. The pressure applied during the blowing stages is approximately 2 bars.

A schematic of the blow and blow forming process can be found in **Figure 2**. Initially, the glass gob is loaded through the funnel into the blank mold, which is placed upside-down (see **Figure 2A**). First, the finish of the container is formed by the neck ring mold. After the loading stage, the baffle is placed on top of the funnel and a plunger is inserted from the bottom of the neck ring. Then the settle blow is performed by blowing pressurized air from the baffle (see **Figure 2B**). Afterward, the funnel is removed and the baffle is placed on top of the blank mold, sealing the blank cavity. The plunger is removed and the counter blow pressure is applied at the glass cavity defined by the plunger, allowing the glass to expand throughout the blank cavity to create the parison (see **Figure 2C**). At this point, the parison is still upside-down. The baffle is then removed and the blank mold is opened allowing the parison, still held by the neck ring, to be transferred into the blow mold by the swing of a mechanical arm (see **Figure 2D**). Once the parison has been transferred and inverted from the blank mold to the blow mold side, the blow mold closes, the neck ring opens and the parison remains hanged on top of the blow mold by the finish (see **Figure 2E**). The blow head is then placed on top of the blow mold, blowing the glass against the walls of the blow mold cavity to create the final shape of the container and defining the glass thickness distribution (see **Figure 2F**). Finally, the blow mold is opened and the tong takes out the finished container to a conveyor belt (see **Figure 2G**). Then the manufactured containers are sent through an annealing lehr, where the cooling rate is controlled to release the internal stresses of the glass containers. Afterward, a quality control inspection is carried out and the perfume containers are packed in boxes and pallets.

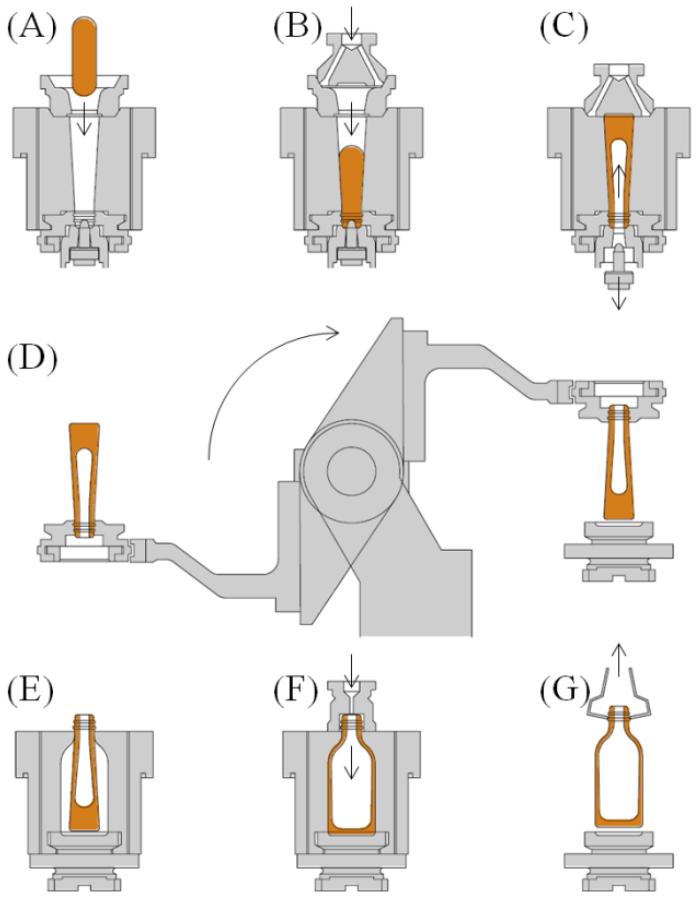

Figure 2. *Container forming IS machine stages of the blow and blow forming process. (**A**) gob loading, (**B**) settle blow, (**C**) counter blow, (**D**) inversion, (**E**) reheat and stretch, (**F**) final blow and (**G**) take out.*

As the machine operation times have an impact on the glass temperature, and glass viscosity depends on temperature, the thickness distribution obtained in the final container may be affected by the production parameters. In **Chapter 4**, numerical simulations of the blow and blow forming process will be carried out to predict glass thickness distribution, taking into account the mold cavities design, machine operation times, glass temperatures and other parameters of the production process.

2.3 RELEVANT MATERIAL PROPERTIES IN GLASSMAKING

As introduced before, glass requires a lot of energy to melt in the furnace. At the end of the forehearth, the glass still conserves most of its energy, remaining at temperatures close to 1,200 ºC. Therefore, the forming process has two objectives, the first is quite obvious: the continuous stream of molten glass must be transformed into discrete glass containers. The second is to reduce the glass temperature to about 650 ºC in a few seconds. So, the forming process will imply rapid variations in all the glass properties that are temperature-dependent.

The most relevant glass properties to be described by the numerical model are the viscosity, the specific heat, the density and the thermal expansion of glass. The material properties are strongly related to the glass composition. Fortunately, these glass properties can be characterized in external laboratories following standard procedures.

(A) Glass Viscosity

Viscosity is a measure of the resistance of a liquid to shear deformation, i.e. a measure of the ratio between the applied shearing force and the rate of flow of the liquid. If a tangential force difference F is applied to two parallel planes of area A, which are separated by a distance d, the viscosity μ is given by the following expression:

$$\mu = \frac{F \cdot d}{A \cdot v} \tag{1}$$

where v is the relative velocity of the two planes. If the velocity varies directly with the applied shear force, the viscosity is independent of force and the liquid is said to behave as a Newtonian fluid. In SI units viscosity is given in Pa·s.

Viscosity is the most important property in glassmaking, not only because it defines the resistance of glass to flow, but also because it has a strong dependence on temperature. The viscosity together with the temperature distribution defines the glass flow in the forming process, especially during the blowing stages. Glass is an amorphous solid, so it has no crystalline structure or melting point. This means that the viscosity of the glass, or its resistance to flow, varies continuously with temperature. At the start of the forming process, the glass temperature is around 1,200 ºC, resulting in viscosity values near 10^3 dPa·s, where glass behaves like a fluid. To have a reference, water viscosity at room temperature is 10^{-2} dPa·s and honey viscosity between 2 and 10 dPa·s. On the other hand, at the end of the forming process, the finished glass containers have temperature distributions around 650 ºC, resulting in viscosities near 10^9 dPa·s. This is a variation of six orders of magnitude, resulting in viscosities so high that the glass almost loses the ability to flow.

For this reason, the stress-strain curve, commonly used to define Young's modulus, the elastic limit or the plastic deformation zone, etc. will not be used to characterize the glass. These would be common parameters in the rigid body dynamics, otherwise, the fluid-dynamic behavior of the glass at high temperatures will be defined using its viscosity curve as a function of temperature

(see **Figure 3**).

For a defined glass composition, the viscosity as a function of temperature defines the working range used to manufacture containers through the blow and blow forming process. Glass viscosity is a very sensitive material property, not only to changes in temperature but also to the glass composition [4]. This includes variations in raw material suppliers, but also small changes in the furnace operation or even weather conditions. Therefore, glass viscosity is periodically characterized in external laboratories to control the viscosity changes over time and maintain a specific working range.

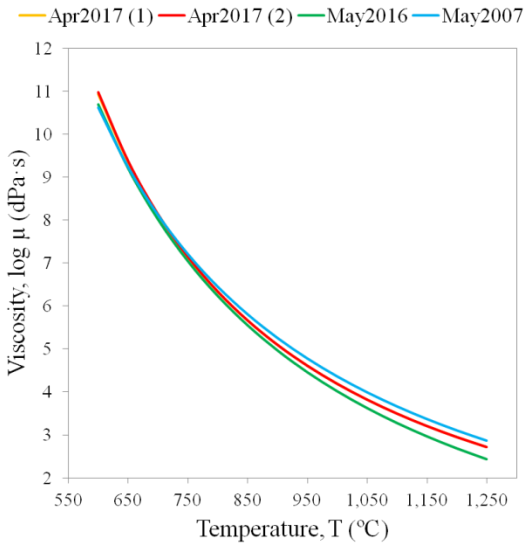

Figure 3. *Curve for viscosity as a function of temperature on a logarithmic scale. Viscosities of different RC soda-lime glass samples are plotted as an example of viscosity variation over the years.*

The strong temperature dependence on glass viscosity is commonly expressed using the VFT (Vogel-Fulcher-Tamman) equation [5]

$$\log_{10}\mu(T) = A + \frac{B}{T - T_0} \tag{2}$$

where A, B and T_0 are empirical coefficients that must be defined for each glass composition.

In the numerical simulations, the viscosity of the glass domain is described using the VFT equation, specifically using the May2016 curve from **Figure 3**.

Additionally, the non-Newtonian behavior of glass due to shear thinning has been characterized in the past [6]. The viscoelastic effects may be relevant in some cases, such as in the NNPB pressing stage, here they can be modeled to predict defects as the glass temperature decreases while it fills the cavity of the neck ring mold [7], [8]. Viscoelastic effects and structural relaxation models have also been taken into account in the numerical simulations of the TV panel pressing process to predict the glass properties and dimensions of the TV panel geometries at the very end of the forming process [3]. However, the non-Newtonian behavior of glass only becomes relevant as the glass temperature descends near its transition temperature

and glass is subjected to high stresses. The lowest glass temperatures in the blow and blow forming process are obtained when the blow mold is opened since the glass viscosity of the finished container should be high enough to withstand gravity and low deformation effects. Even then, the glass temperatures are still above the annealing (541.6 ºC) and strain (511.9 ºC) points and the internal stresses can be quickly relaxed. Therefore, the elastic effects do not need to be taken into account and glass can be considered a Newtonian fluid in the numerical simulations of the blow and blow forming process.

(B) Glass Specific Heat

The specific heat or heat capacity of a material defines the amount of energy that must be added to the sample to achieve a small change in its temperature. Commonly it is referred to as the amount of heat needed to raise the temperature of the sample by one unit. In SI units the specific heat is expressed in J/(kg·K).

The values of specific heat depend on not only the composition and temperature of the glass but also structural changes have an important impact. In **Figure 4** the specific heat dependence on the temperature has been plotted. The structural changes due to the transition of a solid glass into a viscous melt, result in an increase in the enthalpy of the glass and therefore the total specific heat. It can be seen also that after the structural changes in the melt it is possible to neglect the influence of temperature on the heat capacity.

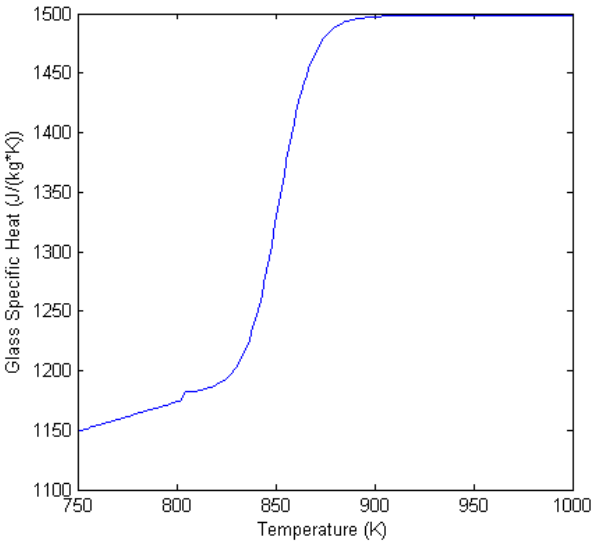

Figure 4. *Specific heat as a function of temperature. The increase in enthalpy due to the transition of a solid glass into a viscous melt can be observed in the heat capacity dependancy.*

As the temperature range of the container forming process is over Tg (533.1 ºC), the heat capacity of the glass can be considered a constant property. For this reason, in the numerical simulations, the specific heat of the glass is defined with a constant value of 1,500 J/(kg·K).

(C) Glass Density and Thermal Expansion Coefficient

The density ρ of a material is the mass of the substance per unit of volume. In SI units the density is expressed in kg/m^3.

The thermal expansion coefficient of a material is a measure of the rate of change in volume, and therefore density, with temperature. The thermal expansion coefficient is defined as the slope of the volume versus the temperature curve, at a specified temperature and constant pressure.

For a specified glass composition, the molecular weight must remain the same. But as the volume will slightly increase with the temperature, the density and therefore the thermal expansion coefficient will be sensitive to changes in the glass temperature. The volume occupied by the atoms also depends on the arrangement of their structure. However, as the temperature range defined in the blow and blow container forming process is over Tg (533.1 ºC), no particular transition in the arrangement is expected.

In the industrial process, a variation in the volume of about 4% is experienced between the molten glass at 1,200 ºC and the glass at room temperature. This thermal expansion must be taken into account when defining the volume of the blank mold cavity, but for the numerical simulations, this variation is not relevant.

In the numerical simulations, the density of the glass is defined with a constant value of 2.5 kg/m^3, which is the most typical value for the density of the soda-lime glasses.

The assumption of a constant value for the glass density will have a minor influence on the predicted results of the glass thicknesses obtained in the containers. In addition, as the mesh of the glass domain will suffer many distortions and will be remeshed many times during the calculation of the numerical simulation, a constant value for the glass density will facilitate the verification of the volume conservation.

2.4 HEAT TRANSFER IN THE CONTAINER FORMING PROCESS

Characterizing the glass properties is an important step since they describe the glass domain in the numerical model. As could be noticed, most of the properties are influenced by the temperature at some point, especially glass viscosity. Therefore, defining the heat transfer, material conductivities and temperatures present in the forming process is a key issue to obtain a better understanding of the thermo-mechanical behavior of the glass and to model the forming process. Heat transfer plays a very important role in the definition of temperatures but this is a complex phenomenon since at the same time the heat transfer also depends on the temperatures. In addition, this thermal phenomenon must be studied directly from the manufacturing conditions in the glass plant.

Heat transfer is divided into three fundamental modes: conduction, convection and radiation. Conduction is the transfer of heat through matter by means of molecular excitement, without bulk motion of the matter. In other words, conduction is the transfer of energy from the more energetic to less energetic particles of a substance due to the interaction between the particles. Convection heat transfer is due to the moving fluid. The fluid can be a gas or a liquid. In convection heat transfer, the heat is moved through the bulk transfer of a fluid with non-uniform temperature. Thermal radiation is generated from the emission of electromagnetic waves that carry the energy away from the emitting body or source. All mater over 0 K emit a certain amount of radiation.

However, a common approach of the thermal problem for the numerical simulations of the blow and blow forming process is to treat the heat transfer not by its modes, but according to where it originates: the heat transfer within the glass and the heat transfer between the glass and the mold.

(A) Heat Transfer within the Glass: Radiation and Conductivity

As will be studied in **Chapter 3**, after the glass is extruded in the gob forming process, small temperature distributions can be defined on the surface of the glass gob. Then, once the gob loads into the blank mold, the heat transfer defined at the glass-mold contact interfaces will result in important temperature gradients in the glass domain. These will define an internal redistribution of the glass temperatures due to conduction. Although glass is a fluid, due to the high values of viscosity, the contribution of convection to the internal heat transfer in the glass during the forming process has not been considered in the numerical simulations. Following the black body approximation, radiation heat transfer is commonly related to heat losses on the surface of a body. But glass is a semi-transparent material and its optical properties vary with wavelength: in the region of 1 to 2.75 μm the glass is highly transparent to infrared; in the region between 2.75 to 4.5 μm its transmission varies with the thickness, and in the region above 4.5 μm glass can be considered opaque to thermal radiation. This variation of the glass transparency with the infrared wavelengths defines then a volumetric emission of transparent radiation within the glass domain. As a result, the emission of thermal radiation comes not only

from the glass surface but also from the deeper layers below the surface. Detailed information explaining how the internal glass radiation is related to the optical properties of glass and the heat transfer mechanisms that can be deduced is found in the literature [6]–[8].

Therefore, the heat flux within the glass domain and to its boundaries can be defined by conduction and radiation components. There are two approaches to treat the contribution of radiation to the total heat transfer depending if the glass sample can be assumed optically thick or not.

The optical thickness is a measure of the ability of a given glass path length to absorb radiation at a defined wavelength. A sample is considered optically thick when the photon mean free path is much smaller than the characteristic length scale of the system, and the radiation process approaches a diffusion process. In that case, the radiation flux can be described by the Fourier equation and the thermal conductivity is replaced by an effective thermal conductivity taking into account the radiative effects. In a physical sense, an optically thick case implies that the attenuation of radiation is so rapid that every element of radiation is directly affected by its neighbors only. On the other hand, an optically thin regime implies that the absorption of photons by the fluid is negligible and radiation emitted by a fluid element will tend to go directly to the surfaces bounding the medium. In this case, to accurately model the radiation exchange that takes place, the spectral discrete ordinates (DO) approach should be implemented.

The discrete ordinates radiation model solves the radiative transfer equation for a finite number of discrete solid angles. Since the glass is not gray (i.e. its emissive power varies with wavelength), the discrete ordinates implementation divides the radiation into several wavelength bands. The radiation transport equation is then integrated over each wavelength band within which the behavior is assumed gray and the total intensity is then summed over the wavelength intervals. The purpose of using the DO model is that it spans the entire range of optical thicknesses and allows for the accurate solution of radiation in semi-transparent media. However, the computational cost associated to solve the radiative transfer equation, together with the already cost-intensive numerical simulations of the container forming process, make this approach currently not feasible.

Thus, the optically thick regime is commonly assumed in mathematical modeling of heat transfer phenomena in the glass forming process. Then, the semitransparent internal radiation of the glass is approximated using an effective conductivity that accounts for the extra amount of heat transferred due to the radiation emitted within the glass in semitransparent wavelengths [9]–[12]. It is true that radiation effects are not negligible and the parison cannot be considered optically thick, but using an effective conductivity compensate for radiative effects during forming. This approximation is valid as the heat flux to the mold that is due to semitransparent radiation is, on average, an order of magnitude less than that which is due to contact conductance [13]. However, the amount of error introduced for the heat transfer in the glass-air interface when the molds are open may be larger (i.e. during the glass reheating before, during and after the parison inversion).

Experimental measurements were performed to obtain the effective thermal conductivity as a function of temperature and thickness [14]–[16], **Figure 5** shows the resulting dependencies. It can be seen that the thickness of the sample plays a relevant role in the definition of the effective thermal conductivity of the sample. This makes sense as the effective thermal

conductivity is including the effects of thermal radiation. Then, the longer the path, the more probabilities of the internal radiation to be absorbed. So, the sample becomes optically thicker. On the other hand, as conductivity is based on the interaction between particles, higher temperatures make the particles more active and the thermal conductivity increases.

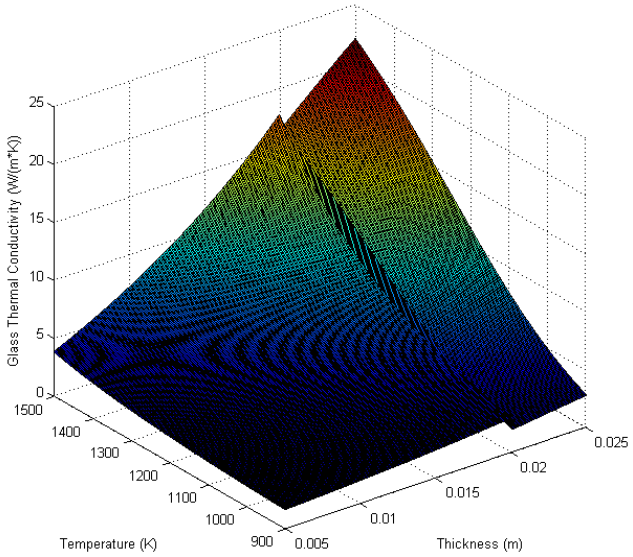

Figure 5. *Effective thermal conductivity including the thermal radiation contribution experimentally determined as a function of the glass thickness and the temperature.*

In the numerical simulations, the effective thermal conductivity approach has been used to define the heat transfer within the glass. An average thickness has been defined for each simulation depending on the glass domain geometry. Then, the effective thermal conductivity is described as a function of temperature, based on the function presented in **Figure 5** [15], [16].

(B) Heat Transfer at the Glass-Mold Interface: Contact Conductance

In the numerical simulations of the blow and blow forming process, the glass domain has two boundary conditions, the glass-air interface and the glass-mold interface. In the glass-air interface, the thermal radiation emitted by the glass contributes to heat losses in the glass domain. However, since most of the time glass is confined inside the mold cavities, this phenomenon is not considered in the numerical model of the container forming process. On the other hand, in the glass-mold contact interface, energy from the hot molten glass is transferred to the cast iron molds, increasing the temperature of the molds and cooling the glass at the same time. The main mode of heat transfer in the boundary conditions in the glass-mold interface is contact conductance. However, between the two materials there is a contact resistance that causes heat transfer to deviate from perfect contact. This resistance is the result of a thin gap of air and combustion products of the lubricant at the glass-mold interface. The thickness of this gas layer initially depends on the surface finish of the mold and varies according to the process conditions: the separation between glass and mold increases due to the thermal contraction of the glass and decreases due to the blowing pressure applied to the glass.

The most complex phenomenon to be measured experimentally under industrial conditions

and, therefore, to be described in the numerical simulations of the blow and blow container forming process is the heat transfer between the glass and the walls of the mold cavity. One of the methodologies to do it is to measure the variation of the mold temperatures next to the surface of the mold cavities, and from there, determine the heat flux between both domains and predict the temperature variation in the glass domain. This can be accomplished using thermocouples with a very rapid response time to measure the rapid increase in the temperature of the metal surface once contacted by the molten glass. The thermocouples are located on the surface of the mold cavity, with the thermocouple junction flush with the surface of the mold cavity [17], [18]. The main drawback of the presented methodology is that thermocouples of these characteristics are very expensive and do not last long due to the harsh conditions present in contact with the molten glass.

Several authors performed experimental studies of these phenomena to characterize the heat flux at the glass-mold contact interface. An extensive amount of work can be found in the literature defining this heat transfer as a function of the glass and mold conditions [11]–[16], [19]–[25]. A comprehensive review of the work performed over the years in this area can be found in the literature [26]. Although these studies have shown that heat transfer may be a function of a multitude of variables, including the operating conditions, temperatures, material properties, pressure, contact time, etc. there is not yet an accurate physical model to predict these phenomena on the glass forming simulations. Until a full understanding is reached, an accepted approach is to define heat transfer with a coefficient. The heat transfer coefficient is usually written as a function of time and adjusted to fit the experimental data.

In the numerical simulations, the heat transfer at the glass-mold contact interface is defined as a function of contact time, specifically using the curve presented in **Figure 6** [27], [28].

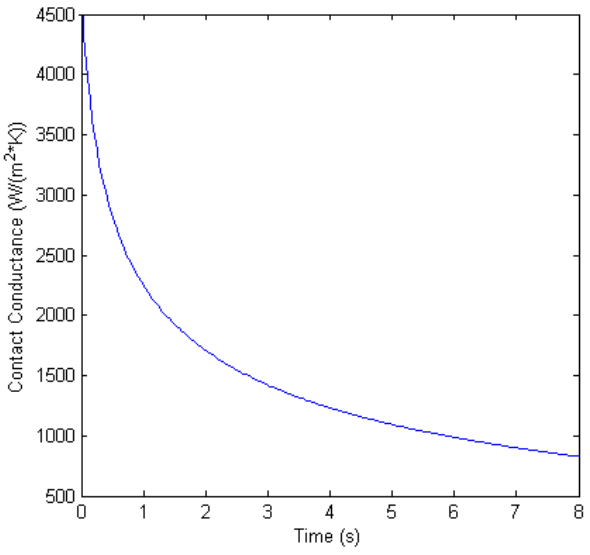

Figure 6. *Heat transfer coefficient at the glass-mold contact interface used in the numerical simulations defined as a function of the contact time.*

2.5 GLASS TEMPERATURE MEASUREMENTS

As previously defined, due to the importance of the glass temperature defining the glass viscosity and its flow, an experimental method is required to measure the glass temperatures and its evolution under manufacturing conditions. As previously presented, machine operators run the IS machine based on empirical knowledge and trial and error. In this sense, a new methodology for Ramon Clemente needs to be defined. Thus, a small review defining different methods to perform temperature measurements is presented in the next section. The purpose of this review is to define the appropriate instrumentation to obtain thermal information related to the heat transfer phenomena occurring during the industrial production of the glass containers. In particular, experimental measurements of the glass temperatures in different stages of the forming process will be performed:

1. Between the orifice ring and the gob distributor, to investigate the temperature evolution during the glass extrusion at the gob forming process.
2. At the end of the delivery equipment, to determine the temperature and velocity of the glass gob at the deflectors exit.
3. During the impact of the glass gobs loaded against a cast iron plate welded to the funnel during the gob drop test, to record the deformation of the molten glass on the plate.
4. After the gob is loaded into the blank mold, to evaluate the temperature of the glass gob as an initial value for the numerical simulations of the gob drop test.
5. At different stages of the blow and blow container forming process, to measure the glass temperatures over time as the container is being manufactured (e.g. gob loading, parison inversion, etc.).

(A) Methods

Different methods can be used to measure glass temperatures in the glass industry. For example, thermocouples and pyrometers are commonly installed in the furnace, working end and forehearth to regulate the glass melting, fining and delivery operations. In fact, temperature measurements provided by these methods are reliable enough to be used as process control setpoints of the aforementioned operations. Therefore, it may seem an easy task to measure glass temperatures, however, it should be noted that in these stages glass conditions are very stable, almost stationary. On the other hand, measuring the temperature of glass in the container forming process is a whole new ballgame. Glass conditions during the forming process are not stationary at all since heat transfer phenomena thermally govern the manufacture of glass containers. This results in strong temperature gradients, very fast cooling rates and a decrease in glass temperatures from 1,200 ºC to around 650 ºC in the few seconds required to form a glass perfume container. In addition, the industrial environment is much more challenging compared to the laboratory conditions required to characterize the previous material properties. Glass manufacturing plants are very hot, loud and dirty and molten glass is corrosive and harsh with everything in contact.

For these reasons, the challenge in measuring glass temperatures in the forming process is not only related to high-temperature values, but rather to the rapid and strong variations of the

property to be measured and the very difficult environment. With all these in mind, an experimental method is required to measure the temperature of glass and its evolution during the industrial production of the containers. Commonly, when considering a particular method and a determined equipment to suit a defined temperature measurement, variables like temperature range, maximum temperature, accuracy, stability, sensitivity, ruggedness, service life, etc. must be considered. Detailed information about these topics can be extensively found in the literature [29], [30]. However, in this case, due to the clear difficulties previously mentioned, the discussion will focus primarily on the type of contact.

Depending on the nature of the contact when performing the temperature measurements of glass, measurement technologies can be divided into two types, invasive and non-invasive methods. Invasive methods require physical thermal contact with the glass. Thermal contact can be achieved through surface adhesion of the sensing probe to the glass surface or by inserting the probe into the glass. On the other hand, non-invasive methods do not require physical thermal contact with glass as the object of interest can be observed remotely, avoiding degradation of the instrumentation in high-temperature or chemically reactive environments.

Contact measurement devices for industrial applications are commonly based on thermocouples due to their range of temperatures, cost, simplicity and robustness. Thermocouples are based on the Seebeck effect, producing an electromotive force in joined dissimilar conductors experiencing a thermal gradient between them. Another great option is resistance temperature detectors (RTD). Although they are more expensive, their temperature measurements are extremely accurate. In this case, the temperature is measured by applying a small current to a platinum wire of known resistance. An alternative to monitoring surface temperatures can be fiber optical probes, as it is possible to channel thermal radiation into a narrow wavelength band via an optical fiber to a wavelength detector. In general, contact measurement devices have fast response times, repeatability and stability, accuracy and wide temperature ranges. The most important disadvantage of these methods in the glass industry is the contact itself, since the gauge may not resist during a prolonged time the corrosive, high-pressure and high-temperature environment of the contact with molten glass. Finally, the use of invasive instrumentation also involves a thermal disturbance, which might be considered for some applications.

In the case of using contact methods to perform glass temperature measurements during the forming process, sensors are commonly installed in the blank and blow molds [17]. In this application, a hole is drilled from the cavity surface through the mold part. The sensing probe, a rapid response thermocouple, is introduced in the previous hole, leaving the sensing end standing out from the cavity surface. Then, the sensing probe is grounded off to match the contour of the mold cavity. With this setup, experimental measurements of the glass temperatures inside the mold cavities can be obtained. The temperatures are measured at the mold surface, therefore, at the glass-mold contact interface. Therefore, these results can be related to the heat flux between both materials [18].

On the other hand, non-contact measurement devices are commonly based on infrared thermography. In this type of sensors, the operation principle is to monitor thermal radiation from emitting sources at different wavelengths in the infrared spectrum. Depending on the field of view of the infrared sensors, these can be divided into pyrometers and thermal cameras. Pyroelectric detectors are manufactured using crystal wafers. A change in the temperature of the

crystal due to the absorption of infrared radiation in a certain period produces a proportional electrical signal. Pyroelectric detectors have a fast response time and good accuracy. However, temperature measurements are restricted to single-point measurements. On the other hand, infrared thermal cameras commonly use bolometers as detectors. Bolometers are thermal detectors in which the incident thermal radiation produces a change in the electrical resistance of the detector. In general, bolometers can be comparatively slower than pyrometers, but infrared thermal cameras offer a full field temperature map that determines the spatial distribution of temperatures.

To conclude, non-contact measurement devices stand out in applications where contact methods are impossible or inaccessible, for example, to measure a moving object or when the source is hot enough that contact devices would not survive. However, infrared thermal cameras are complex and expensive devices as they include an optical system, a detector and a control and analysis system. Therefore, its flexibility and durability must be paid. For single-purpose temperature measurements, thermography might not be a cost-effective solution. Finally, as the thermal radiation depends on the emissivity of the measured source, this value needs to be defined to obtain precise temperature values.

(B) Infrared Thermal Camera

As deduced from the previous review, infrared non-contact measurement devices are probably the easiest and most flexible option to measure glass temperatures throughout the manufacture of a glass container, to define the thermal conditions of the gob, parison and final container using a single device. At the same time, one of the most important advantages of the infrared thermal camera over pyrometers is its enhanced field of view. The working principle is very similar; however, a pyrometer only gives a single temperature value, and sometimes may be difficult to define where the pyrometer is measuring at. On the other hand, using a thermal camera a thermogram or even a thermal recording is obtained, resulting in much more information available of the glass and its surroundings.

Once convinced of the infrared thermal camera capabilities, other variables must be taken into account according to the specific application as the temperature range, accuracy, response time, stability or sensitivity. There is a wide variety of brands and specifications in the market. After testing some distributors, a FLIR A325sc infrared thermal camera has been chosen to carry out infrared temperature measurements of the glass surface in the forming process. Its infrared detector is an uncooled microbolometer with a spectral range from 7.5 to 13 μm. This IR camera has two thermal calibrations to measure temperatures in different ranges: from 0 to 500 ºC (low-temperature calibration) and from 300 to 2,000 ºC (high-temperature calibration). The data acquisition frequency of the sensor is 60 Hz, so a frame is recorded every 1/60 s or 16.67 ms. Detailed specifications are defined in the product datasheet of the manufacturer [31].

A detailed description of the working principle of an infrared thermal camera is presented. An infrared thermal camera takes digital pictures or videos that display thermal information. This thermal information is related to the amount of electromagnetic radiation emitted by the bodies present in a shot at a certain instant of time. A microbolometer is used as an infrared thermal detector, which is sensitive to the infrared radiation that comes from the shot, through

the camera lenses. Once the radiation is absorbed by the detector, it heats up and changes its electrical resistance. This change in the sensor properties leads to an electrical signal, which after being amplified and digitally processed will be proportional to the amount of radiation absorbed by the infrared sensor. This process is repeated again and again every 60 Hz to obtain each of the frames composing an infrared recording. Then, the amount of absorbed radiation in each of the pixels is represented with different colors depending on the thermal palette used.

It is important to take account that the radiation detected by the IR sensor comes from the shot, but there may be different sources: the different bodies present in the shot emit thermal radiation, but radiation may also be reflected on the surface of these bodies and the air in between the bodies and the camera emits radiation too. The software of the camera can compensate for the air radiation based on the distance between the body and the camera. And reflections are minimal when the camera is positioned normal to the surface of the measured body. But even then, thermograms should be analyzed carefully, as reflections on the body surface should not be mistaken with the results of the emitted radiation measurements.

Finally, a small example showing the potential of the wide field of view of the infrared thermal cameras is presented. Playing with different calibrations and thermal palettes, very powerful thermal information of the gob forming process can be obtained. The presented details would probably remain unnoticed using other methods.

Figure 7 shows two shots taken at the same instant of time using the two thermal calibrations and displaying the results with different thermal palettes. In **Figure 7A** a shot with a low-temperature (LT) calibration and a palette from 25 to 500 ºC is presented. Here, the layout of the gob forming process can be identified, including the orifice ring, the shear blades, the graphite tube and spray nozzles of the shear lubricant. On the other hand, **Figure 7B** shows the same shot taken with a high-temperature (HT) calibration and displayed with a palette from 250 to 1,200 ºC. As can be observed, shots using the LC calibration help to locate the different elements of the layout and the HT calibration together with thermal palettes in a range from 700 ºC up to 1,200 ºC are commonly used to define the glass geometry (see **Figure 7C**).

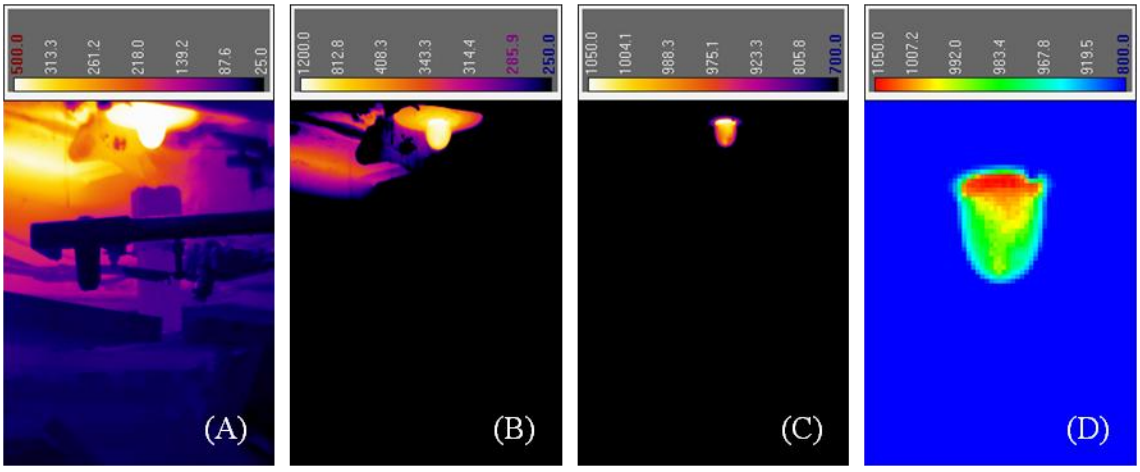

Figure 7. *Same infrared thermogram taken with two thermal calibrations and displayed using different palettes. (**A**) shows a LT calibration and a palette range from 25 to 500 ºC. (**B**) shows a HT calibration and a palette range from 250 to 1,200 ºC. (**C**) shows a HT calibration and a palette range from 700 to 1,200 ºC. (**D**) shows a HT calibration and a high contrast*

palette with a range from 800 to 1,050 ºC and a 2x zoom.

In addition to the calibrations, high contrast thermal palettes highlight important details on the glass surface. In **Figure 7D**, a highly contrasted thermal palette reveals two different thermal zones in the extruded glass during the gob forming process. The red-orange ellipse observed at the top of the glass geometry is defined as the orifice ring area. Temperature readings of the orifice ring area are between 1,005 and 1,045 ºC and the mean value is 1,022 ºC. The yellow-green shape under the red-orange ellipse is defined as the extruded gob area. Temperature readings of the extruded gob area are between 960 and 1,000 ºC and the mean value is 983 ºC.

Therefore, a clear temperature drop can be measured between the top of the glass gob, right below the hole of the orifice ring, where there is the most freshly extruded glass; and the rest of the glass gob, which has been previously extruded and remains hanging out the feeder and the orifice ring until it is cut by the shear blades. This will be a recurrent phenomenon in all the infrared measurements performed on the gob forming process. For this reason, the temperature evolution of the surface of the glass gob will be evaluated separately for the two defined areas, stated henceforth as Box1 and Box2.

(C) Emissivity

The infrared camera sensor measures the intensity of the thermal radiation coming from a body, but one wants to determine the temperature of that body. The emissivity (ε) defines the relationship between the amount of thermal radiation emitted by the body and its temperature. The emissivity depends on the material, surface quality of the body, temperature or even wavelength. Emissivity can be defined theoretically based on the optical properties of the material or can be defined experimentally: measuring simultaneously the temperature with a contact probe (i.e. a thermocouple) to obtain the temperature of the body and then, with the infrared thermal camera, adjust the emissivity to obtain the same temperature reading.

Several emissivity values can be found in the literature. For instance, an emissivity value of 0.91 was defined by Gardon [7] for glass sheets at high temperatures and opaque wavelengths. From the experimental study published by McMahon [6], where the emissivity, reflectivity and transmissivity were determined for different glass compositions, much information can be obtained about the optical properties of the glasses. **Figure 8** shows the values of these three optical properties measured from a sample of flint container glass, which was 3.175 mm (1/8 inches) thick at 537.8 ºC (1,000 ºF). It can be seen how the optical properties vary with the wavelength, but generally do not vary markedly with temperature [6], [21].

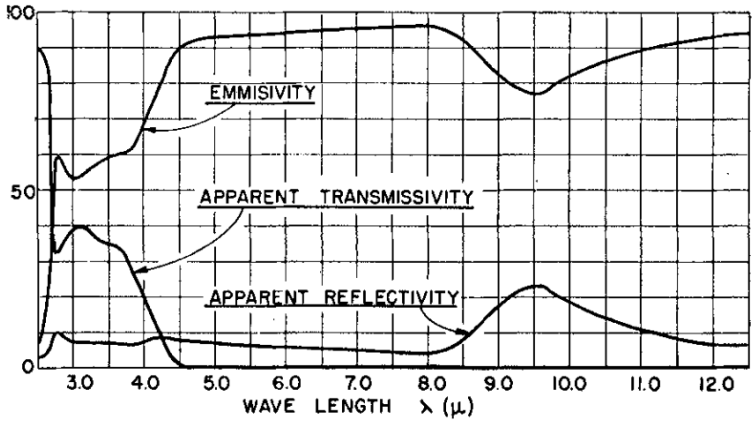

Figure 8. *Emissivity, reflectivity, and transmissivity measured from a sample of flint container glass, which was 3.175 mm (1/8 inches) thick at 537.8 ºC (1,000 ºF) [6].*

Previously in **Chapter 2**, it was stated that as glass behaves as a semi-transparent material, the emission of thermal radiation is a volumetric phenomenon. However, **Figure 8** shows that at wavelengths beyond 4.5 μm, the transmissivity of soda-lime glasses tends to 0. Therefore, for practical purposes, when measuring the temperature with an IR thermal sensor in the wavelength range from 7.5 to 13 μm, soda-lime glasses can be considered as an opaque material. Thus, only thermal radiation emitted from the glass surface will be detected by the infrared thermal camera. On the other hand, although flint glasses are opaque in the wavelength range of interest and its emissivity is pretty high, one must be careful with the metallic reflection band near the 9.5 μm [6], where reflectivity rises to values near 0.23 and, therefore, emissivity is reduced to 0.77. The area defined by the emissivity curve in **Figure 8** has been integrated between the wavelength range from 7.5 to 13 μm, obtaining a total emissivity of 0.89 from that sample of flint container glass.

In addition to that, the air has a high transmissivity in the infrared region from 8 to 15 μm or also called the long-wavelength infrared region (LWIR). So it can be considered almost transparent and its contribution to the measured radiation at these wavelengths will be very small.

In this thesis, all the measurements with the infrared thermal camera have been recorded assuming a default value of 0.95 for the glass emissivity, without any particular adjustment to the specific conditions of each measurement. Therefore, the temperature values obtained in the infrared measurements can deviate from the actual glass temperatures. However, the temperature setpoint of the last forehearth section is specified as a reference temperature in each case. In any case, when processing the IR measurements, different emissivity values can be defined to adjust the measured temperatures if necessary. The software of the infrared thermal camera uses an almost linear function to adjust the measured temperatures as a function of the emissivity of the body. When the temperature values using a reference emissivity of 0.95 are compared with an emissivity of 0.91, the maximum deviation introduced would be around 3% taking as a reference a temperature value of 1,050 ºC; or around 5% using an emissivity of 0.891.

2.6 CONCLUDING REMARKS

One of the main concerns of glass manufacturers is to produce perfume containers with the desired quality and glass thickness distribution, reducing the number of defects and rejected bottles to increase the rate of produced containers and maximize the throughput. This can be achieved with the proper definition of the mold cavities and the operation of the IS machine during the development and manufacturing tests of a new container. The design of the mold cavity is a key issue for the development of each new container and its mold equipment as it defines the thickness distribution of the manufactured containers. In spite of that, the design of the mold cavities is still based on trial and error and empirical knowledge. Furthermore, glass forming is a complex process, as the glass conditions, the mold equipment and the many sequential operations of the IS machine are completely interrelated, defining the heat transfer, temperature and viscosity of the glass inside the molds. For these reasons, several iterations may be required until the final design is obtained. These manufacturing tests, although being extremely useful, are expensive, increase the time to market and involve huge downtimes in the production line.

Therefore, a numerical model of the blow and blow forming process will be very helpful to improve the development of glass perfume containers. The numerical simulations will predict the glass thickness distribution obtained in the manufactured containers, in the same way that is currently done with production tests on the IS machine but using a virtual environment. Nevertheless, the complexity of the industrial glassmaking process makes this proposal a very ambitious goal. For this reason, in this initial chapter, the glass forming process has been studied in depth to define a framework. First, the operation of the industrial process to manufacture glass perfume containers has been extensively detailed. Afterward, the material properties, thermal phenomena and glass temperatures present during the forming process were defined. Difficulties to measure and define these parameters and phenomena under industrial manufacturing conditions were presented, therefore, different approaches were used to describe each of them in the numerical model. The gathered information defines a framework to model the blow and blow forming process. This will be very useful to overcome the many and different difficulties that will be encountered throughout the realization of this thesis.

In this chapter, a detailed description of the industrial manufacture of glass perfume containers has been presented. In addition to the several operations performed by the IS machine during the blow and blow container forming process, previous stages as the glass melt delivery and the gob forming process, delivery and loading operations have also been defined. Special attention was paid to the evolution of the glass conditions throughout the process.

Once the operation of the industrial process was defined, the most relevant material properties were determined to describe the glass domain in the numerical model. Glass viscosity is the most important property in glassmaking due to its strong dependence on the temperature and chemical composition of glass. For this reason, the viscosity of Ramon Clemente's glass was characterized in an external laboratory. Other glass properties were also defined, as the specific heat, density and thermal expansion coefficient. In contrast to the material properties, glass thermal conditions in the forming process (i.e. glass temperatures and heat transfer within the glass and to the boundaries) need to be defined under industrial manufacturing conditions.

This fact makes it complex not only the acquisition of experimental values but also the proper description and understanding of the heat transfer phenomena and the validation of the predicted temperatures by the numerical simulations. Thus, the effective thermal conductivity and the contact conductance approximations will be used to model the heat transfer phenomena in the simulations of the blow and blow forming process.

Finally, a study of the existing methods to measure the glass temperatures was performed. Temperature, pressure and corrosive conditions inside the mold cavities and next to the glass surface result in a very harsh environment. From this review, it can be concluded that, in addition to its durability, non-contact measurement devices perform measurements in many different situations. The field of view of the infrared thermal cameras and its flexibility allows recording much thermal information of the forming process. For these reasons, an infrared thermal camera FLIR A325sc will be used to carry out temperature measurements by measuring the infrared radiation emitted by the glass surface. This methodology will be applied to study the glass temperatures and thermal phenomena in several operations of the forming process.

In the next chapter, experimental measurements of the glass temperatures will be performed using an infrared thermal camera. These thermal measurements will be performed on the gob surface at different stages previous to the container forming process. It will allow the definition of additional thermal phenomena present in the glass gobs and to determine the initial conditions of the glass gobs in the container forming process. Later on, in **Chapter 4**, the framework presented in this initial chapter will be used as the foundation of the numerical model, implemented to describe and predict in a virtual environment the glass conditions during the container forming process.

2.7 REFERENCES

[1] L. D. Pye, A. Montenero, and I. Joseph, *Properties of Glass-Forming Melts*. Boca Ratón, FL, USA: CRC Press, 2005.

[2] M. R. Hyre and K. Paul, "The Effect of Shear Angle on Gob Formation," *Conf. Glas. Probl.*, pp. 87–107, 2000.

[3] O. O. Den Camp, D. Hegen, G. Haagh, and M. Limpens, "TV Panel Production : Simulation of the Forming Process," in *Conference on Glass Problems*, 2003, vol. 24, no. 1, pp. 1–19.

[4] A. Fluegel, "Glass viscosity calculation based on a global statistical modelling approach," *Glas. Technol. - Eur. J. Glas. Sci. Technol. Part A*, vol. 48, no. 1, pp. 13–30, 2007.

[5] G. S. Fulcher, "Analysis of Recent Measurements of the Viscosity of Glasses," *J. Am. Ceram. Soc.*, vol. 8, no. 6, pp. 339–355, 1925.

[6] H. O. McMahon, "Thermal Radiation Characteristics of Some Glasses," *J. Am. Ceram. Soc.*, vol. 34, no. 3, pp. 91–96, 1951.

[7] R. Gardon, "The Emissivity of Transparent Materials," *J. Am. Ceram. Soc.*, vol. 39, no. 8, pp. 278–287, 1956.

[8] I. H. Farag, M. J. Beliveau, and R. L. Curran, "Heat Transfer During Glass Forming," *Chem. Eng. Commun.*, vol. 52, pp. 21–32, 1987.

[9] H. Rawson, "Physics of glass manufacturing processes," *Phys. in Technol.*, vol. 91, no. 5(2), pp. 91–114, 1974.

[10] K. C. Granger and R. Gardon, "Interaction of Radiation and Conduction in Glass," *J. Am. Ceram. Soc.*, vol. 52, no. 10, pp. 548–553, 1969.

[11] W. Trier, "Temperature Distribution and Heat Flow in Glass in Blank Molds of Container Machines," *J. Am. Ceram. Soc.*, vol. 44, no. 7, pp. 339–345, 1961.

[12] J. Manthuruthil, T. R. Sikri, and G. A. Simmons, "Simplified Mathematical Model Simulating Heat Transfer in Glass-Forming Molds," *J. Am. Ceram. Soc.*, vol. 57, no. 8, pp. 345–350, 1974.

[13] K. Storck, M. Karlsson, and D. Loyd, "Analysis of the blank mould - a transient heat transfer problem in glass forming," *Trans. Eng. Sci.*, vol. 5, pp. 175–182, 1994.

[14] M. R. Hyre, "Numerical Simulation of Glass Forming and Conditioning," *J. Am. Ceram. Soc.*, vol. 85, no. 5, pp. 1047–1056, 2002.

[15] M. R. Hyre, "Effect of Mold to Glass Heat Transfer on Glass Container Forming," in *Advances in Fusion and Processing of Glass III*, 2004, pp. 271–279.

[16] M. R. Hyre and B. L. Underwood, "Experimental Measurement of Glass to Mold Heat Transfer for Computational Modeling of Container Production," in *ASME International Mechanical Engineering Congress and Exposition*, 2004, pp. 319–324.

[17] D. M. Shetterly and N. T. Huff, "Mold Surface Temperatures During Glass Container Forming," *J. Non. Cryst. Solids*, vol. 38–39, pp. 867–872, 1980.

[18] N. T. Huff, D. M. Shetterly, and L. C. Hibbits, "Glass to Metal Heat Flow During Glass Container Forming," *J. Non. Cryst. Solids*, vol. 38–39, pp. 873–878, 1980.

[19] C. J. Fellows and F. Shaw, "A Laboratory Investigation of Glass to Mould Heat Transfer During Pressing," *Glas. Technol.*, vol. 19, pp. 4–9, 1978.

[20] R. Kent, "Mould Temperature and Heat Flux Measurements and the Control of Heat Transfer During the Production of Glass Containers," *IEEE Trans. Ind. Appl.*, vol. IA-12, no. 4, pp. 432–439, 1976.

[21] D. A. McGraw, "Transfer of Heat in Glass During Forming," *J. Am. Ceram. Soc.*, vol.

44, no. 7, pp. 353–363, 1961.

[22] S. K. Pchelyakov and Y. A. Guloyan, “Heat Transfer at the Glass-Mold Interface,” *Steko i Keramika*, no. 9, pp. 14–15, 1985.

[23] P. Moreau, J. M. A. César de Sá, S. Grégoire, and D. Lochegnies, “Integration of Heat Transfer Coefficient in Glass Forming Modeling With Special Interface Element,” *AIP Conf. Proc.*, vol. 908, pp. 750–764, 2007.

[24] S. Grégoire, J. M. A. César de Sá, P. Moreau, and D. Lochegnies, “Modelling of heat transfer at glass/mould interface in press and blow forming processes,” *Comput. Struct.*, vol. 85, pp. 1194–1205, 2007.

[25] P. Moreau, D. Lochegnies, S. Grégoire, and J. M. A. César de Sá, “Analysis of lubrication in glass blowing: Heat transfer measurements and impact on forming,” *Glas. Technol.*, no. February, 2008.

[26] M. Brown, “Computer simulation of the glass pressing process: A review,” *Int. J. Mater. Prod. Technol.*, vol. 33, no. 4, pp. 335–348, 2008.

[27] M. R. Hyre, “Container forming modeling: Sensitivity to boundary conditions, material properties, and underlying physics modelling,” in *Seminar presented at the “Jornada sobre Simulación en Procesos de Fabricación de Vidrio” at IQS, Barcelona, Spain.*, 2017.

[28] A. Biosca, S. Borrós, V. Pedret, M. R. Hyre, and A.-A. García Granada, “Numerical and experimental study of blow and blow for perfume bottles to predict glass thickness and blank mold influence,” *Int. J. Appl. Glas. Sci.*, vol. 10, no. 4, pp. 1–15, 2019.

[29] P. R. N. Childs, J. R. Greenwood, and C. A. Long, “Review of temperature measurement,” *Rev. Sci. Instrum.*, vol. 71, no. 8, pp. 2959–2978, 2000.

[30] D. Ross-Pinnock and P. G. Maropoulos, “Review of industrial temperature measurement technologies and research priorities for the thermal characterisation of the factories of the future,” *Proc. Inst. Mech. Eng. Part B J. Eng. Manuf.*, vol. 230, no. 5, pp. 793–806, 2016.

[31] “FLIR A325sc Datasheet,” in *FLIR Product Catalog 2018*, 2018, pp. 71–73.

CHAPTER 3
EXPERIMENTAL ANALYSES OF THE GLASS AT THE GOB FORMING, DELIVERY AND LOADING OPERATIONS

3.1 INTRODUCTION

Although the blow and blow forming process is the most relevant stage when defining the produced glass perfume bottles, it is important to realize that the container forming is only the last stage of the glass manufacturing operation. As explained in **Chapter 2**, the raw materials and cullet are melted and converted into molten glass in the furnace. Then, the molten glass is refined, conditioned and delivered through the forehearth to the different IS machines. At the end of this process, molten glass is obtained at the desired viscosity (and ideally at a uniform chemical composition and temperature). Finally, the flow of molten glass is converted into discrete glass gobs in the feeder during the gob forming process and then distributed to each of the individual sections of the IS machine. It is not until the glass gobs are loaded into the blank mold when the container forming process really starts. The result of all these previous stages determines the initial conditions of the glass gob at the start of the container forming process inside the blank mold. Thus, despite the efforts made during glass conditioning to achieve a homogeneous temperature distribution of the glass melt at the end of the feeder; the operation of the spout, rotating tube and feeder plunger will produce thermal distortions to the glass flow resulting in temperature distributions within the formed glass gobs. Moreover, the glass gobs will also suffer heat losses during their delivery through the loading equipment to the blank molds.

It is common knowledge in the glass manufacturing industry that the feeder and delivery equipment operations affect the homogeneity of the glass temperatures, resulting in thermal distributions within the gob. Moreover, as stated earlier in **Chapter 2**, temperature variations in glass have a strong influence on the glass viscosity and its flow. Nevertheless, only a few

authors have studied these stages previous to the glass container manufacturing process compared to the amount of literature dealing with the container forming process itself. Most of the time, those effects on the initial glass temperature distributions, which can be observed under industrial conditions, are not considered as initial conditions in the numerical simulations of the container forming process. One of the few examples in literature that study the gob forming process is a series of publications from HVG (Research Association of the German Glass Industry). There, experimental measurements were conducted to study the temperature distribution of the glass gobs. In these publications, explanations defining the causes of the temperature distributions were also presented to allow understanding the physical and thermal phenomena during the gob forming process.

Temperatures near the surface of amber glass gobs were measured after being cut. Axial and radial temperature distributions were determined with a pyrometer mounted in a rotating device below the shear blades [1]. Infrared measurements were performed using a pyrometer with a fixed wavelength of 3.9 μm. For the studied amber glass, the measured temperatures could be assigned to a penetration depth between 2 and 5 mm. There was a small axial temperature distribution from the top to the bottom of the gob due to radiative heat losses during the glass gob extrusion. Radial temperature variations were measured related to non-homogeneities of the molten glass inside the feeder. It was also defined that: article changes require a different pull rate and orifice ring diameter, substantially modifying the glass flow and gob temperatures; and small variations in the temperature setpoints of the delivery channels have a huge impact in the gob length due to the strong dependence of the glass viscosity.

Later on, a second measuring point was added after the deflectors to study the influence of the thermal contact with the delivery system. Moreover, pyrometers with different wavelengths were used to measure the glass gob temperatures at different depths [2]. Three pyrometers were used with wavelengths of 1.46 μm, 3.9 μm and 5.14 μm. As glass is a semi-transparent material, the visibility depth is the reciprocal of the absorption coefficient. Which for the studied amber glass was 4 mm at 1.46 μm and 2.5 mm at 3.9 μm. The 5.14 μm measurements referred to the temperature on the glass surface. The gob temperature distributions obtained at different depths showed lower radial variations. However, there was a temperature gradient from the inside of the glass gob to the surface even just after the cutting. This was too large to be explained only by radiation losses, it had to come from heat losses inside the feeder in contact with the refractory walls. Temperature measurements of the glass gob after the deflector showed heat losses by radiation and contact with the delivery equipment over all IS machine sections. It could also be noted how surface temperatures were especially influenced by the trough lengths.

Finally, the previously presented thermal data of the glass gob from the different measurements with the addition of a 9 point grid thermal distribution at the end of the forehearth were introduced into a numerical model [3]. The goal was to predict the temperature distribution of the glass gob at any point in the delivery system, although only partial results were obtained.

As presented, relevant results about temperature distributions in the gobs can be obtained solely from experimental measurements of the glass temperature under manufacturing conditions. On the other hand, together with experimental measurements, several authors went one step beyond, developing different numerical models to gain a better understanding of the underlying physics and thermal phenomena of glass during gob forming. In the following cases, the thermal conditions of the glass flow at the end of the delivery channel, feeder and spout, were modeled based on experimental measurements. Then, numerical simulations of the gob

forming process were performed defining the geometry of the gobs and the thermal properties of the extruded glass. These results were later used to define the initial conditions of the glass in the simulations of the forming process, that is, the container and TV panel manufacturing operations, respectively. The most relevant numerical and experimental publications about the gob forming process are presented.

Numerical simulations to study the flow and thermal conditions of molten glass in a double gob feeder using Fluent/UNS numerical code were carried out by Emhart. Numerical results determined that gob weight differences between inner and outer gobs in a double gob feeder were related to different temperature and viscosity profiles in the gobs as a result of different glass pathlines and residence times inside the feeder [4]. A new spout design was developed to reduce gob properties variation and increase gob weight consistency and thermal uniformity [5]. The temperature profiles obtained in the feeder using Fluent/UNS were also used to initialize the temperature field in a gob forming numerical model using Polyflow [6]. The previous results of the gob forming model were used as initial values of the gob thermal condition for simulations of the gob loading into the blank mold. The influence that the inner and outer gob variations had at the end of the container forming process was presented in [7], showing the effects during the parison inversion and in the final thickness distribution of the container. Outer gobs were hotter, resulting in a container with more glass distributed at the bottom, due to lower viscosity and more glass flowing down to the bottom of the parison during the stretching. Finally, a fully integrated simulation approach for the container glass forming process was presented in [8], where several numerical models defining the complete process (i.e. glass melting, delivery and forming) were reviewed. With this approach, the effects of each step of the process can be used for the subsequent steps to control the final thickness distribution of the manufactured bottles.

TNO (Netherlands Organization for Applied Scientific Research) also carried out simulations of the complete TV panel forming process [9]. Simulations included the feeder operation and the gob forming process as initial stages to provide reliable data for the pressing model. The initial temperature input from the feeder model was measured with a 9 position grid of thermocouples. The flow and thermal evolution of glass at the spout were calculated, using a rotating and vertically striking gobber to push the glass through the orifice ring. As glass in this stage cannot be considered optically thick, a fast heat radiation model for the glass domain was implemented. Overlapping meshes and concentration methods were used to avoid time-consuming remeshing techniques. The shape, weight and 3D temperature distribution of the formed gobs as a function of time were obtained as a result. To validate the full model of TV glass pressing averaged temperature simulation results over a cycle were compared with experimental measurements using infrared thermal cameras and optical pyrometers. The computed and measured weights of the glass gob were also compared.

As presented, very powerful results can be obtained from a reliable numerical model of the complete glass manufacturing process. However, to implement this type of numerical tools, many properties, parameters and conditions of the industrial process are required. Most of the time, this will imply conducting complex, expensive and time consuming experimental measurements under manufacturing conditions. In addition, when a model grows in size, it also becomes more complex, due to the interrelation of subsequent operations. Therefore, due to the huge amount of work required, trying to integrate all the stages may be a very ambitious challenge. Therefore, many authors also followed a simpler approach, studying operations

individually, isolated from the rest of the manufacturing process, rather than dealing with the complete process. Small numerical and experimental studies can be conducted to gain a better understanding of the relationships between different material properties and process variables [10], [11]. In very complex processes, as glass manufacturing, this simpler approach can provide guidance to improve the performance of the model or to solve manufacturing problems related only to that forming operation.

For these reasons, while performing an in-depth investigation to model the thermo-mechanical behavior of glass in the container forming process to determine how the mold cavities and the conditions of the IS machine operation define the thickness distribution of the manufactured glass containers, due to the high sensitivity of the thermal conditions to the glass flow, this final stage cannot be isolated from the previous stages. Therefore, it seems wise to consider how ideal the previous stages are: defining how the gob forming operation influences temperature distributions present in the glass gobs. In this sense, as explained in **Chapter 2**, the versatility of an infrared thermal camera and its capability to perform non-contact temperature measurements allow obtaining thermal information of the glass in many stages of the manufacturing process. Thus, the use of an IR camera is not only restricted to the container forming process. Therefore, the methodology presented in **Chapter 2** will be applied in this chapter, using an infrared thermal camera to perform non-contact temperature measurements on the glass surface. In particular, in the first part of this chapter, an analysis of the temperature distributions within the glass gob will be performed under different industrial conditions to gain a better understanding of the thermal phenomena that occur during the gob forming process.

So far, variations in the glass melt temperature and viscosity at the forehearth and feeder stages have been presented. These may cause deviations in the temperature distribution and weight of the formed gobs. On the other hand, once the molten glass is converted into discrete glass gobs in the feeder, gobs must be delivered and loaded through the delivery equipment into the blank mold. During these stages, even more distortions occur to the glass gob until the container forming process starts. In this sense, a non-optimal glass gob delivery results also in higher heat losses as the gob has more friction and less velocity. If the loading is not vertical and centered into the blank mold, the glass gob may bend or induce hot spots due to the repeated dragging at the sides of the blank mold cavity. All these deviations have an impact on the quality of the manufactured containers causing container defects, poor wall thickness distribution and variations in the temperature of the mold cavities.

Moreover, to maximize the production rate of the IS machines, the number of sections and mold cavities per section has been increasing over the years. The largest IS machine configurations can have up to 10 or 12 individual sections and one to three or even four mold cavities per section. At the delivery equipment, the glass gob in contact with the scoop and the deflector is horizontally accelerated and decelerated to obtain a vertical load into the blank mold. Gob issues related to friction with the delivery equipment became more relevant for the larger machine configurations where there are more sections and gobs need to travel longer horizontal distances. As the conditions of the glass gob may show some differences as a function of the individual section where are loaded, the quality of the produced containers can be affected by these deviations, obtaining variability in the properties of the containers throughout the production. Deviations in the glass temperature and viscosity defined during the gob forming process also become even more evident when working with multiple gobs at the feeder. In the early nineties, an experimental study [12] indicated how container quality

deviations could be reduced modifying the orifice rings alienation in double gob feeders.

Therefore, as many deviations obtained at the delivery and loading operations cannot be later corrected in the container manufacture and result in container defects, for many years authors have shown their interest in gaining a better understanding of the underlying physics and thermal phenomena of the gob delivery operation. Continuing with the previously presented approach of studying single and isolated stages of the glass forming process, numerical and experimental studies have also been helpful for, once the difficulties present in that step have been understood, improving its operation. For instance, the optimization of the design of the delivery equipment resulted in an improvement of the gob loading conditions.

In this sense, misalignment among the delivery components and the impact of the glass gob transitioning between components introduce variations in velocity, length and arrival time of the gobs when loaded into the blank mold that results in a final bottle quality inconsistency. The length and velocity of the gobs were monitored using fiber optic light sensors mounted at the shear blades, scoop entry, trough entry, trough exit and deflector exit [13]. The measured experimental data of the gob was used to gain insight into these problems, and be addressed at their root cause, redesigning and improving the delivery components to deliver a better glass gob to the blank molds.

On the other hand, deflector trajectories were optimized to reduce friction and improve the gob delivery in large IS machines where gobs need to travel longer horizontal distances (e.g. IS machines with 10 or 12 sections) [14]. New deflectors with optimized curvatures were developed and experimentally tested to reduce the variation of the gob velocity between the different IS machine sections. The reduction of friction on the deflectors was demonstrated by measuring the gob velocities with a high-speed camera. Recently, a new deflector's design [15] based on a very similar idea was released by Emhart in conjunction with the new constant cone delivery equipment [16] to enhance the gob loading.

As presented, the quality of the delivered glass gobs and consistent blank mold temperatures has been a major concern for the container manufacturing industry. Traditionally, glass manufacturers have relied on the operators experience to set up job changes and control productions. Many adjustments are needed during production to ensure that the gob maintains a uniform temperature and shape, and also that it is loaded vertically and centered inside the blank mold cavities. IS machines need very fine adjustments to control thermal issues to obtain optimal parisons and produce consistent containers. Nevertheless, manual adjustments are done by trial and error and depend upon the operator skills. So, in recent years, the need for glass manufacturers to have more reliable control of the production process gave room to reduce human intervention. Thus, new industrial applications have been commercially available based on the treatment of experimental data to automatically adjust process parameters related to the gob.

XPAR has developed an application to detect defects on the glass gobs related to the delivery equipment [17]. A high-speed camera monitors the velocity, shape and position of the loaded gobs into the blank molds of each individual section to maintain an optimal gob loading.

Tiama has implemented a gob weight control system [18] using an infrared thermal camera under the shear blades to monitor the gob during production. The gob temperature and shape are monitored to define its volume and a closed-loop controls the feeder parameters to obtain consistent glass gob weights.

Emhart also has developed a temperature control system of the mold equipment on the blank side [19] and a gob monitoring system that measures the loading conditions of the glass gobs

during production [20]. Either both systems can be used as a source of information to help the machine operator to control the production or as an automatic closed-loop control [21], where the blank mold cooling system adjusts the cooling time for each section of the IS machine to maintain the blank mold temperatures within a defined temperature range over time.

Although the concerns by many authors and companies to reduce defects in the loading and delivery operations, to produce glass perfume containers Ramon Clemente currently works only with single gob IS machines with 4 and 6 individual sections, so deviations and defects produced during the gob delivery and loading operations are not expected to be as relevant as in the case of larger machine configurations. However, due to the unusual amount of experimental measurements of the velocity [10], [13], [14], [21], [22] and temperature [1], [2] of the glass gobs at the delivery equipment that were published in the past, it seemed interesting to carry out the same measurements in a small IS machine and see how they relate to the results published in larger machine configurations. Therefore, in the second part of this chapter, an experimental study during the delivery and loading operations will also be carried out: infrared measurements of the temperature, velocity and geometry of the glass gobs will be performed to define the loading conditions of the glass gobs. This study will define the influence of the delivery equipment and variations in the loading conditions of the glass gob as a function of the loaded section of the IS machine. At the same time, by measuring the loading conditions of the glass gob, the initial conditions of the glass at the start of the blow and blow container forming process will be defined.

To summarize, different approaches followed in the past to study several topics related to glass conditions and the production process have been presented, including also a few examples of the most recent advances applied in the industry. These so ambitious but useful improvements would not have been possible without the knowledge previously acquired by conducting experimental and numerical analysis on the gob forming, delivery and loading operations. In this sense, a new methodology for Ramon Clemente will be used in this chapter**.** Experimental measurements of the glass gob with an infrared thermal camera will be carried out to define the temperature distributions, thermal phenomena and loading conditions of the glass gobs. Knowledge about the glass gob conditions will be improved, while very useful experience in non-contact thermal radiation measurements will also be acquired. This is a necessary step to later achieve more ambitious goals, such as modeling the thermo-mechanical behavior of glass in **Chapter 4**.

In this sense, as glass viscosity has a strong dependency on temperature, the resulting temperature distributions and conditions of the glass gobs when loaded into the blank mold, may impact the properties of the manufactured containers by the blow and blow forming process. Therefore, the main objective of this chapter is to **carry out experimental analyses to define the conditions of the glass gobs under manufacturing conditions.** This includes **performing infrared measurements of the glass gobs during the operations of gob forming, delivery and loading.** The thermal information gathered in this chapter related to the glass gobs will be used later in the numerical simulations. Infrared measurements are required to define the initial temperature conditions in the glass domain and to validate the predicted results.

To achieve this objective, the following tasks were proposed:

- Perform temperature measurements on the surface of the glass gobs during the gob

forming, delivery and loading processes using an infrared thermal camera.

- Conduct a thermal analysis during the gob forming to define the resulting temperature distributions in the glass gob and the thermal phenomena related to them.

- Study the variations of the glass gob properties at the delivery and loading stages as a function of the position of the individual sections.

- Evaluate the influence of the previous results when used as initial conditions in the numerical simulations of the container forming process.

3.2 METHODOLOGY

The methodology presented in **Chapter 2** was applied to obtain thermal information of the glass in different stages of the forming process. In particular, a FLIR A325sc infrared thermal camera was used to measure experimental temperatures on the surface of the glass gobs at several stages of the following operations:

1. Between the orifice ring and the gob distributor, to investigate the temperature evolution during the glass extrusion at the gob forming process.
2. At the end of the delivery equipment, to determine the temperature and velocity of the glass gob at the deflectors exit.

In the first part of this chapter, temperatures of the glass gobs were measured to investigate temperature distributions and their evolution at the gob forming process. A thermal analysis was performed as the glass flow extruded through the orifice ring and until the gob was cut. The orifice ring is at a distance of about 4 meters above the ground. On top of the IS machine, there is a small platform at the height of a first floor to have access to the orifice ring, shear blades mechanism and gob distributor. Temperature measurements with the infrared thermal camera of the gob forming process were taken from that platform. Infrared thermal measurements describe the glass gob as it is extruded through the orifice ring. Under the spout and right below the orifice ring, there is the shear plane where two shear blades met to cut the glass and form the gob. After being cut, the glass gob accelerates in free fall, passing through a graphite guide to the gob distributor and then being delivered to the corresponding IS machine. The gob acceleration results in blurred shots and incorrect temperature readings due to the limitations of the uncooled microbolometer. The graphite guide is used to correct the verticality of the free-falling glass gobs and obtain a reliable gob loading into the scoop of the gob distributor.

In the second part of this chapter, delivery times, velocity, temperature and geometry of the glass gobs were performed to define the loading conditions of the glass gobs. An experimental study during the delivery and loading operations was carried out at the end of the delivery equipment. The infrared measurements of the gob loading conditions were performed from the blank side of the IS machine, below the platform used in the previous measurements of the gob forming process. From there, the troughs, deflectors and the operation of the blank mold can be observed. Thus, once the glass gobs are distributed by the scoop, they can be recorded sliding through the delivery equipment and loading into the blank molds of all the different sections of the IS machine.

3.3 RESULTS AND DISCUSSION

3.3.1 GLASS THERMAL ANALYSES OF THE GOB FORMING PROCESS

As stated before, a thermal analysis of the glass flow extrusion through the orifice ring will be performed under different industrial conditions. This analysis will be carried out by measuring the temperature distribution in the glass gobs and their evolution during the gob forming process, until the gobs are cut. The motivation of this study is to gain a better understanding of the thermal phenomena that occur during the gob forming process.

First, to test the new methodology, initial glass gob measurements were conducted at Ramon Clemente. The performed infrared measurements were very similar to those presented in the HVG publications. However, due to variations in the experimental conditions, the temperature results were not as expected. Literature about temperature distributions and thermal phenomena within glass gobs was presented before. Nevertheless, due to unexpected differences in the results of the conducted temperature measurements, these publications were reviewed again, focusing on the experimental conditions, temperature results and their causes. Finally, both results were compared and discussed. Then, several thermal analyses based on infrared measurements were performed to define and validate a hypothesis that could explain the most probable causes of the thermal phenomena measured in the glass gobs.

(A) Initial Glass Gob Temperature Measurements

As defined before, to test the new methodology, infrared thermal measurements were conducted under different industrial manufacturing conditions. The results of these measurements describe the temperature evolution on the glass surface during the gob forming process.

Initially, the gob forming process was studied with the production of two different glass perfume containers, defined as Case 1 and Case 2. Relevant manufacturing parameters defining the conditions of the glass gob for both cases are presented in **Table 1**. The container produced in Case 1 is much heavier than in Case 2. Therefore, a larger orifice ring is required to form that glass gob. In addition, as the amount of glass defines the energy stored within the gob, lower glass gob temperatures and longer dwell times are required to manufacture that container. Otherwise, the viscosity of the glass container would not be high enough to withstand gravity deformations after the blow mold is open.

Table 1. *Industrial manufacturing conditions of the containers produced during the IR measurements of Case 1 and Case 2.*

	Case 1	**Case 2**
IR Measurement Ref.	136R063 on 20170516	191R087 on 20170710
Container Name	BRAVO MM 100	SIERRA 60
Glass Weight (g)	207	91

Orifice Ring Ø (mm)	38	28
Production Rate (bpm)	40	58
Forehearth Temp. SetPoints (ºC)	1,240 – 1,209 – 1,200 – 1,144 – 1,135	1,220 – 1,210

In this sense, it can be stated that the parameters of the gob forming process are defined based on the specifications of each container. At the same time, these parameters influence the manufacturing conditions of the container. Two different containers were selected to perform the initial measurements and define if there is any influence of the gob forming process parameters on the temperatures of the glass gob.

As explained in **Chapter 2**, two thermal areas were evaluated separately. Box2 defines the temperature measurements of the glass in the orifice ring area and Box1 defines the temperature measurements of the glass in the extruded gob area. These two areas defined as Box1 and Box2 were described with squares in **Figure 1**. The position of these areas is the same for all the frames of the thermal camera measurements, although the hot spots may slightly move depending on the maximum temperatures on the glass surface.

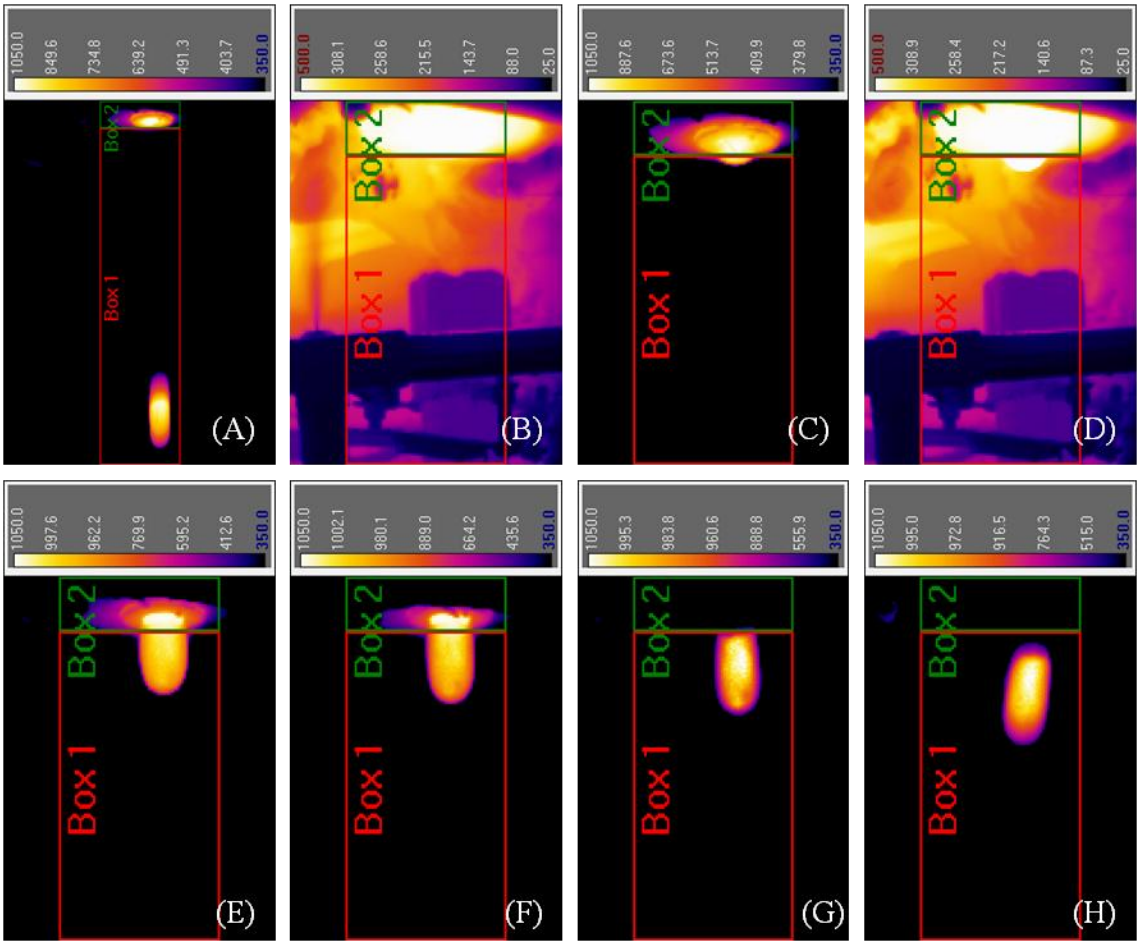

Figure 1. *IR thermal camera shots showing the extruded glass at different frames during the gob forming process in Case 1 temperature measurements. (**A**) refers to frame 1,479; (**B**) to 1,488 (115); (**C**) to 1,500; (**D**) to 1,521 (141); (**E**) to 1,540; (**F**) to 1,543; (**G**) to 1,549 and (**H**) to 1,553.*

A detailed review explaining the evolution of the glass temperatures during the gob forming process under the manufacturing conditions defined in Case 1 is presented. In addition, the maximum temperature values measured with the infrared thermal camera of the orifice ring area (Box2) and the extruded gob area (Box1) are plotted in **Figure 2**.

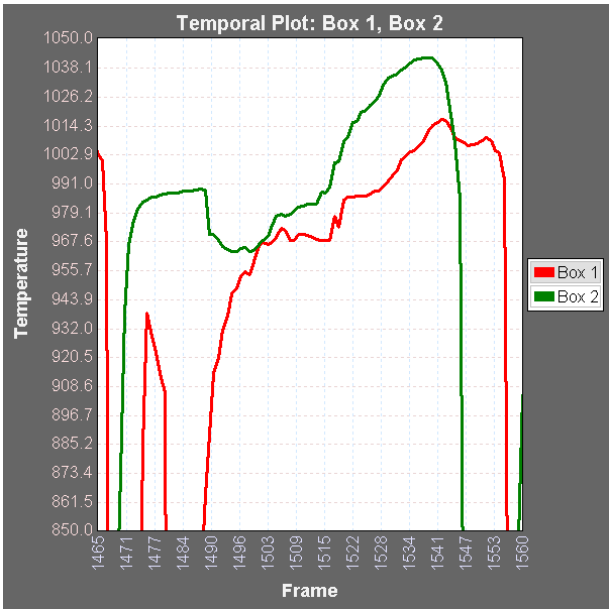

Figure 2. *Maximum temperature readings throughout the gob forming process in the orifice ring (Box2) and the extruded gob (Box1) areas for the infrared measurements performed under Case 1 conditions.*

First, the temperature evolution in the orifice ring area (Box2) is defined. At the beginning of the gob forming process, the shear blades are still closed and the glass temperature cannot be measured as glass in the orifice ring area is not visible yet. Initial glass temperature in the orifice ring is 985.6 ºC (see frame 1,479 in **Figure 1A**) and increases slightly until 988.5 ºC (at frame 1,490). When the shear lubricant emulsion starts to be sprayed (see frame 1,488 in **Figure 1B**), a mist is created that results in sawtooth interferences and the maximum temperature measured at the orifice ring drops to 963.2 ºC (at frame 1,500). The feeder plunger acts as a piston controlling the flow of molten glass with an oscillating vertical motion. During the initial long upward movement the plunger ascends, allowing the molten glass of the spout to slowly start flowing through the orifice ring due to the low glass viscosity and gravity (see frame 1,500 in **Figure 1C**). Then, there is a fast downward stroke of the plunger to push and extrude the glass through the orifice ring to form a gob of the desired weight. During the extrusion, the glass temperature near the orifice ring has grown up to 1,042.0 ºC (see frame 1,540 in **Figure 1E**). The upward plunger motion starts right before the cut, then the glass gob is sucked to allow a better cut and to minimize the contact of the remaining glass with the cold shear blades. Finally, the shear blades cut the gob (see frame 1,549 in **Figure 1G**) and it accelerates in free fall to the gob distributor and the delivery equipment.

On the other hand, the temperature drop due to the shear lubricant spraying appreciated in Box2 is not present in the extruded gob area (Box1). This is because, at that time, the gob has not yet been extruded enough to reach Box1 area (see frame 1,488 in **Figure 1B**). It is not until the glass begins to extrude that it can be measured by Box1, then the glass temperature at the

bottom of the gob is 954.0 ºC (see frame 1,500 in **Figure 1C**). When the shear lubricant emulsion spraying ends and the mist disperses an increase in temperature up to 984.2 ºC can be detected (see frame 1,521 in **Figure 1D**). While the glass is being extruded, the temperature keeps rising to 1,016.8 ºC (see frame 1,543 in **Figure 1F**). Finally, when the shear blades have cut the glass gob, it has a maximum temperature of 1,009.5 ºC (see frame 1,553 in **Figure 1H**). Note that once the gob acceleration starts, it will result in blurred shots and incorrect temperature readings (see frame 1,479 in **Figure 1A**).

In Case 2, infrared measurements were performed very similar to the presented in Case 1. Obviously, since a different container was being manufactured, the gob forming conditions were also different. As expected from the forehearth temperature setpoints in **Table 1**, glass temperatures in Case 2 were higher than in Case 1. The higher production rate of the IS machine can also be appreciated with a much faster gob forming operation. On the other hand, the measurements were carried out another day, so the camera position and the elements in the shot layout may slightly vary. Nevertheless, the same approach evaluating separately the two thermal areas defined as Box1 and Box2 was followed. The maximum temperature values measured with the infrared thermal camera of these two areas during the gob forming process under the manufacturing conditions defined in Case 2 are plotted in **Figure 3**.

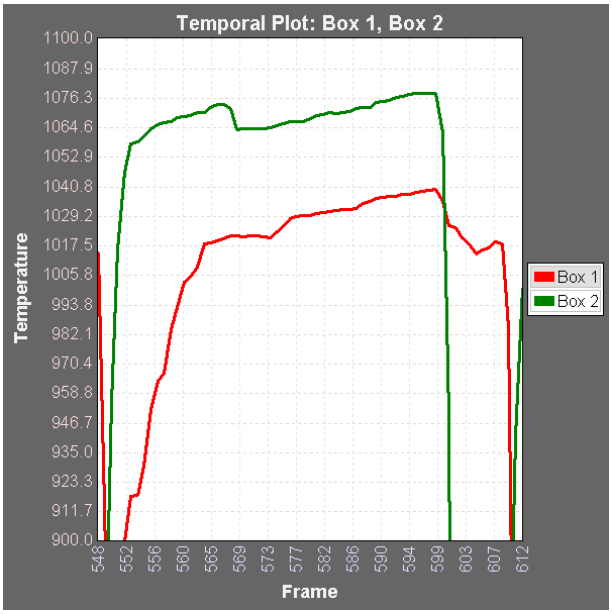

Figure 3. *Maximum temperature readings throughout the gob forming process in the orifice ring (Box2) and the extruded gob (Box1) areas for the infrared measurements performed under Case 2 conditions.*

In this case, the experimental infrared measurements were performed in MIS 4 instead of MIS 5, because it was observed that the lubricant spraying onto the shear blades was much cleaner in MIS 4 rather than in MIS 5. In Case 2, the spraying still creates a mist, but the splashes and drops observed earlier in Case 1 that caused a lot of interferences in the temperature measurements were considerably reduced. The interference reduction allowed obtaining smoother and more accurate plots, therefore more reliable thermal readings of the process. In this sense, **Figure 3** shows a clear phase difference between the two thermal areas defined as Box1 and Box2. Now it can be appreciated much better that there is an almost

constant and linear temperature increase over time during the glass gob extrusion in both temperature measurements plotted in **Figure 3**. The same thermal phenomena presented in the previous measurements of Case 1 appear in this second case, the temperature drop due to the lubricant spraying in the orifice ring area (Box2) at frame 570 becomes evident as well. However, as a result of the reduced splashes in Case 2, the temperature drop was considerably minimized from 25 ºC to 10 ºC.

Despite the differences between Case 1 and Case 2, it is possible to define a trend by comparing the evolution of the maximum temperatures represented in both cases. Because the manufacturing conditions and gob forming parameters were different, the temperature setpoints of the forehearth and the range of thermal readings obtained in both infrared measurements were different too. Even then, from these two cases, it can be concluded that although the gob forming conditions were modified, there is repeatability in the evolution of the maximum temperatures measured in the glass surface during the gob forming process. Nevertheless, another conclusion can also be obtained, that is, the temperature results of the initial measurements of the gob forming process carried out at Ramon Clemente are very different from the temperature results presented in the literature. The largest difference is that any increase in temperature was previously reported in the literature. However, in the measurements performed there is a visible increase in temperature over time during the extrusion of the glass gob. The reasons for this strange phenomenon will be discussed in the following sections.

(B) Thermal Phenomena in the Gob Forming Process

Due to unexpected differences in the results of the conducted temperature measurements in the gob forming process, the literature was reviewed again, focusing on the experimental conditions, temperature results and their causes.

As cited before, HVG performed experimental measurements to study temperature distributions in amber glass gobs [1], [2]. In these studies, measurements were made when the gob was already cut, at 0.5 and 0.6 m below the shear blades with an approximate gob velocity of 3 m/s. Initially, with the pyrometer mounted on a rotating device, multiple temperature measurements at the top, middle and bottom of the gob were performed at several angular positions to obtain the axial and angular temperature distributions of the glass gob. Afterward, using infrared pyrometers with different wavelengths, temperatures at several depths were also obtained to define a temperature distribution within the glass gob.

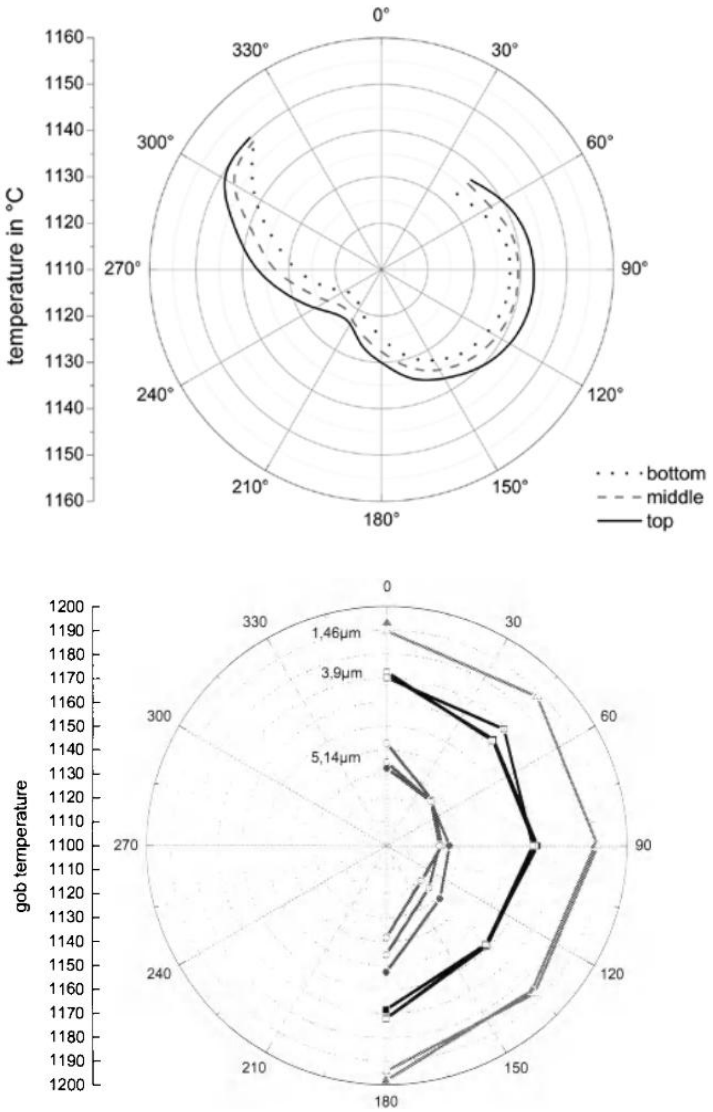

Figure 4. *Gob temperature results from HVGs publications. (**Top**) shows the axial and angular temperature distribution [1] and (**Bottom**) shows the radial temperature distribution as a function of depth [2].*

The results of the glass gob temperature distributions from the mentioned publications are shown in **Figure 4**. It can be seen how the measured temperatures deviate from the desired homogeneous thermal distribution. Along with the infrared measurements, the authors also explained the causes of these distributions. A linear increase in the temperature along the length of the gob can be observed. This was defined due to radiative heat losses. The portion of the gob that has already left the feeder losses heat by radiation during the extrusion and the free fall between the shears and the scoop, where the infrared measurements were performed. In the angular direction, there were also temperature differences due to the influence of the feeder. Finally, a radial temperature profile was determined. The measured temperature gradient was too large to be explained only by radiative heat losses. Thus, it was deduced that the gob is carrying a temperature profile previously induced by the feeder.

These were the only publications found about experimental temperature distributions in the glass gobs. Nevertheless, few authors also developed numerical models of the feeder and gob

forming operation, predicting temperature distributions in the glass domain. Their goal was not to determine the temperature distribution of the glass gobs. Even then, the numerical models took into account some thermal phenomena that resulted in glass gob temperature distributions.

For instance, the previously presented numerical simulations of the TV panel forming process [9] included a numerical model of the gob forming process to provide reliable thermal data for the pressing model. The glass flow and temperature distributions were computed in the spout as a function of time and the forming of the gob itself; while the gob was cooled down due to radiative heat losses to the environment. Thermal phenomena occurring during the gob forming process were not explained, but vertical and horizontal sections of the feeder were presented showing the predicted temperature distributions in the glass domain. Both sections presented clear temperature profiles, showing that glass temperatures near to the refractory walls were up to 80 ºC lower than glass flowing in the center of the feeder, which gives a better idea of the feeder influence presented by HVG.

On the other hand, Emhart [4] carried out a numerical investigation on the flow and thermal conditions of molten glass during its passage through a double gob feeder. Simulations included thermal heat losses from the feeder and temperature non-uniformities at the equalizing section outlet. Variations in gob weight between orifices were found to be due to deviations in gob temperature profiles. This was a result of the different glass residence times and different paths taken by the glass flow to each orifice ring. To eliminate the problems of gob thermal variations the bottom of the feeder was designed for equalization of the flow. It allowed for additional insulation, which helped to minimize uncontrolled heat losses from the walls. The simulation results showed that thermal variations between the inner and outer gobs were practically eliminated as a direct result of the increased feeder insulation and decreased glass residence time in the feeder.

(C) Discussion of the Initial Results

A detailed description of the evolution of the glass temperatures measured at RC during the gob forming process was detailed above. From the infrared thermal measurements presented in Case 1 and Case 2 (see **Figures 2** and **3**), it could be seen that the maximum temperature values on the surface of the glass gobs showed an increase over time as the glass was being extruded through the orifice ring. The lowest temperature value was measured at the start of the gob forming process, when the extruded glass was visible for the first time after opening the shear blades. Then, during the gob extrusion, the maximum temperature increased over time. Until the shear blades started closing to cut the extruded glass, when the highest temperature value was measured. To summarize, the results from the initial infrared measurements performed at Ramon Clemente showed relevant differences with the temperature distributions previously reviewed.

Therefore, due to the strange findings in the conducted temperature measurements, literature discussing about glass temperatures in the gob forming process was reviewed again. Showing special interest in the experimental conditions, temperature results and thermal phenomena presented in the HVGs publications. It is important to note that RC measurements were carried out **during** the gob forming process and HVGs results were obtained **after** the gobs were cut. Therefore the increase in temperature observed during the glass gob extrusion could have gone unnoticed by measuring the glass temperature at 0.5 or 0.6 m below the shear blades. This

suggests that some thermal phenomena may be happening during the gob forming process or before the gob reaches the pyrometer position of HVGs measurements. Moreover, the thermal conditions of the glass gobs during the infrared measurements performed by HVG could not be exactly reproduced as after the shears cut the gob, it starts to accelerate, resulting in blurred shots and incorrect temperature readings. Other conditions that also differed between both studies were the wavelengths of the infrared sensors; the optical properties of the glass gobs as the glass compositions were different (soda-lime glass against amber glass); the thermal conditions inside the feeder, etc.

To conclude, in their publications HVG explained some provable causes of the measured temperature distributions. In addition, other causes were defined by different authors using numerical simulations. Even HVG worked in mathematical interpolations to calculate the temperature distribution of the gob at any point in the delivery. But in any of these publications, no information was presented on thermal phenomena resulting in the measured temperature distributions. For all these reasons, an in-depth analysis of the infrared measurements presented in Case 2 will be performed along with further temperature measurements to obtain a better understanding of the thermal phenomena occurring within the glass during the gob forming process. The main use of the infrared thermal camera is to measure the temperatures on the glass surface. However, as will be presented in the following sections, much more information can be obtained besides the temperature comparing the differences between subsequent frames.

(D) Analysis of the Flow of Extruded Glass

As stated before, in the following sections, several thermal analyses will be performed to describe the thermal phenomena observed in the initial measurements of the glass gob forming process. The most surprising phenomenon was a temperature increase of the extruded glass during the gob forming process.

First, it is necessary to define the place where the highest temperatures were measured. From the initial infrared measurements, it can be defined that the hottest part of the glass gob is always located near the orifice ring, at the top of the extruded gob. Therefore, at every frame, the most recently extruded section of glass has the highest temperature. This makes sense, in fact, it was already noticed before, when playing with the camera's calibrations using a single frame in **Chapter 2** and it was rightly decided to divide the glass gob measurements into two areas using Box1 and Box2. At the same time, it can be defined that the increase in the glass temperature is probably related to the glass extrusion itself, that is, as more glass is extruded, the extruded flow becomes hotter. Thus, to validate that affirmation, the approach will be to try to relate the increase in temperature with the increase in the flow of extruded glass during the gob forming process.

The flow of extruded glass at the gob forming process depends on several parameters as the orifice ring diameter, the rotating tube height and the temperature setpoints of the forehearth sections. Once all these parameters are defined, sequential gobs with a constant weight can be obtained. Then, it can be stated that the flow of extruded glass as function of time is only modified by the plunger vertical motion, glass viscosity and gravity. To relate the plunger vertical motion with the variation of glass flow through the orifice ring over time, the flow of

extruded glass will be quantified by measuring the length of the glass gob at every frame. From there, try to relate the gob forming operation with the increase in the glass temperature.

The following results are from the infrared thermal measurements performed under the industrial gob forming conditions presented in Case 2. A thermal palette showing only pixels at temperatures over 600 ºC was used to track at every frame the position of the top (y_{top}) and bottom (y_0) of the extruded glass gob during the entire gob forming process (see **Figure 5**).

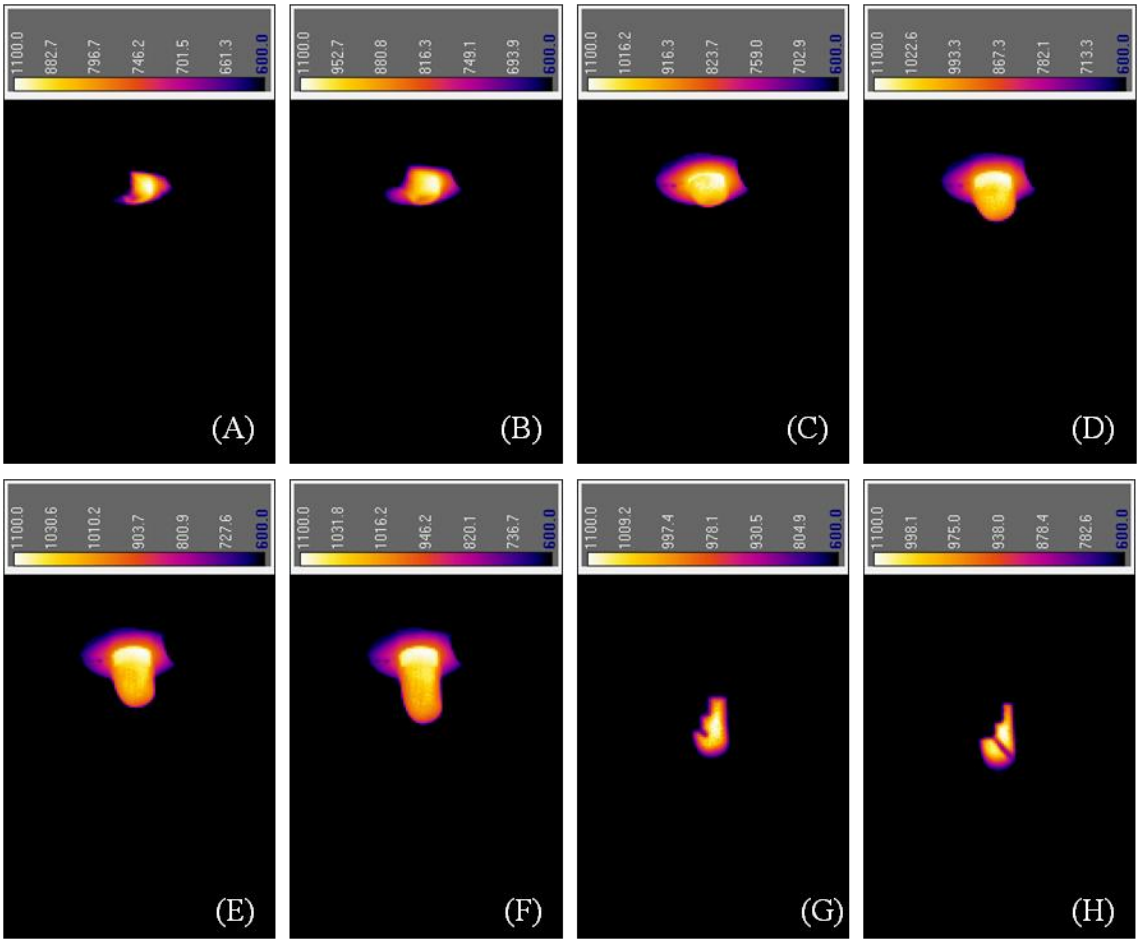

Figure 5. *IR thermal camera shots showing the extruded glass at different frames during the gob forming process measured under Case 2 conditions. (**A**) refers to frame 551; (**B**) to 552; (**C**) to 556; (**D**) to 575; (**E**) to 584; (**F**) to 592; (**G**) to 604 and (**H**) to 606.*

The coordinate of the bottom (y_0) of the glass gob was defined as the lower pixel in the extruded gob area with a temperature of over 600 ºC. The coordinate of the top (y_{top}) of the glass gob could be obtained from the position of the orifice ring hole. Once defined the vertical position of these two points, an estimate of the gob length can be obtained in each frame by counting the pixels between the top and bottom coordinates of the extruded glass gob (see **Figure 6**). In fact, it only was necessary to track the coordinate of the bottom (y_0) of the glass gob as the orifice ring position could be defined as a constant value for all the frames. Due to this simplification, however, when the gob was cut and started falling inconsistent values of gob length were obtained.

Very useful information can be obtained by measuring distances with pixels. However, this is

a relative and unusual length unit. The equivalence between pixels and millimeters can also be defined at each infrared thermal measurement. The diameter of the orifice ring is a known and constant dimension present in all the shots, this dimension will be used as a reference. In Case 2 measurements, the orifice ring required for the container production was 28 mm. Defining how many pixels measure the diameter of the extruded glass, or the hole of the orifice ring, the equivalence between pixels and millimeters can be obtained. The diameter of the orifice ring and the extruded glass geometry measures 18 pixels wide (see **Figure 5F** for instance). Therefore, an equivalence of 1 pixel equal to 1.56 mm can be defined for length measurements in Case 2.

For ease of use, in this section, distances will still be determined in pixels. However, interesting information can be obtained with the defined equivalence. For instance, the length of the extruded glass can also be measured in millimeters to validate the volume and weight of the gob. As the surface tension of hot glass is pretty high, the volume of the gob after being cut can be approximated to a cylinder with half-spheres in both ends. The shear blades cut the glass gob in frame 604 (see **Figure 5G**), then the measured gob length is 45 pixels or 70 mm resulting in a calculated glass weight of 93.4 g. The weight specification of the glass perfume container manufactured during Case 2 was 91 ±1 g, so there is a deviation of 2.6% in the calculated glass weight. As the infrared thermal camera is not normal to the gob axis, the gob length has been measured using the orifice ring position instead of the coordinate of the top (y_{top}) of the glass gob and the coordinate of the bottom (y_0) of the gob was defined as the lower pixel with a temperature of over 600 ºC; a deviation of 2.6% in the glass weight calculations based on the infrared thermal measurements compared to the real container weight is considered more than acceptable.

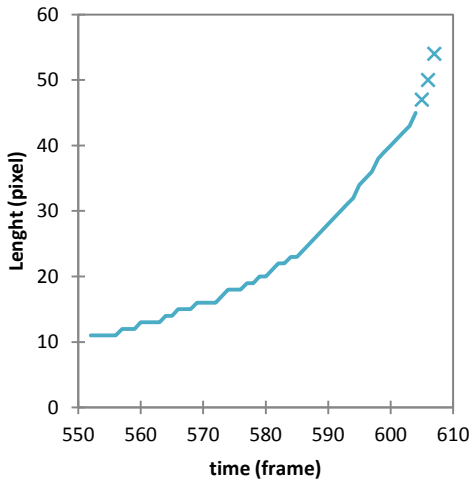

Figure 6. *Gob lengths obtained tracking the top and bottom coordinates of the extruded glass at each frame during the gob forming process for Case 2.*

The measured length of the extruded glass during the gob forming process is represented in **Figure 6**. If the slope of the curve plotted in **Figure 6** is calculated at each frame, the relative length increment of the extruded glass gob over time can also be defined (see **Figure 7**).

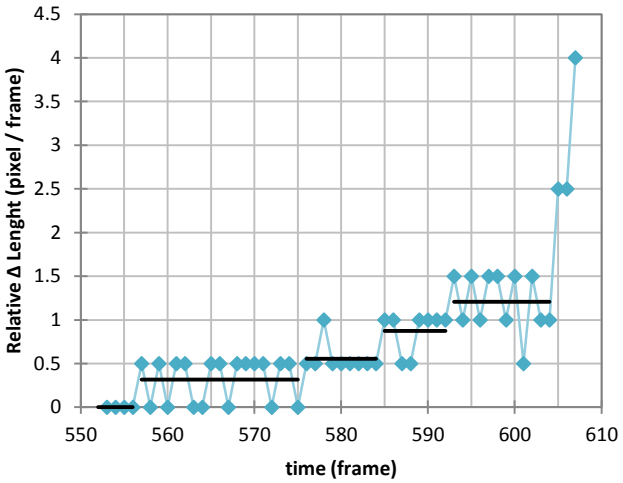

Figure 7. *Relative length increments of the extruded glass gob over time. Several time intervals can be defined during the gob forming process based on the values of the length increments.*

Until now the length and the relative length increase of the glass gob were measured during the forming process. However, as the area of the orifice ring hole remains constant during the gob forming process, the relative length increment of the glass gob over time is proportional to the volumetric flow of extruded glass during the gob forming process. As can be seen in **Figures 6** and **7**, the length increase or the flow of the extruded gob is not constant over time. At the beginning of the process, glass flows very slowly through the orifice ring. In the end, glass flows faster.

Once presented the experimental results, to understand the variations in the glass flow and to correlate them to the gob forming operation, a detailed description of the evolution of the length measurements during the gob forming process is presented.

The length measurements of the gob start when the shear blades, after cutting the previous gob, are open again (see frame 552 in **Figure 5B**). Until that moment the glass in the orifice ring cannot be properly measured as it is not visible by the infrared thermal camera (see frame 551 in **Figure 5A**). Then, several time intervals can be defined as a function of the relative length increment values: from frame 552 to 556 (see **Figure 5C**) there is not any appreciable increase in length and the mean value is 0 pixel/frame; from frame 557 to 575 (see **Figure 5D**) the increase in length oscillates between 0 and 0.5 and the mean value is 0.32 pixels/frame; from frame 576 to 584 (see **Figure 5E**) the increase in length is near 0.5 and the mean value is 0.56 pixels/frame; from frame 585 to 592 (see **Figure 5F**) the increase in length is near 1 and the mean value is 0.88 pixels/frame and from frame 593 to 604 (see **Figure 5G**) the increase in length oscillates between 1 and 1.5 and the mean value is 1.23 pixels/frame. All the values defined in these time intervals have been summarized in **Table 2**. As can be seen in **Figure 7**, after frame 604 the relative length increment values start increasing excessively compared with the previous values, this was defined as the instant when the shear blades cut the glass gob. In frame 606 (see **Figure 5H**) the shear blades are completely closed and the glass gob geometry is already slightly blurred.

Table 2. *Time intervals defined as a function of the extrusion flow values during the gob forming process presented in Figure 7.*

Relative Δ Length (pixel/frame)	**Mean Value (pixel/frame)**	**Time (frame)**	
		From	**To**
0	0	552	556
between 0 and 0.5	0.32	557	575
near 0.5	0.56	576	584
near 1	0.88	585	592
between 1 and 1.5	1.21	593	604

Similar to the previous description of the measurements, the observed variations in the gob length over time, that is, the extruded flow of glass can also be related to the vertical motion of the plunger and, therefore, to the operation of the gob forming process in the feeder.

As stated before, the flow of extruded glass is determined by the plunger vertical motion, gravity and the viscosity and temperature distribution of glass in the spout. In particular, the oscillating velocity profile of the feeder plunger is defined with three steps: initially, there is a long upward movement, followed by a fast downward stroke and just before the cut of the gob the upward movement starts again. **Figure 7** shows the incidence of the plunger motion to the flow of extruded glass. During the upward motion, the plunger ascends, allowing the molten glass to slowly start flowing through the orifice ring due to the low glass viscosity and gravity. This is represented approximately by the three initial time intervals. As the glass gob remains hanging, the pull rate increases with the amount of glass slowly added to the extruded gob. Later, during the downward stroke of the plunger, the molten glass is pushed and extruded through the orifice ring to form the gob. This short stage controls most of the glass flow during the gob forming process, defining the weight and geometry of the extruded glass gob. It is represented approximately by the fourth and fifth-time intervals. When the upward plunger motion starts again, negative pressure is obtained to suck the glass gob and allow a better cut. If necessary, this negative pressure can even counter gravity after the cut and suck the remaining glass gob back to the orifice ring. As only the bottom of the gob has been tracked, huge relative length increments are perceived after the shear blades cut the gob.

Once the vertical movement of the plunger and the extruded glass flow through the orifice ring have been related, the phenomena defining the increase in temperature still need to be defined.

As explained above, in **Figure 7**, several time intervals were defined as a function of the relative length increment values. This information was summarized in **Table 2**. Once the time intervals were defined, plotting the mean values of these intervals in the middle of every time interval, one can see that those points follow a linear trend (see **Figure 8**).

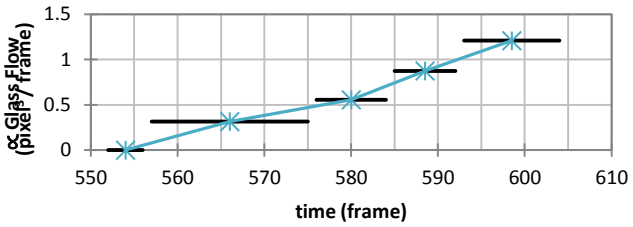

Figure 8. *Flow of extruded glass during the gob forming process. The mean values of each time interval show a linear distribution over time.*

In other words: the flow of extruded glass, which was proportional to the relative length increment of the extruded glass measured over time, shows a linear increase during the gob forming process under Case 2 conditions (see **Figure 8**). In the same way, the maximum glass temperatures plotted in **Figure 3**, also showed a similar linear increase over time, during the gob forming process. Thus, as the flow of extruded glass increases over time and the maximum temperatures on the freshly extruded glass sections near the orifice ring also show an increase, both presenting a similar linear trend; it can be concluded that the most probable cause of the measured increase in temperature is defined by an increase in the flow of glass through the orifice ring.

As mentioned before, numerical simulations on the flow and thermal conditions of molten glass in the feeder showed that some refractory elements as the spout or the orifice ring may not be properly insulated and tend to have relatively high local heat losses, resulting in strong variations in the glass temperatures near these refractory walls. To conclude, an increase in the glass flow through the orifice ring during the glass gob extrusion was experimentally measured and defined based on the gob forming operation and the vertical motion of the feeder plunger. At the same time, it can be measured a increase in temperature at the top sections of the glass gob. A reasonable explanation of this phenomenon is that as the flow of extruded glass increases there is a reduced influence of the heat losses present at the walls of the orifice ring, resulting in a temperature increase proportional to the variation of the glass flow.

(E) Temperature Evolution of the Glass Gob

Once defined the thermal phenomena that caused the unexpected increase in temperature during the extrusion of the glass gob, the next step is to study the radiative heat losses in the glass throughout the gob forming process. The explanation presented in the literature about radiative heat losses resulting in an axial temperature distribution in the gob seems plausible and can be validated by conducting more infrared temperature measurements. Therefore, an analysis of radiative heat losses and temperature distributions along the longitudinal axis of the glass gob under Case 2 industrial manufacturing conditions is presented below.

In this case, not only the coordinates of the bottom (y_0) of the glass gob were tracked at every frame, but also more sections were defined at different heights along the extruded glass gob (y_{+10}, y_{+11}, y_{+15}, y_{+20}, y_{+25} and y_{+30}). The coordinates of the bottom (y_0) of the glass gob were previously defined as the lower pixel in the glass gob area with a temperature of over 600 ºC. Once tracked that height for each frame, defining the position of the other glass gob sections

becomes redundant. Then, the respective temperatures at each section were recorded during the entire gob forming process. Glass temperatures could be measured once each gob section was already extruded. However, frames where the sections were not yet below the orifice ring area were omitted. Temperatures of all the sections were measured until just before the glass gob was sheared. An exception was made to sections y_{+25} and y_{+30}, since as they were very close to the shear blade mechanism, when the shear blades began to cut the gob, these two sections were no longer visible (see **Figures 5G** and **5H**).

In **Figure 9**, the evolution of the maximum temperatures during the gob forming process of the glass gob sections positioned at 10, 11, 15, 20, 25 and 30 pixels higher than y_0 is presented.

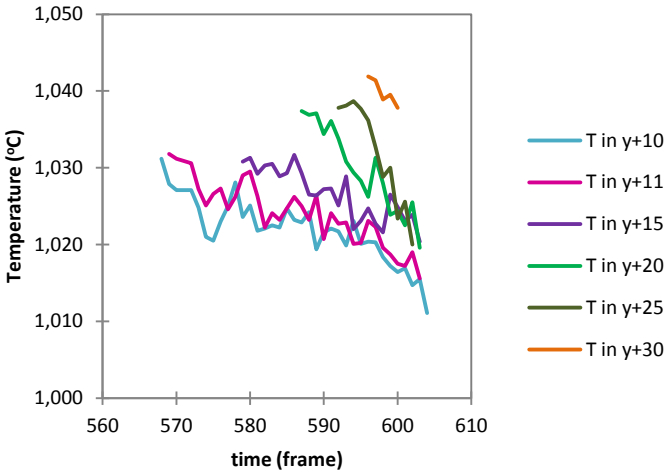

Figure 9. *Evolution of the maximum glass temperatures measured at different sections of the extruded gob tracked during the gob forming process.*

From the temperature values plotted in **Figure 9**, it can be concluded that in all the tracked sections of the glass gob, once extruded, the maximum temperature value decreases over time. In relation with the results presented in the previous section, it can be appreciated that, as the y_{+10} section is the first to be extruded, its initial maximum temperature is lower than the initial temperature in the y_{+30} section, which is extruded almost before the cut, when the extruded glass flow is higher. On the other hand, as previously defined in the literature, radiative heat losses of the glass result in a decrease in temperature. Therefore, as y_{+10} is the first section to be extruded, it will accumulate more radiative heat losses over time compared with the top sections of the gob, which were extruded later. Focusing on the radiative heat losses, linear trend lines could be adjusted to each of the temperature plots to obtain a rough estimate of their slope. These slopes would define the cooling rates of the different sections of the glass gob. Once each glass gob section is extruded, the cooling rate is mostly defined by radiative heat losses. Thus, as the total emissive power of a body depends on its absolute temperature to the fourth power, obtaining different radiative heat losses as function of the initial temperatures of each glass section seems reasonable. For this reason, as in the glass sections near the top the initial glass temperature is higher, steeper cooling rates are observed.

From these two thermal phenomena presented, a theoretical temperature distribution along the longitudinal axis of the glass gob can be defined, with lower temperatures at the bottom and higher at the top. To experimentally validate the axial temperature distribution, the evolution of

the maximum glass temperature along the vertical axis of the gob was also measured during the glass extrusion.

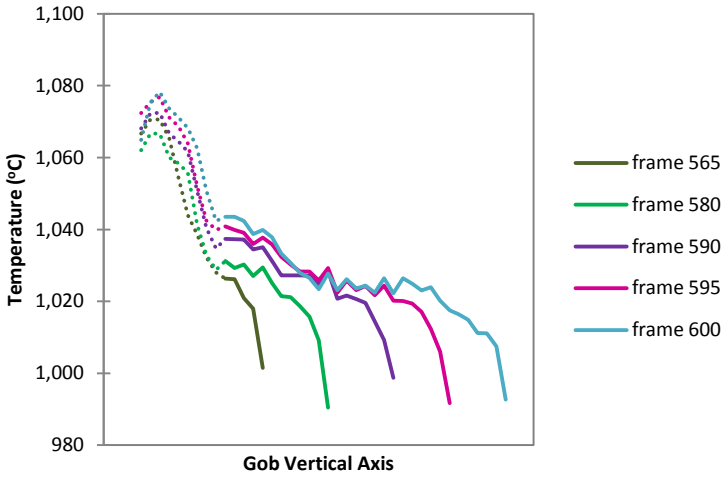

Figure 10. *Maximum temperatures measured along the vertical axis of the gob at different frames during the gob forming process.*

In **Figure 10**, several vertical profiles with the measured temperatures are presented. The dotted plots on the left side are the temperature readings from the orifice ring area (Box2). On the right side of the plot, there are the temperatures measured along the extruded glass area of the gob (Box1). As the length of the extruded gob increases over time during the gob forming process, an increase in the plot width is defined over time. As expected, few axial temperature distributions along the gob can be appreciated during the glass extrusion at different instants of time, with higher temperatures at the top of the gob and lower temperatures at the bottom. This temperature distribution becomes more than evident in frame 600 when the gob is almost completely extruded. It can be also appreciated the increase in temperature of the freshly extruded glass gob sections near the orifice ring.

Therefore, after performing the presented infrared measurements, it can be concluded that there is an axial temperature distribution along the glass gob. Nevertheless, this is not only related to radiative heat losses once the glass was extruded, but also with conductive heat losses present inside the feeder during the glass extrusion. The additional thermal phenomena occurring during the glass gob extrusion obviously could not be observed when measuring the temperature of the glass gobs after being cut, as HVG did.

Finally, some variability in the measured temperature values presented in **Figures 9 and 10** can be observed. Therefore, it was interesting to plot the temperature of two adjacent pixels (i.e. y_{+10} and y_{+11}) in **Figure 9**, to see if there was a real temperature oscillation in the glass gob surface or the variability was related with interferences during the experimental measurements. The average difference between the temperature values measured in sections y_{+10} and y_{+11} over time is only 3 ºC and the acquisition accuracy of the infrared thermal camera is ±2 ºC. Therefore, the variability of the measured temperatures must be considered correct. At the same time, it is clear that something is distorting the real temperature values as the difference between two adjacent pixels (1.56 mm) should be more reliable in **Figure 9**. On the other hand, the very same peaks appear at the same abscissa position but at different instants of time are observed in

Figure 10. In that case, it is clear that the very same peaks are appearing at the same abscissa position but different frame plots. Therefore, both interferences might be related to the layout of the shot.

(F) Thermal Phenomena between Subsequent Gobs

Up to now, based on the infrared measurements conducted during the gob forming process, an increase in the glass temperature of the most recent extruded sections was related to an increase in the extruded glass flow. On the other hand, it was also described how glass starts losing energy due to thermal radiation once it is extruded. To conclude the thermal analysis of the gob forming process, it is necessary to answer one last question: What happens to the glass temperature between subsequent gobs? **Figure 11** shows the evolution of the maximum temperature values of two subsequent gobs. When the final temperature of the previous gob is compared to the initial temperature of the next one, a temperature drop can be observed.

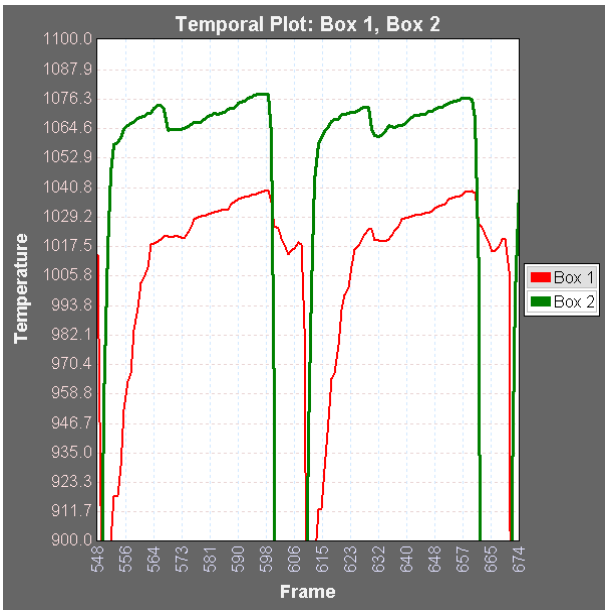

Figure 11. *Maximum temperature readings along the gob forming process of two subsequent gobs in the orifice ring (Box2) and the extruded gob (Box1) areas for the Case 2 infrared measurements.*

After each cut, a lubricant and cooling oil/water emulsion is sprayed onto the shear blades to obtain a reliable cut and avoid shear marks on the tips of the glass gobs. In the same direction, when the shear blades are going to cut the extruded glass, the feeder plunger starts an upward motion and negative pressure is obtained to suck the gob. These two actions result in a clean cut, minimizing the contact of the remaining glass with the cold shear blades. Even then, a decrease in the maximum temperature of the remaining glass is obtained when the shear blades open again. Unfortunately, when the shear blades are closed, they block the view of the orifice ring. Therefore, it is not possible to measure the glass temperature at that interval using an infrared thermal camera. But it is common sense that the temperature of the glass section in contact with the cold shear blades must be severely distorted. Even to the naked eye, different glass coloration can be observed at the bottom of the gob, probably due to the temperature

difference compared to the rest of the glass gob. In addition, since extruded glass that remained below the orifice ring but above the shear plane will be hanging outside the feeder, it will accumulate radiative heat losses until the next gob is extruded. At the same time, the extrusion flow is almost stopped. The glass volume inside the feeder that will be extruded in subsequent gobs may be also accumulating heat loses from the spout and orifice ring areas, inducing a thermal gradient in the glass near the refractive walls. On the other hand, there should be an internal redistribution of heat in the spout area, due to thermal conductivity, the flow generated by the rotating tube and even partial absorption of thermal radiation. These thermal phenomena would explain the temperature evolution between two subsequent gobs.

So far, supported by experimental measurements of the gob forming process, it was deduced that temperature non-uniformities in the gob forming process are defined when the glass is extruded throughout the orifice ring. However, many thermal phenomena take place in the gob forming process, especially the ones inside the feeder, and are very complex to be experimentally defined. In this sense, as presented before in the literature, conducting experimental measurements is a very useful methodology to obtain information about the manufacturing process. Since in many cases, the measured data may be enough to understand or experimentally validate different phenomena. In other cases, due to the complexity of the studied phenomena, the use of a numerical model would be a much powerful method, for instance, to define the temperature gradients and heat transfer phenomena within the glass in the feeder area. In any case, as will be presented later in **Chapter 4**, obtaining experimental data of the problem is the foundation of the numerical model, as precise experimental data will be required to initialize or validate the numerical simulations. For this reason, more thermal measurements of the glass gob will be performed in the following sections to define how conditioned is the glass at the end of the delivery equipment.

3.3.2 GOB CONDITIONS AT THE DELIVERY AND LOADING STAGES

As presented in the previous section, it is clear that gobs are not thermally uniform. Many thermal phenomena condition the temperature distribution before, during and after the gob forming process. However, more thermal measurements should be conducted to define how conditioned is the glass when loaded into the blank mold. Therefore, in this section, the glass gob conditions will be studied in the delivery equipment.

A detailed description of the delivery equipment will be presented, showing the theoretical implications of having different delivery paths to each individual section of the IS machine. In addition, an experimental study during the delivery and loading operations will also be carried out: infrared measurements of the temperature, velocity and geometry of the glass gobs will be performed to define the loading conditions. This study will also define the influence of the delivery equipment and variations in the loading conditions of the glass gob as a function of the loaded section. The gob properties and the repeatability of measurements will be evaluated and compared with previously published results. At the same time, by measuring the loading conditions of the glass gob, the initial conditions of the glass at the start of the blow and blow container forming process will also be defined.

(A) Influence of the Delivery Equipment to the Gob Loading Conditions

As presented in Chapter 2, the delivery equipment distributes the formed glass gobs to the blank molds of the IS machine. It consists of three components: the scoop, trough and deflector. There is a single scoop and one trough and deflector per each individual section. The feeder plunger, orifice ring, shear blades and scoop are vertically aligned in the middle of the IS machine, describing a vertical axis that defines the machine centerline. In a six-section container forming machine, the defined centerline is placed between IS3 and IS4. Then, on both sides of the centerline, there are three individual sections placed symmetrically. Therefore, the components of the delivery equipment used in the side sections (IS1 and IS6), IS2 and IS5 and the middle sections (IS3 and IS4) are symmetric. The IS machines commonly have an even number of sections, so the pieces of the delivery equipment are always paired.

Detailed technical drawings with the dimensions of the delivery equipment components were not available from the manufacturer. Hence, the dimensions of the different parts were measured before being assembled on the IS machine (see **Table 3**). A 3D model of the several components of the delivery equipment assembled in the same position as when mounted on the IS machine was build to check that all the measurements were correct (see **Figure 12**). The slopes of the troughs mounted on the IS machine were measured and there was a variation in the slopes between 27º and 30º, depending on the individual section. As it was difficult to see any differences to the naked eye in the curvature of the deflectors when the three deflectors were overlapped, the curved inner section of all the deflectors was considered the same.

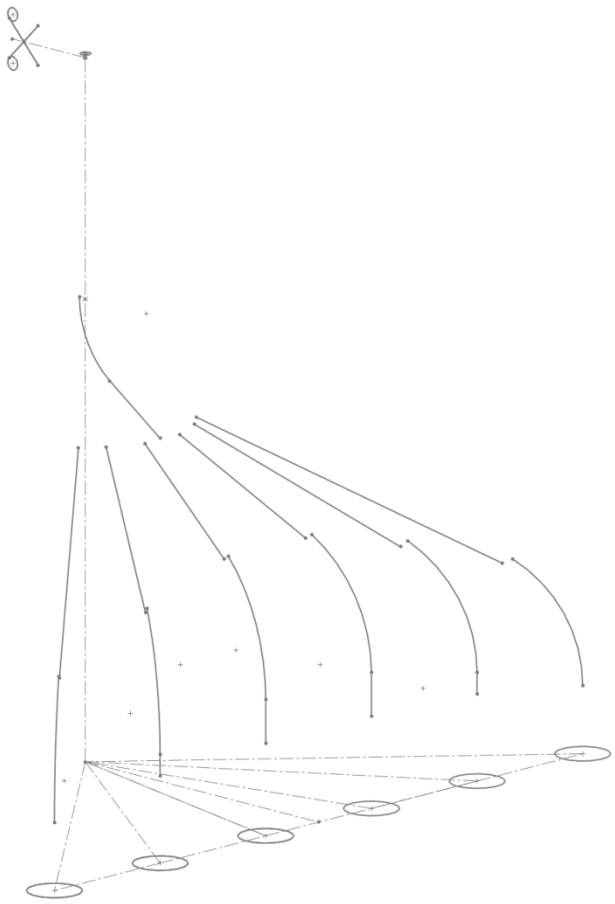

Figure 12. *3D model of the delivery equipment components assembled in the same position as when mounted on a six-section IS machine to define the delivery trajectories of the glass gobs from the orifice ring to each blank mold cavity.*

Table 3. *Length measurements of the different parts of the delivery equipment according to the position of the individual section where they are assembled.*

	Length (m)		
	Side Sections (IS1 and IS6)	**IS2 and IS5**	**Middle Sections (IS3 and IS4)**
Horizontal distance	1.77	1.42	1.20
Scoop	0.62	0.62	0.62
Trough	1.22	0.85	0.61
Trough increase	+100.0%	+39.3%	0% (reference)
Deflector	0.56	0.63	0.72
Deflector increase	-22.2%	-12.5%	0% (reference)
Total delivery equipment	2.40	2.10	1.95
Total delivery equipment increase	+23.1%	+7.7%	0% (reference)

As can be seen in **Table 3**, troughs and deflectors have different lengths depending on the individual section where they are mounted. Thus, the delivery equipment is not the same for the side sections (IS1 and IS6) and the middle sections (IS3 and IS4). Troughs from the middle sections are shorter due to the smaller horizontal distance between the machine centerline and the blank molds. Then an extra straight section can be added at the end of the deflectors to improve the gob loading. As the section position moves away from the machine centerline, the

troughs must be longer to cover a larger horizontal distance and then the straight section at the end of the deflectors is shortened.

For instance, in a six-section IS machine, when the delivery equipment of the side section is compared to the middle section, the trough length is doubled (+100.0%), then the deflector needs to be a 22.2% shorter. In the end, the total length increase of the delivery equipment is 23.1%. In larger IS machines, with 10 or 12 individual sections, these differences between the delivery equipment dimensions may become even more relevant. As there are more sections, the total width of the IS machine increases and then the horizontal distance between the outermost section and the machine centerline is much longer too. That would result in a reduction in the slope of the external troughs and an increase in the friction with the glass gob during the delivery, obtaining even more deviations in the loading conditions of the glass gobs due to the delivery operation. To compensate for this issue, the total height of the IS machine and the delivery equipment length increases with the number of sections to obtain steeper troughs at the outermost sections and try to contain the variation of the loading conditions between sections.

The vertical distance between the orifice ring and the top of the blank mold in the six-section IS machine number 5 (MIS 5) at Ramon Clemente glass plant is 2.69 m; this is the total vertical separation that the gobs must travel before loading. Simplifying the path traveled by the glass gobs as if it was a free-fall scenario, from the equations of the uniformly accelerated rectilinear movement it can be deduced that the time required for a glass gob to travel that distance would be 0.73 s and the loading velocity would be 7.14 m/s. But in an IS machine, gobs also have to be distributed horizontally to all the individual sections, so, between the shear blades and the blank molds, there is the delivery equipment. In the delivery, glass gobs slide through the channels of the delivery system to be translated horizontally to each individual section. As the glass gobs are in contact with the delivery equipment, friction forces will appear due to the relative velocity between them. Friction between the gob and the surface of the delivery equipment results in a reduction in the gob velocity and an increase in the delivery time. Glass gobs may also suffer elongation and the surface of the delivery channels will be eroded too. In addition to deviations of the gob physical properties, a temperature distribution will appear on the glass surface, caused by heat losses of the hot glass due to thermal radiation and contact conductance with the cold delivery equipment.

The length differences between the troughs and deflectors of the delivery equipment as a function of the individual section position against the machine centerline will affect the properties and loading conditions of the glass gob. An inconsistent gob loading can lead to uneven container forming conditions that will result in container defects. These deviations of the glass gob properties are more relevant at the outermost sections of the machine, where the distance traveled by the gob through the delivery equipment is longer. Comparing the glass gob conditions of the side sections (IS1 and IS6) against the middle sections (IS3 and IS4), it can be stated that:

- The horizontal distance from the orifice ring to the blank molds is longer. Longer troughs and shorter deflectors are needed to cover that distance and deliver the glass gobs.
- Longer delivery equipment implies prolonged contact between the glass gob and the delivery channels. Then, there will be more friction and contact heat transfer.
- Friction with the delivery equipment will tend to slow down and elongate the delivered gobs and also erode the inner surface of the delivery equipment components.

- As the path is longer and there is more friction, the gob will spend more time being delivered. This will result in slightly higher heat losses due to thermal radiation.

Thus, based on the length differences between the components of the delivery equipment, it can be noted that the glass gobs loaded into the blank molds might have different loading conditions according to the position of the individual section where they are loaded. Gobs loaded into the blank molds of the IS1 and IS6 machine sections will tend to have lower velocities and accumulate more heat losses. These deviations will be experimentally determined by measuring the glass gob properties at the end of the gob delivery operation with an infrared thermal camera.

(B) Measurements of the Gob Delivery Time

To define the influence of the delivery equipment in the loading conditions of the glass gobs, the glass gob delivery operation has been recorded with the infrared thermal camera from the blank side of the IS machine. In **Figure 13** it can be seen the layout of the delivery equipment during the infrared measurements. On the top-right corner of the shot, there is the feeder with the shear blades and the orifice ring. The extrusion of the glass gobs during the gob forming process can be observed in the recording. The instant of time when the extruded gob is cut by the shear blades and starts free-falling into the delivery equipment can be determined. On the other hand, at the lower half of the shot, the deflectors and the end of some troughs can be observed. In **Figure 13** there is a glass gob traveling through the second deflector and the third deflector is hidden behind a pillar. Finally, at the bottom of the shot, there are six blank molds mounted on the IS machine.

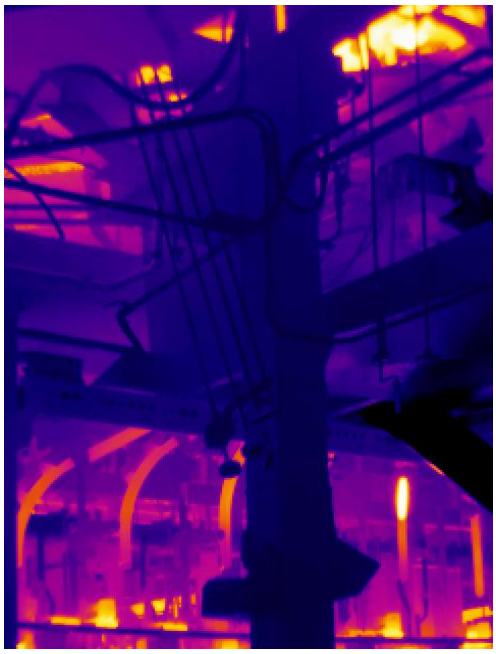

Figure 13. *An infrared shot of the IS machine viewed from the blank side using the low-temperature calibration. The glass gobs traveling through the delivery equipment and the amount of time spent in that operation can be determined.*

During the infrared thermal recordings, the glass gobs being delivered through the delivery equipment and loading into each of the blank molds can be observed. The loading sequence of the gobs is defined by the gob distributor and it is IS1, IS2, IS5, IS6, IS3 and finally IS4. The gobs traveling through the scoop and the troughs cannot be identified in this shot, but the glass gobs at the deflector and until they are loaded into the blank mold can be clearly defined. At the bottom of the shot, there is a horizontal bar, which can be defined as an approximate reference of the position of the top of the blank molds. Therefore, when the glass gobs arrive there, the instant of time in which the glass gob is loaded into the blank mold is defined. Then the total delivery time of the glass gobs, defined as the time interval since the gob is cut until it is loaded, can be determined as a function of the relative position of the individual section and the machine centerline.

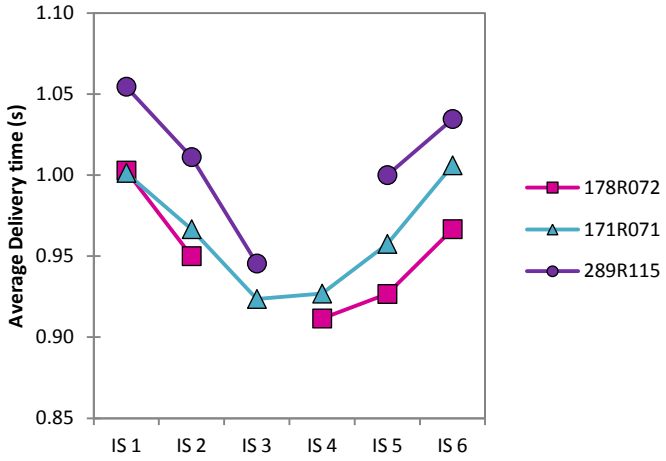

Figure 14. *Results of the average delivery time of the glass gobs measured under different conditions at the six individual sections of the IS machine number 5.*

The glass gob delivery time at each section has been determined as the average delivery time measured in ten consecutive gobs. **Figure 14** shows the results of the average delivery time of the gobs measured under different conditions. As expected, the gob delivery time depends on the horizontal distance that the gob needs to travel between the orifice ring and the blank mold. The side sections of the machine are farther, so, the delivery equipment components need to be longer. This results in prolonged contact between the glass and the surface of the delivery equipment channels. Therefore, in **Figure 14** it can be observed that as the average delivery time of the glass gob depends on the longitude of the delivery equipment, the delivery time is smaller for the middle sections (IS3 and IS4) and larger for the side sections (IS1 and IS6) of the IS machine. The variability of the delivery time is almost zero between consecutive gobs. There is also a good agreement of the experimental measurements performed under different gob forming and delivery conditions, showing all three similar deviations on the gobs delivered to the different sections. The variation of the delivery time between sections, although it is small, results in a variation of the contact time between the glass gob surface and the walls of the blank mold cavity at the initial stage of the container forming process.

(C) Measurements of the Gob Velocity

Once defined the influence of the delivery equipment to the time spend by the glass gobs in being delivered, it seems clear that the gob velocity will also be influenced. Therefore, the velocity of the glass gob passing through the deflector of each section of the IS machine was also measured. As a consequence of the high speed of the glass gobs during the delivery its geometry cannot be clearly defined. Then, the hot spot present on the surface of the glass has been taken as a reference to track the displacement of the gobs during the delivery. Due to the high speed of the gob, the interval of time analyzed is very small, only four frames or 66.67 ms. Then, it can be assumed that there is not any relevant heat transfer modifying the position of the hot spot during these four infrared thermal measurements. To measure the loading velocity of the glass gob, the position of the hot spot on the glass gob surface has been tracked during four consecutive frames while the gob is passing through the curved section of the deflector.

To be able to compare the measured velocities of the glass gobs while they are traveling through the deflector of sections IS1, IS2 and IS3; the infrared thermal camera was always positioned normal to the inner surface of the channel deflector and approximately at the same distance. Initially, it was expected to use the dimensions of the baffle of each section as a length reference to define the equivalence between pixels and meters for the infrared thermal measurements performed at each individual section. However, as the deflector orientation varies with the position of the individual sections of the machine, when the camera was positioned normal to the inner surface of the deflector, the distance between the camera and the corresponding baffle was not consistent for the three infrared measurements and could not be taken as a reference. Thus, in this case, the velocity measurements of the glass gobs could only be determined in units of pixels/frame.

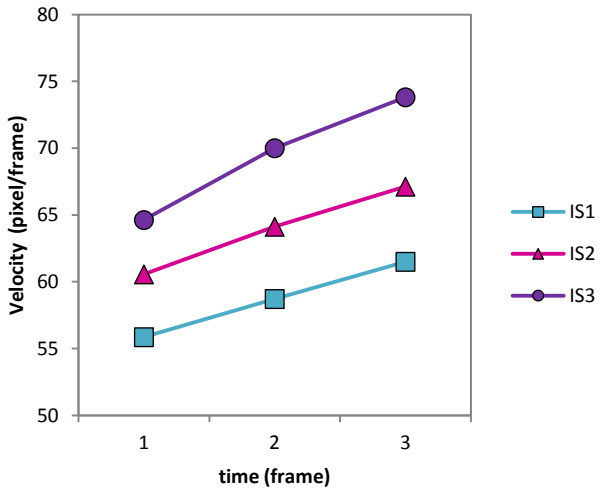

Figure 15. *Evolution of the velocity of the glass gobs measured when being delivered through the deflector of section IS1, IS2 and IS3.*

Figure 15 shows the average results of the loading velocities measured at ten consecutive glass gobs passing through the deflector of section IS1, IS2 and IS3. As expected, the velocity of the glass gobs varies with the horizontal distance between the orifice ring and the blank mold. The side sections of the machine are farther, so, the delivery equipment components need to be

longer. This results in prolonged contact and more friction between the glass and the inner surface of the delivery equipment channels. Therefore, the velocity of the glass gob is higher when loaded to the middle sections and lower on the side sections of the IS machine. This makes sense with the previous measurements of the loading times. The gob velocity measured at each of the deflectors is consistent for the ten consecutive gobs. One can also appreciate an increase in the glass gob velocity over time, as the gob passes through the curved section of the deflector before loading vertically into the blank mold.

It can be concluded that there is a clear deviation in the loading conditions of the glass gob as a function of the individual section position due to the variation in the length of the delivery equipment components. Comparing IS1 and IS3 it can be defined that: the side section troughs are 100.0% longer than the middle section ones and the side section deflectors are 22.2% shorter; then, there is an increase in the total length of the delivery equipment on the side sections of a 23.1%; finally, the slope of the troughs on the side sections is also lower. This results in an increase in the measured delivery time of the glass gobs at the side sections between 8 and 10%. At the same time, the loading velocity is reduced by around 16% when the side and middle sections are compared. The delivery equipment and the measured kinetic properties of the gobs loaded in sections IS2 and IS5 are halfway between the values presented for the side (IS1 and IS6) and the middle (IS3 and IS4) sections.

Although the influence of the delivery equipment on the gob loading conditions has been defined analyzing the displacement of the glass gobs in consecutive frames, pixels/frame is a relative and uncommon velocity unit. To define the velocity of the glass gobs in m/s to be able to compare it with the values presented in the literature, and use that value in further numerical simulations, the equivalence between pixels and meters needs to be defined for each infrared thermal measurement. For this reason, measurements of the gob loading velocity were performed again at the deflector of the side section IS6. In this second case, a ruler with a known length was positioned next to the studied deflector and at the same distance from the thermal camera to be used as a length reference. The real length of the ruler is 0.32 m and when measured in the infrared shot the length of the ruler is 96 pixels (see **Figure 16A**). Therefore, an equivalence of 3 pixels equal to 0.01 m can be defined for this specific infrared measurement. Then, the velocity of the glass gobs loaded at section IS6 can be defined in m/s.

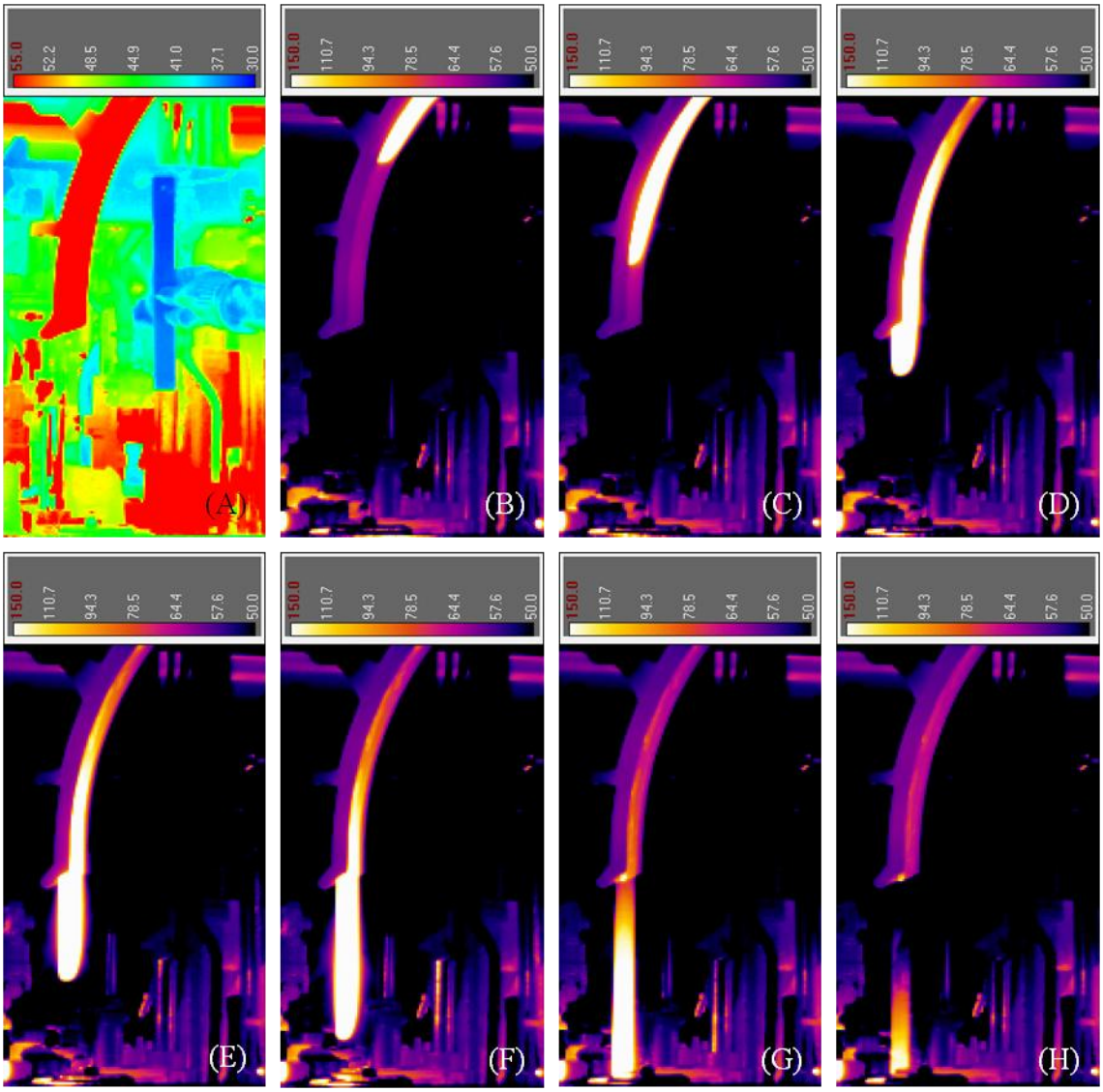

Figure 16. *Delivery of a glass gob into the IS6 blank mold. (**A**) shows the reference dimension of the ruler using a high contrasted thermal palette. (**B**) to (**H**) show some of the frames used to track and measure the loading velocity of the gob at the end of the delivery equipment: (**B**) refers to frame 79; (**C**) to 81; (**D**) to 83; (**E**) to 84; (**F**) to 85; (**G**) to 87 and (**H**) to 89.*

Figure 16 shows different frames describing the delivery of a glass gob into the blank mold. As the ruler was at room temperature, to be able to use it as a reference, the measurements were performed using the low-temperature calibration of the infrared thermal camera (see **Figure 16A**). Then, as the surface of the glass gob was saturated at 150 ºC and a hot spot could not be identified, a different reference point was needed to define the relative displacement of the glass gob between frames. In this case, the position of the bottom of the glass gob has been tracked at every frame. It can also be observed that the gob traveling at high speed leaves a trail behind it due to the limitation of the uncooled microbolometer. The velocity of ten consecutive glass gobs was measured at the end of the delivery equipment of the side section IS6. In this case, the velocity measurements were performed while the gob was traveling through the deflector but also until it was loaded into the blank mold to determine the velocity of the glass gob at the loading stage. As explained before, the deflector mounted on the side sections of the

IS machine does not have a linear section at the end to improve the verticality of the loaded gobs but still, a vertical loading can be observed in the measurements (see **Figure 16F**).

As the reference point used to measure the gob displacement at every frame was the same, consistent velocity measurements of the loaded gobs could be obtained. All the repetitions of the velocity measurements of the gobs loaded at the side section IS6 were almost exactly the same. A small increase in the velocity can be defined as the glass gob passes through the curved section of the deflector, but when the gob leaves the deflector and it falls vertically into the blank mold, the glass gobs have a constant velocity of 5.2 m/s when loaded into IS6. The evolution of the gob velocity measured passing through the deflector is consistent with the previous measurements in pixel/frame units.

The variation in the loading velocity of the glass gobs as a function of the individual section has been a concern in the past. Several authors published experimental measurements of the glass gobs traveling through the delivery equipment and the results are summarized in **Table 4**. As can be seen, most of the measurements were performed on a 12 section IS machine where these issues became more relevant. At the same time, the total height of the IS machine increases with the number of sections to obtain a minimum slope in the troughs of the outermost sections. This results in a higher vertical distance between the orifice ring and the top of the blank molds (e.g. 3.3 m in [2] and 3.6 m in [10]), higher potential energy and therefore higher gob loading velocities compared to a six-section IS machine. A variation of the loading velocities between 5.5 and 7 m/s as a function of the individual section can be observed in [2], which are slightly lower but consistent with the values presented in [10], [14], [22]. The publications [13], [14] present different optimizations in the components of the delivery equipment, obtaining an increase in the loading velocities of the glass gobs up to 8 m/s. The measured values of the gob loading velocity in a six-section IS machine, although smaller due to the lower height of the IS machine and the orifice ring, are considered consistent with the several published measurements performed on larger IS machines.

Table 4. *Published results on the gob velocities measured experimentally at different positions of the delivery equipment.*

Source	Type of IS Machine	Position	Distance from Shears (m)	Velocity (m/s)
[22]	12 section DG	gob loading	-	6.8 – 7.0
[2]	12 section	after shears	0.5	2.5
		trough	1.7	5.2 – 5.6
		deflector	3.3	5.5 – 7.0
[10]	12 section TG with a constant cone of 28º	after shears	0.4	3.0
		trough	1.8	5.4
		deflector	3.2	6.8
		before blank	3.6	7.1
[13]	-	after shears	-	3.8
		trough entry	-	6.5
		middle of the trough	-	6.8
		deflector	-	7.5 – 8.0
[14]	10 or 12 section	blank entrance (old deflector design)	-	6.7 – 7.5
		blank entrance (new deflector design)	-	7.9

(D) Measurements of the Glass Gob Temperature

Until now, the influence of the delivery equipment on the loading conditions has been defined by measuring the delivery time and velocity of the glass gobs at the end of the deflector. According to the description of the delivery influence presented before, glass gobs loaded on the side sections should also present lower temperatures. Since, in addition to the previously defined temperature distributions in the gob forming process, during the delivery, glass gobs accumulate heat losses due to thermal radiation and contact heat transfer with the cold surface of the scoop, troughs and deflectors. Therefore, the longer paths and higher delivery times present in the side sections should result in lower gob temperatures.

Using the FLIR A325sc infrared thermal camera, accurate temperature measurements of the glass gobs cannot be obtained in the delivery equipment, since the high gob loading velocities result in blurred shots and incorrect temperature readings. This problem was detected after the shear blades cut the extruded glass in the gob forming process. However, in the delivery, due to the much higher speed of the glass gobs, the infrared sensor limitations become even more evident. In this sense, a test was performed with a much more sophisticated detector lent by the supplier. A FLIR A6752sc infrared thermal camera equipped with a cooled indium antimonide detector was used to measure the glass gob at the end of the deflector. This detector had an integration time of only 0.127 ms (more than one hundred times less than the FLIR A325sc), which resulted in clear shots of the glass gob at high velocities and consistent temperature measurements when compared with the glass temperatures at the gob forming process. From this test, it was concluded that the blurred shots and incorrect temperature readings were related to the high integration times of uncooled microbolometers. Therefore, only qualitative temperature values will be measured at the delivery with the actual camera.

On the other hand, due to the heat losses in contact with the delivery equipment, it is important to note that the temperature measured on the surface of the glass gob may not be consistent with the glass temperatures within the gob. In this sense, when measuring the gobs from the blank side of the IS machine, the surface of the gob that remains visible at the deflectors is the one that has been previously in contact with the inner surface of the scoop and troughs. Thus, by measuring the glass temperature on the gob surface at the deflector, a disturbance can be observed which may not be representative of the temperature of the glass within the gob. These thermal phenomena were discussed in one of the HVG publications, where the glass temperatures were measured with pyrometers from both sides of the gob [3], the one in contact with the scoop and trough from the blank side and the one in contact with the deflector from the blow side of the IS machine. Temperature variations up to 100 ºC were determined when measuring the gobs from both sides. Even a reheat could be observed on the gob surface visible at the deflector. Nevertheless, these measurements are out of scope due to the limitations of the type of sensor that the infrared thermal camera uses. In fact, even the most recent and budget-unfriendly state-of-the-art industrial applications used to monitor and automatically adjust process parameters related to the gob loading are not capable yet to measure the temperatures in the glass gobs.

Therefore, after presenting all these considerations, qualitative temperature measurements of

the glass gobs while traveling through the deflector of the sections IS1, IS2 and IS3 were conducted with the infrared thermal camera. The temperature measurements were performed following the same methodology as presented in the velocity measurements. The infrared thermal camera was positioned normal to the inner surface of the channel deflector and approximately at the same distance to have comparable temperature measurements at the different deflectors. As the measurements were performed from the blank side of the IS machine, the visible side of the gob was the one in contact with the inner surface of the scoop and trough.

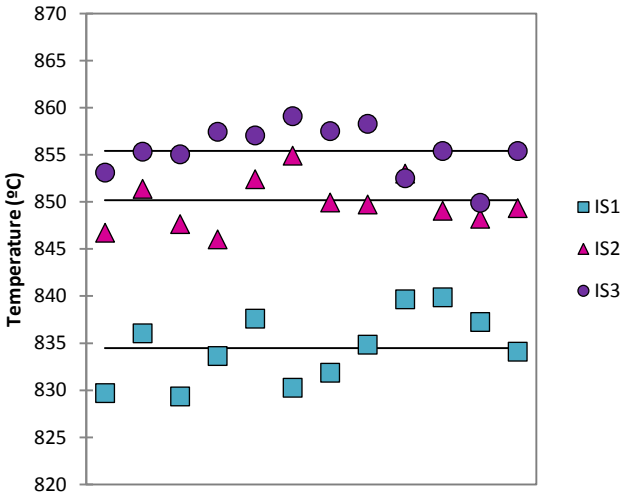

Figure 17*. Maximum glass temperatures on the surface of the gobs measured when being delivered through the deflector of section IS1, IS2 and IS3.*

The maximum glass temperatures were measured on 12 consecutive gobs delivered at sections IS1, IS2 and IS3. The results are presented in **Figure 17**. Horizontal lines with the average temperature values in the glass gobs delivered to the different individual sections of the IS machine have been plotted too. Each series of results show a variability of the temperature values under ±5 ºC which is considered an acceptable repeatability. Nevertheless, it can be seen that the sensibility of the temperature measurements on the glass surface is much greater than other glass properties measured before (e.g. the delivery time or the velocity) where the variability was almost zero. Glass gobs loaded at the side section IS1 show lower temperature values than gobs at IS2 and the middle section IS3. AS expected, when the side and middle sections are compared, the longer trough and the reduced delivery velocity result in a prolonged contact between the glass gob and the inner cavity of the trough and a decrease in temperature is detected on the glass surface. Although only qualitative temperature values could be measured at that stage of the process, it can be observed that the dependency of the gob properties as a function of the position of the individual section against the machine centerline is also present in the temperatures measured at the surface of the glass gob.

3.4 CONCLUDING REMARKS

As has been stated, there is not an extensive collection of publications dealing with the gob forming process. Only one set of publications about experimental temperature measurements of the glass gob was found in the literature. In that study axial, radial and angular temperature distributions of an amber glass gob measured below the shear blades were presented along with explanations of the possible causes of the temperature non-uniformities. Few publications related to numerical models of the gob forming process complete the information available. From the literature, it can be stated that the main causes of the thermal deviations present in a glass gob after being cut are: strong temperature profiles present or induced inside the feeder due to temperature non-uniformities in the glass delivery, distortion of the flow related to the rotating tube and uncontrolled heat losses. Radiative heat losses with the environment are also present once the glass gob is extruded.

Using the methodology presented in **Chapter 2**, an infrared thermal camera was used to measure the evolution of the glass temperatures during the gob forming process under industrial manufacturing conditions. From the infrared thermal measurements presented in Case 1 and Case 2, it can be concluded that the maximum temperature values on the surface of the glass gob increase over time as the glass is being extruded through the orifice ring. This phenomenon is not explained by the experimental bibliography; provably this has gone unnoticed by measuring the temperatures after the gobs were cut instead of during the glass extrusion. Thus, an in-depth analysis of the measurements presented in Case 2 was performed in the first part of this chapter to obtain a better understanding of the thermal phenomena occurring during the glass extrusion of the gob forming process.

The position and temperature of several sections of the gob were tracked during the gob forming process. Then, the length of the extruded molten glass was defined. As the orifice ring remained constant, the relative increase of the gob length over time was proportional to the extruded glass flow, which showed a linear increase during the gob forming process. In turn, the maximum glass temperature at the most freshly extruded glass gob section also showed a linear increase during the gob extrusion, revealing that the probable cause of this increase in temperature was the increase of the extruded glass flow. Therefore, the unexpected temperature increase was related to the reduced influence of the heat losses present at the spout and the orifice ring area due to the increase in the flow of extruded glass. On the other hand, studying the temperature evolution of the several tracked sections of the gob it was concluded that once every glass gob section was extruded, it started having radiative heat losses, resulting in a local temperature decrease in these sections. As the glass was extruded continuously over time during the gob forming process, once the entire gob was extruded, the bottom of the gob accumulated more radiative heat losses in comparison with the top, which was extruded in the last moment. These thermal phenomena, together with the increase in flow, resulted in an axial temperature distribution along the surface of the extruded glass gobs. In addition to that, it was stated that temperature non-uniformities in molten glass could even be defined before the gob forming process, taking place inside the feeder and also coming from the delivery channel. Numerical simulations of the previous process would give more information about the temperature deviations within the glass domain. So, it is clear that after the forming process the glass gobs are not thermally uniform, as many thermal phenomena conditioned the temperature distribution

before, during and after the gob forming process.

To summarize, in the first part of this chapter a thermal analysis of the temperature distributions within the glass gob was performed under different industrial conditions to gain a better understanding of the thermal phenomena that occur during the gob forming process. On the other hand, to define how conditioned the temperature distribution will be when the gob is loaded into the blank mold additional thermal measurements are necessary after the gob forming process, during the gob delivery and loading operations. This leads to the second part of this chapter, where the properties of the glass gobs were measured traveling through the delivery equipment.

The delivery equipment distributes the freshly extruded glass gobs vertically and horizontally using the scoop, troughs and deflectors from the orifice ring to the blank mold of each individual section of the IS machine. The conditioned molten glass is severely disturbed during the forming and delivery operations of the gob, defining a temperature and viscosity distribution within the glass gob before the container forming process. A non-optimal delivery results in higher heat losses, more friction and a reduction in the loading velocity of the gob. These issues became more relevant in larger machine configurations where the gob needs to travel a longer horizontal distance. As many deviations obtained at this step of the glass forming process cannot be later corrected, these deviations have an impact on the properties of the final container, resulting in a variability in the quality of the manufactured containers throughout a production. For this reason, the delivery time, velocity and temperature of the glass gobs have been experimentally measured as they travel through the deflectors at the end of the delivery equipment. Variations in the loading conditions of the glass gob have been determined as a function of the length of the delivery equipment and the relative position of the individual sections and the centerline of the IS machine.

In summary, it can be concluded that there is a clear deviation in the loading conditions of the glass gob as a function of the individual section position when measured in a six-section IS machine. Comparing IS1 and IS3 it can be defined that: the side section troughs are 100.0% longer than the middle section ones and the side section deflectors are 22.2% shorter; then, there is an increase in the total length of the delivery equipment on the side sections of a 23.1%; finally, the slope of the troughs on the side sections is also lower. All this results in a consistent increase in the delivery time of the glass gobs loaded at the side sections between 8 and 10%. Although the absolute variation of the delivery time is small, it defines a longer contact time between the glass gob surface and the walls of the blank mold cavity at the initial stage of the container forming process. At the same time, as a result of the longer delivery equipment, prolonged contact and more friction in the glass gobs loaded at the side sections, the loading velocity is also reduced around 16% when the side and middle sections are compared. The measured values of the gob loading velocity, although lower due to the IS machine dimensions are consistent with the published measurements performed on larger IS machines. Finally, only qualitative temperature measurements on the surface of the glass gobs before loading into the blank mold were possible using the uncooled sensor of the infrared thermal camera. Nevertheless, it could be observed that the dependency of the gob properties as a function of the position of the individual section was also present in the temperature readings. The delivery equipment dimensions and the measured properties of the gobs loaded in sections IS2 and IS5 are in all the cases halfway between the values presented for the side (IS1 and IS6) and the middle (IS3 and IS4) sections.

Finally, it has been theoretically and experimentally stated that there is a significant deviation in the loading conditions of the glass gob as a function of the loading position, even in a small six-section IS machine. This can lead to a variability in the quality of manufactured containers. In fact, by analyzing the defects and thickness distribution in the containers manufactured throughout a production, a variability can be determined empirically. However, it is very difficult to relate this variability with the loading deviations, since the variability in container defects is random and does not obey a pattern related to the position of the individual sections where the containers were produced. Therefore, it cannot be defined a relationship between the quality issues of the glass perfume containers and deviations in the loading conditions due to differences in the delivery equipment. During the container forming process there might be other deviations from undefined sources that result in the perceived variability in the container quality bigger than the probable deviations induced by the loading conditions of the glass gobs. This phenomenon will be treated again during the gob drop tests presented in **Chapter 4**.

To summarize, in this chapter an in-depth study of the thermal conditions of the glass gob was presented. However, the container forming process starts when the gob is loaded into the blank mold. Then, the glass gob will remain inside the blank cavity, without the possibility to be seen again until the parison is transferred to the blow mold. The approximations that will be used to describe the heat transfer phenomena in the numerical model were presented in **Chapter 2**. However, the difficulties to perform infrared measurements inside the mold cavities will be a limiting factor to validate the glass temperatures predicted by the numerical model of the blow and blow forming process. These problems will be addressed in **Chapter 4**, before modeling the blow and blow glass forming process.

3.5 REFERENCES

[1] G. Bergmann and H. Müller-Simon, "Measurement of the temperature distribution in glass melt gobs after cutting," *Glas. Technol. - Eur. J. Glas. Sci. Technol. Part A*, vol. 51, no. 6, pp. 231–234, 2010.

[2] H. Müller-Simon, G. Bergmann, and K. Kessler, "Temperature Distributions in Glass Gobs Between Shears and Blank Mold: Calculations and Measurements," in *Conference on Glass Problems*, 2010, vol. 31, no. 1, pp. 151–158.

[3] G. Bergmann, H. Müller-Simon, N.-H. Löber, and K. Kessler, "Changing of Gob Temperature From Spout to Blank," in *Conference on Glass Problems*, 2012, vol. 33, no. 1, pp. 147–158.

[4] M. R. Hyre and K. Paul, "The Effect of Shear Angle on Gob Formation," *Conf. Glas. Probl.*, pp. 87–107, 2000.

[5] "Emhart Glass Technical News Bulletin 71: Metering Spout Systems," 2002.

[6] M. R. Hyre and A. L. Harrison, "Effect of Feeder Design and Operation on Gob Shape," in *6th European Society of Glass, Monpellier, France.*, 2002.

[7] M. R. Hyre, "Numerical Simulation of Glass Forming and Conditioning," *J. Am. Ceram. Soc.*, vol. 85, no. 5, pp. 1047–1056, 2002.

[8] M. K. Choudhary, R. Venuturumilli, and M. R. Hyre, "Mathematical Modeling of Flow and Heat Transfer Phenomena in Glass Melting , Delivery , and Forming Processes," *Int. J. Appl. Glas. Sci.*, vol. 1, no. 2, pp. 188–214, 2010.

[9] O. O. Den Camp, D. Hegen, G. Haagh, and M. Limpens, "TV Panel Production : Simulation of the Forming Process," in *Conference on Glass Problems*, 2003, vol. 24, no. 1, pp. 1–19.

[10] X. J. Liu, M. R. Hyre, G. S. Frost, and S. A. Austin, "Numerical Simulation of Heat Transfer for the Gob Delivery System in Glass Container Production," in *ASME International Mechanical Engineering Congress and Exposition*, 2008, vol. 10, pp. 569–576.

[11] A. Biosca, S. Borrós, V. Pedret, and A.-A. García, "Glass Gob Modeling and Experimental Validation Using a Drop Test," in *MATEC Web Conf. (IC4M)*, 2018, vol. 167, pp. 1–6.

[12] P. Giacobbo, "Optimization of the Ultralight Glass Container Production Process," in *1992 International Glass Packaging Forum*, 1992.

[13] B. McDermott, X. Ding, and J. Simon, "Characterization and Improvements of Gob Delibery Systems," in *Conference on Glass Problems*, 2011, vol. 32, no. 1, pp. 195–202.

[14] K. Hiltmann and T. Neubauer, "Case study: Gob loading in a glass moulding machine," in *Procedia CIRP*, 2016, vol. 39, pp. 203–208.

[15] "Emhart Glass Technical News Bulletin 280: Enhaced Gob Loading, Constant Cone Bezier Delivery," 2019.

[16] "Emhart Glass Technical News Bulletin 235: Constant Cone Delivery, Enhanced Gob Loading & Flexible Change of Setups," 2015.

[17] P. Schreuders, "Gob Assist: a lot to gain!," *Glass Worldwide*, vol. July, 2010.

[18] L. Barel, "When Gob Weight Monitoring Opens the Way Towards Glass Container Weight Decrease," *Glass Machinery Plants & Accessories*, no. 3, pp. 34–38, 2014.

[19] "Emhart Glass Technical News Bulletin 215: Temperature Control System - TCS," 2012.

[20] "Emhart Glass Technical News Bulletin 265: Blank Radar," 2018.

[21] J. Simon and B. McDermott, "Closed Loop Control of Blank Mold Temperatures," in

Conference on Glass Problems, 2012, vol. 33, no. 1, pp. 167–175.
[22] "Emhart Glass Technical News Bulletin 44: Deflector Series 18000," 1996.

CHAPTER 4
NUMERICAL AND EXPERIMENTAL STUDIES TO MODEL THE BLOW AND BLOW CONTAINER FORMING PROCESS

4.1 INTRODUCTION

As defined in **Chapter 1**, this thesis aims to implement a numerical model that predicts the thermo-mechanical behavior of glass during the blow and blow forming process to define the glass thickness distribution of the manufactured containers. This is a very ambitious proposal as physical and thermal phenomena modify the temperature, viscosity, flow and geometry of the glass domain during the container forming process. Ramon Clemente has been producing glass perfume containers for almost a century. Despite the accumulated experience in glassmaking, due to the complexity of industrial production, a better understanding of the blow and blow forming process is still required. To achieve this goal, craftsmanship and empirical knowledge in glassmaking must be translated into scientific knowledge. In other words: the operation of the IS machine, material properties and physical, thermal and mechanical phenomena present in the container forming process need to be modeled using mathematical equations.

The evolution of numerical models applied to the glass forming process has been extensively reviewed in the past [1], [2]. The first attempts to apply the use of numerical simulations in the glass industry were performed during the 1980s. The first study modeling the container forming process was presented in 1984. It was a simulation limited to the final blow operation of a pressed parison [3]. However, it was a starting point to evaluate the feasibility of numerically predicting the container forming process. These results encouraged few glass companies to work on the problem and in 1986, the International Partners in Glass Research (IPGR) commissioned the development of an axisymmetric numerical model to simulate the coupled thermo-mechanical press and blow forming process [4]. This model included both the blank and blow sides, allowing the effects of the pressing operation at the blank mold to be followed to the

blow side and final container. In the 1990s many advances in the development of numerical techniques together with an improvement in computational capabilities allowed taking a numerical approach to study the manufacture of glass containers. Thus, in the new century, very powerful results were obtained with the integration of all the operations in the forming process [5], [6]. These studies coupled several numerical models and also included accurate experimental measurements to validate the predicted results.

The presented numerical advances, together with improved sensors and new measurement technologies to perform more precise experimental studies in the production line, led to a better understanding of the glass flow and heat transfer phenomena during the container forming process. As a result, several authors in the glass industry started using numerical models to study several topics. For example, numerical simulations were used to determine the causes of container defects and find solutions to improve production rates [7]. Also to validate experimental studies of thermal and mechanical properties at the glass-mold contact interface [8]–[10] and to define how the use of lubricants is related to heat transfer [11] and friction coefficients [12]. On the other hand, numerical models were used by different authors for predicting and optimizing different parameters of the production process, such as mold temperatures in conjunction with vertiflow cooling systems [13]–[16]. Optimization techniques were also used to improve the mechanical properties of glass containers while reducing their weight [17], [18]. Despite the importance of aesthetics in glass perfume containers, only a few authors presented numerical results on the prediction of glass thickness distributions of manufactured containers [19]–[22]. Moreover, hardly any results about numerical simulations were based on glass containers for the perfume industry [23], [24]. Finally, reverse engineering algorithms were also presented to optimize the design of the blank mold cavities using Bezier curves for perfume bottles [24] but also glass containers [25].

In summary, it can be stated that many publications presented numerical models of the NNPB forming process; probably, as detailed in **Chapter 1**, because most of the world production of glass containers is for the food and drink industry. However, despite differences in the gob loading and parison forming stages, the production process remains very close to the blow and blow forming process. In addition, it can be concluded that many authors were only interested or limited to the numerical approach of the problem, neglecting the importance of experimental measurements under industrial conditions to define and validate the numerical model and the simulation results. Although process conditions may have been provided by glass manufacturers in some cases, they did not pursue an actual validation of the numerical model, presenting only numerical results for generic simulation cases.

Therefore, there is a significant lack of literature defining actual process conditions, relevant material properties and boundary conditions; or comparing both numerical and experimental results, for example presenting cross-section profiles of manufactured glass containers to demonstrate the reliability of the numerical model defining glass thickness distributions. In this sense, it is also evident that as happened during the last centuries, glass manufacturers are not interested in revealing their secrets on journal publications. Therefore, **this will be one of the important contributions of this thesis to the field, presenting a sincere discussion about the experimental and numerical studies carried out to obtain results in the prediction of thickness distributions.**

At this point in the thesis, the challenges in modeling the blow and blow forming process

have been presented; in fact, many of them have already been covered in the previous chapters. Nevertheless, once the container forming process is modeled, its numerical solution also presents important challenges as large free surface deformations, complex contact phenomena, high-temperature dependent viscosity, conjugate heat transfer or evolving coupled boundary conditions at the glass-mold contact interface, etc. Moreover, although a few examples of numerical models were presented above, most of them were developed by glass manufacturers, so any information could be shared. For these reasons, and due to the limited experience in this kind of simulations at the beginning of this thesis, a collaboration with CIMNE (International Centre for Numerical Methods in Engineering) was initiated to carry out initial simulations of the counter and final blow stages. In this sense, an isothermal and axisymmetric model based on their particle finite element method (PFEM) [26], [27] was used to evaluate the capabilities to succeed in the numerical prediction of the glass flow.

In particular, numerical simulations of the counter blow stage were initially performed with PFEM. These simulations described the isothermal expansion of the glass inside the blank mold cavity during the counter blow stage; obtaining, as a result, the distribution of glass in the parison. As expected, different process conditions and blank mold cavities resulted in variations in the predicted geometry of the glass domain. In addition, CIMNE also developed and implemented an automated two-stage simulation to couple the numerical results of the counter and final blow stages. In this case, the predicted geometry of the counter blow simulation was automatically introduced as the initial geometry of the glass domain in the final blow simulation, obtaining the glass thickness distribution of the manufactured container. However, despite the promising initial results to numerically predict the flow of glass in the counter blow simulations using the isothermal model, when both operations were numerically coupled, the thickness distribution obtained as a result was far away from the expected. Then, the importance of using a numerical model with non-isothermal formulations became evident. Therefore, glass viscosity as a function of temperature must be characterized and implemented in the numerical model to couple the thermo-mechanical phenomena within the glass domain. In fact, CIMNE also had a non-isothermal model to predict the thermal evolution of the glass domain during the blowing simulations. However, relevant difficulties experienced with that non-isothermal model to handle heat transfer phenomena and temperature distributions at the glass-mold domain interface, as well as the lack of flexibility to simulate other cases apart from the blowing operation, led to dismiss the use of the PFEM software for the following steps of this thesis.

So far, relevant experience in numerical simulations was acquired working with CIMNE. At the same time, the shortcomings in their numerical model made evident the steps to be taken to implement and validate a reliable numerical simulation. For these reasons, a robust software with a much more flexible [5] and friendly environment as ANSYS Polyflow was chosen to continue modeling the glass flow and its thermo-mechanical behavior. In addition to the presented numerical difficulties, once preformed these simulations with CIMNE, it was also stated the importance of obtaining even more experimental information from the industrial process. This is because simulations require many input values sensitive to the glass conditions (i.e. material properties, process temperatures and heat transfer phenomena at the boundary conditions) to obtain an accurate prediction. In fact, the development of a numerical model and the accuracy of its results are often limited to the possibilities of experimental validation, which are extremely difficult under industrial manufacturing conditions. So, in order to obtain accurate simulation results, accurate input values must be previously defined from Ramon Clemente container production lines.

This leads to many of the tasks already covered in the previous chapters to model the glass forming process. In this sense, the operation of the industrial manufacture of glass perfume containers was detailed in **Chapter 2**. Along with that, a framework was presented characterizing the material properties, heat transfer and boundary conditions necessary to model the glass domain. However, heat transfer phenomena and boundary conditions must be related to the real production process and glass thermal conditions. These are two key phenomena to successfully describe glass behavior in a numerical model. For this reason, a methodology was defined to perform experimental measurements of the glass temperature. Thermal analyses of the glass at the forming, delivery and loading operations were presented in **Chapter 3**. There, infrared temperature measurements were performed to study the conditions of the loaded glass gobs at the start of the container forming process. Therefore, at this point, many of the shortcomings related to the lack of experimental data present in the simulations with CIMNE have already been successfully addressed.

However, once the numerical model is properly defined, much more information is required to validate the results of the simulations. As presented in **Chapter 3**, experimental measurements were performed to determine the loading conditions of the glass gobs, including the thermal conditions of the glass at the start of the container forming process. As previously defined, two blowing stages modify the glass geometry in the blow and blow forming process. First, the counter blow transforms the glass gob into a parison inside the blank mold. Later, the final blow expands that parison into the shape of the final container inside the blow mold. However, once the glass gob is loaded into the blank cavity, many thermal phenomena condition the glass temperature. Then, when the counter blow is about to start, the initial temperature distribution of the glass gob previously defined has evolved. That second temperature distribution, which results, in turn, in a viscosity distribution, is the one that governs the glass flow at the counter blow stage.

Therefore, the blank mold design and the heat transfer during the initial dwell time define the temperature and geometry of the glass parison; which after the final blow, will result in the thickness distribution of the manufactured container. As presented, the thermo-mechanical behavior of glass is very complex to model, as several thermal phenomena take place inside the mold cavities, even before start blowing. At the same time, as the glass is not accessible inside the mold cavities, very limited information can be obtained from the intermediate states. Thus, an easier and more controlled problem needs to be defined to implement and evaluate a non-isothermal numerical model in ANSYS Polyflow, that is, coupling the glass viscosity with the thermal conditions and heat transfer phenomena present in the forming process to describe the thermo-mechanical behavior of glass. In this sense, a glass gob drop test has been defined.

This gob drop test will consist of welding a cast iron plate on the top of a funnel arm. This arm will be mounted in one section of the IS machine and blocked in the loading position. For security reasons, the remaining operations of that section will also be blocked. Then, following the normal operation of the delivery equipment, glass gobs will be loaded on that plate to define a very visual description of the glass flow as a function of the glass temperature and viscosity. There are several reasons to perform a drop test. First, the ease to observe the glass and measure its properties compared with the difficulties presented during the container forming process. The glass gob is visible during all the operations previous to the drop test, so it can be experimentally measured with the infrared thermal camera to define the initial conditions of the

numerical simulation. On the other hand, this is a much simpler problem to be modeled. Although temperature variations may be present due to heat losses by thermal radiation and contact conductance with the delivery equipment, once the initial conditions of the glass gob are determined, the main heat transfer phenomenon during this test will be the contact conductance between the glass and the cast iron plate after the impact. At the same time, kinetic energy present on the loaded gob will be dissipated during the impact, resulting in the deformation of the glass gob geometry. This glass deformation, as occurs on the cast iron plate, can also be experimentally recorded with the infrared thermal camera.

For all these reasons, a glass gob drop test is a very interesting numerical simulation case to start with ANSYS Polyflow. This initial case will be used to solve many modeling and data acquisition issues, defining the thermo-mechanical behavior of glass using the characterized viscosity and the VFT equation and experimentally defining the initial loading conditions of the glass gob based on the measurements presented in **Chapter 3**. Furthermore, a better understanding of the numerical simulations using ANSYS Polyflow will also be obtained. In this sense, numerical simulations of the glass gob drop test will be performed using Newtonian non-isothermal formulations and the characterized glass viscosity to describe the glass flow over time and as a function of its temperature and viscosity. All the learned knowledge in this "small scale" problem will later be applied to the much more complex simulations of the blow and blow glass forming process. Finally, as the deformation of the glass gob will be recorded using the infrared thermal camera, a validation of the numerical model will be performed establishing a correlation between the numerical and experimental deformation of the glass gobs after the impact with the plate.

To summarize, after successfully conducting thermal analyses of the glass gobs with the infrared thermal camera and due to the difficulties encountered in the non-isothermal simulations performed with CIMNE, another study involving glass gobs will be carried out. Nevertheless, this study will not only be experimental, but also numerical simulations will be conducted. Therefore, in the first part of this chapter, a glass gob drop test has been specially designed to validate the numerical model in ANSYS Polyflow before start working again with the simulations of the blow and blow forming process.

Once the non-isothermal formulations have been successfully validated to predict the dependence of the glass viscosity on the temperature and other glass material properties, simulations of the blow and blow forming process will be carried out. This time, the numerical model used in the glass gob drop test, will be adapted to describe the manufacture of glass perfume containers. Therefore, in the second part of this chapter, numerical and experimental studies of the blow and blow container forming process will be performed to predict the glass thickness distribution of the final container. In this sense, to validate the numerical model, the simulation results will be correlated with experimental infrared measurements of the glass temperature and the thickness distribution obtained sectioning containers manufactured in the production line.

Ramon Clemente produces a very broad range of glass perfume containers, including different capacities, weights, geometries, etc. which also results in a wide range of manufacturing conditions depending on the container requirements. Therefore, since the numerical model must support the development of new glass perfume containers, it was very relevant to demonstrate the influence of blank mold cavity design and industrial manufacturing

conditions on the numerical results of glass thickness distribution in the final containers. For this reason, to validate the blow and blow numerical model under different conditions, two very different perfume bottles from Ramon Clemente and several mold designs have been selected. These two examples are representative of the broad variety of perfume containers manufactured by Ramon Clemente and its forming process conditions. In this sense, the choice of these two perfume containers to ensure that the numerical model could handle glass-forming simulations in a wide range of scenarios was made covering the aspects presented in **Table 1**.

Table 1. *Relevant specifications of the glass perfume containers selected to cover a wide range of industrial manufacturing conditions.*

	SIERRA 60	**ALFA 200**
Brimful capacity (ml)	68	211
Glass weight (g)	95	293
Production machine rate (bpm)	58	32.3
time to produce a single container (s)	11.1	20.7
External bottle volume (ml)	107.5	328.5
Cross-sectional area (cm^2)	31.6	72.5

Both containers had a similar mass-capacity ratio. However, the desired aspect for both containers once manufactured was very different. Therefore, different approaches in the design of each container and its blank mold cavity were taken into account. In the case of SIERRA 60, it was intended to obtain a light container with a uniform glass thickness distribution throughout its section profile. Thus, the main priority during its development was to avoid thin and fragile areas, especially at the edges of the bottle. On the other hand, ALFA 200 followed the opposite principle, as an overweighed aspect was desired to enhance the aesthetic properties of the glass packaging. In this sense, several manufacturing tests using different blank molds were performed to obtain a thick base, trying to gather a large accumulation of glass at the bottom of the container using a limited weight of glass.

On the other hand, the process conditions of the industrial manufacture depend to a large extent on the shape and weight of the manufactured glass container. Therefore, the production machine rate, process temperatures, glass conditions and operation times of the IS machine must be adjusted accordingly to obtain a tailor-made parison for each container. In this case, SIERRA 60 bottle is three times lighter than ALFA 200 bottle. This results in a much more faster production rate, as the lower mass of glass results in less thermal energy stored within. So, shorter dwell times inside the mold cavities are required to manufacture that container. These differences in the glass conditions and the machine operation times were taken into account when defining the numerical simulations of each container.

Finally, due to the relevant differences between both containers and their manufacturing conditions, the numerical parameters used in both simulations were also different. In this sense, two scales of time and space were defined for each case. Depending on the size of the glass domain and the total simulation time, different values of mesh size and time step were necessary to keep computation times reasonable without compromising the accuracy of the predicted results. The different time scale of each simulation, defined by the *time to produce a single container* in the IS machine, was especially relevant in the definition of the boundary conditions of the glass domain. Since as presented in **Chapter 2**, the heat transfer coefficient at the glass-mold contact interface was defined in the numerical model as a function of contact time.

To summarize, many of the tasks necessary to model glass behavior were covered in the

previous sections. Now is the time to reach the main goal of this thesis. Therefore, the objective of this chapter is to **perform different numerical and experimental studies to model and validate the blow and blow container forming process to predict the glass thickness distributions of the manufactured containers**. The implemented simulation tool will be used by Ramon Clemente to support the design of the blank mold cavities and the definition of the machine operation times in their new developments while reducing the amount of trial and error testing.

To achieve this objective, the following tasks were proposed:

- Build a non-isothermal model on ANSYS Polyflow to describe the thermo-mechanical behavior of the glass gobs during the impact on a cast iron plate.

- Conduct experimental glass gob drop tests and record them with the infrared thermal camera to correlate and validate the predicted results by the numerical model.

- Perform a numerical and experimental study to simulate the blow and blow container forming process with different containers and validate the obtained glass thickness distributions.

- Define the significance of numerical results to support the development of new glass perfume containers by Ramon Clemente.

4.2 METHODOLOGY

The methodology presented in **Chapter 2** was applied again to obtain thermal information of the glass in different stages of the forming process. In particular, a FLIR A325sc infrared thermal camera was used to measure experimental temperatures on the surface of the glass gob, parison and manufactured containers at several stages of the following operations:

3. During the impact of the glass gobs loaded against a cast iron plate at the gob drop test, to record the deformation of the molten glass on the plate.
4. After the gob is loaded into the blank mold, to evaluate the temperature of the glass gob as initial value for the numerical simulations of the gob drop test.
5. At different stages of the blow and blow container forming process where glass is visible, to measure the glass temperatures over time as the container is being manufactured (e.g. gob loading, parison inversion, etc.).

Infrared thermal measurements of the glass gob drop test were performed from the blank side of the IS machine, following exactly the same methodology as when studying the loading conditions of the glass gobs in **Chapter 3**. On the other hand, to study the blow and blow forming process, infrared measurements from the blank side were complemented with additional experimental studies from the blow side of the IS machine. From there, the blow mold operation and all the manufactured glass containers can be easily observed. Although parison inversion takes place outside both mold cavities and it can be observed from both sides of the IS machine, it is one of the most complex operations to be experimentally defined. This is due to the high velocity of the inversion, reheating of the glass parison and difficulties to extract physical glass samples without modifying the parison geometry. Then, additional infrared measurements from the sides of the IS machine were carried out when possible.

All the experimental data obtained from the glass gob drop tests and the industrial manufacture of glass containers was used to define the initial conditions of the glass domain in the numerical model. In addition, once the numerical results were obtained, more experimental data was used to validate the predicted results as will be presented through this chapter. In the second part of this chapter, along with the mathematical equations used in the numerical model of the blow and blow forming process, a detailed description of the many information required to perform a single numerical simulation is presented, including the geometry of the mold cavities and glass domain, glass material properties, boundary conditions, machine operation times, process conditions, glass and mold temperatures, etc. Once validated, the material properties, mathematical formulation and boundary conditions will be the same. However, the other parameters are specific to the manufacture of each container and must be defined again for each new simulation case.

4.3 RESULTS AND DISCUSSION

4.3.1 NUMERICAL AND EXPERIMENTAL GLASS GOB DROP TEST

In this section, the results of the glass gob drop test will be discussed. Performing numerical and experimental studies of the gob drop test will be very useful to validate the dependence of the glass viscosity on the temperature. First, during the drop tests, experimental information is recorded with the infrared thermal camera as presented in the previous chapters. Then, numerical simulations of that gob drop test are also conducted. Finally, both numerical and experimental results are compared. As a result, an accurate description of the thermo-mechanical behavior of the glass flow using non-isothermal formulations with ANSYS Polyflow is presented.

(A) Experimental Analysis of the Gob Drop Test

Glass gob drop tests were performed at the blank side of the IS machine, following the normal operation of the delivery equipment to reproduce the loading conditions of the gob in the container forming process. A plate made from the same cast iron used for the blank molds was machined to obtain a surface finish similar to the mold cavities. This plate was welded on the top of a funnel arm, which was mounted in an individual section of the IS machine. The arm was blocked in the loading position; for security reasons, the other operations of that individual section were also blocked. Then, glass gobs delivered through the delivery equipment were loaded on that cast iron plate to conduct several drop tests. These tests were recorded with the infrared thermal camera to define a very visual description of the glass flow as a function of its temperature and viscosity. In addition, the loading conditions of the glass gobs were determined following the same methodology as presented in **Chapter 3**. Finally, the initial temperature of the glass gob and its evolution after the contact with the cast iron plate were also determined.

Gob drop tests were performed on a six-section IS machine. This allowed using glass gobs formed under the same conditions to perform drop tests at the middle and side sections of the IS machine, to study if deviations present in the loading conditions as a function of the loading position had any influence on the glass deformation after the drop test. In this sense, the loading conditions of the gobs were measured again at the end of the deflector at each individual section of the IS machine. As expected, measurements of the delivery time, impact velocity and glass temperature were consistent with previous experimental measurements presented in **Chapter 3.** Delivery time of gobs loaded at the side section was longer than in the middle section and impact velocities showed slower values when compared to the central sections of the IS machine. On the other hand, previous limitations in obtaining accurate temperature measurements of the glass gobs due to high loading velocities were not experienced in this case. After the impact of the gobs with the cast iron plate, precise temperature measurements could be conducted on the glass surface. Gobs loaded at the side sections also showed lower temperatures when compared to the ones loaded at IS2 or IS3. As previously determined, side section gobs tended to accumulate more heat loses due to an increase in the delivery time and extended

contact with the delivery equipment. Nevertheless, because of the blurred shots before the impact, it was not possible to define any variation on the length and diameter of the glass gobs loaded in the side sections in relation to an increase in friction with the delivery equipment.

(B) Modeling and Numerical Simulations of the Gob Drop Test

After conducting experimental glass gob drop tests at the production line, an axisymmetric and non-isothermal model of the drop test was also implemented in ANSYS Polyflow. The numerical model described the impact of the gob against a cast iron plate and the subsequent deformation of the glass gob geometry. This was a simple simulation case to start with, as potential energy was converted into kinetic energy to define the impact velocity of the gob. Then, that stored energy was dissipated during the impact, resulting in the deformation of the glass domain. At the same time, the flow of glass on the cast iron plate was defined by its viscosity and temperature distribution, which was influenced by the heat transfer between the glass and the plate.

The numerical model defined in ANSYS Polyflow consisted of two domains. A generalized Newtonian non-isothermal material was used to define the glass domain. Glass viscosity dependence on temperature was defined with the externally characterized viscosity and the VFT equation. Other glass properties were also set, including density, thermal conductivity and heat capacity per unit mass. The initial geometry of the glass domain was assumed as a cylinder with rounded edges, defined by the length and diameter of the gob. Diameter of the gob was defined between the hole of the orifice ring and the funnel diameter. Finally, the volume of the glass domain was defined in concordance with the weight of the glass container manufactured during the drop test. On the other hand, the domain of the cast iron plate was also described as non-isothermal. The geometry and position of the plate were completely fixed throughout the simulation. To define the thermal contact at the glass-plate interface, material properties of the cast iron blank molds were used to set the material properties of the plate domain. Density, thermal conductivity and heat capacity per unit mass were specified in this case.

As previously stated, much information is required to define the initial conditions of the numerical simulations. Therefore, infrared measurements of the glass gob drop tests conducted at the side and middle sections were used to define relevant information of the glass domain. In this sense, impact velocities were defined from the loading velocities of the glass gobs. Infrared thermal measurements were also performed to determine the initial temperature of the glass domain. During delivery and loading operations, glass accumulated heat loses due to contact conductance with the delivery equipment and thermal radiation. Then, different temperatures were experimentally measured on the surface of the drop-tested gobs as a function of the individual section where it were delivered. However, the temperature of the glass inside the gob was considered uniform. Thus, a temperature distribution was defined within the glass domain by conducting a transient cooling simulation on the gob surface during the delivery time prior to the impact with the cast iron plate. Then, after the impact, heat transfer phenomena were described as a contact conductance at the glass-plate interface and radiation heat losses from the glass surface.

Due to the extreme high deformations suffered by the glass domain during the impact with

the cast iron plate, an adaptive remeshing technique was used to control the quality of the mesh elements of the glass domain after each time step. Volume conservation was also verified so as not to modify the initial volume of the glass domain at the end of the numerical simulation due to continuous remeshing. Planes of symmetry were used whenever possible to reduce the computational cost of the numerical simulations, so only one section was required to carry out simulations with the axisymmetric model.

(C) Comparison of the Numerical and Experimental Results

Numerical simulations of the glass gob drop test were successfully carried out in ANSYS Polyflow. Different stages were taken into account to describe the glass gob drop test in the numerical model. Before comparing both numerical and experimental results, a description of the numerical simulation is detailed. The simulation started with the glass gob at a determined height and zero velocity. Then, the gob accelerated with a free-fall movement until the impact velocity was obtained before reaching the plate. Subsequently, the glass gob impacted the surface of the cast iron plate. During the impact, the geometry of the glass domain experienced an extreme deformation flowing over the surface of the plate. As a result, the initial shape of the glass gob ended up being a kind of amorphous medallion. After a few seconds, glass stopped flowing due to its viscous behavior and the heat transfer at the glass-plate contact interface.

Figure 1 shows some representative numerical results of the glass domain obtained at different simulation time steps. A local scale was used in the temperature contours in each figure, to appreciate initial small temperature gradients within the glass domain, but also large temperature distributions present in the final time steps of the simulation (see **Figures 1A** and **1E,** respectively). In particular, **Figure 1A** shows the glass gob before the impact, with a temperature distribution based on the experimental infrared measurements. **Figures 1B** and **1C** are intermediate simulation steps that describe the initial deformation of the glass gob due to the impact energy. In **Figure 1D,** most of the energy was already dissipated in the deformation of the gob. However, glass continued flowing over the plate surface due to its high temperature and low viscosity. After the impact, the contact conductance at the glass-plate interface defined a heat transfer from the glass to the cast iron plate. Thus, there was an increase in the glass viscosity over time and then glass stopped flowing (see **Figure 1E**).

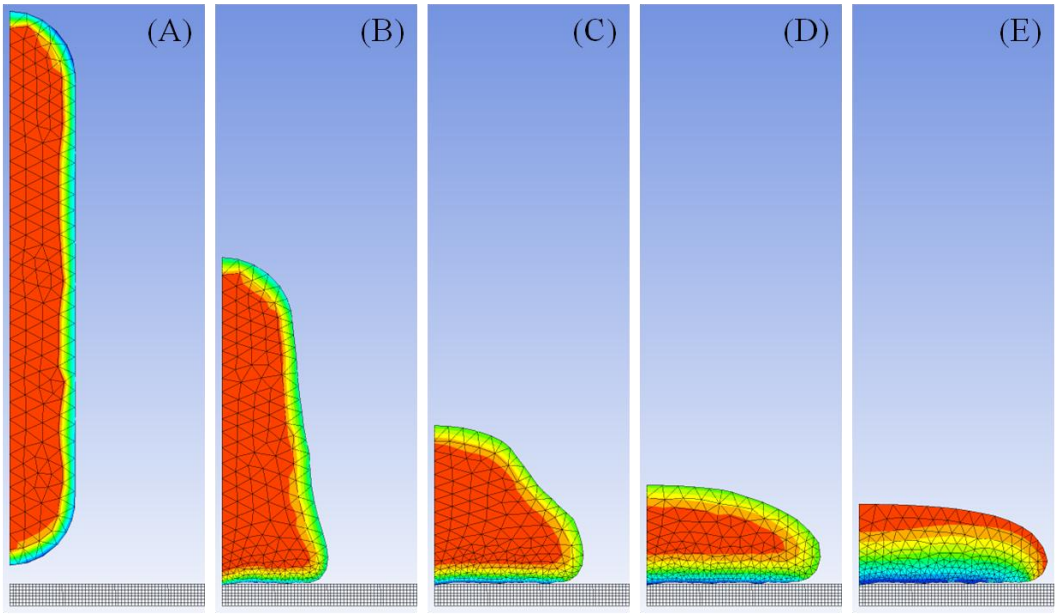

Figure 1. *Representative numerical results of the glass gob drop test obtained at different simulation steps. (**A**) shows the glass gob before the impact. (**B**) and (**C**) are intermediate steps that describe the initial deformation. (**D**) defines the glass flow over the plate surface until it stops in (**E**).*

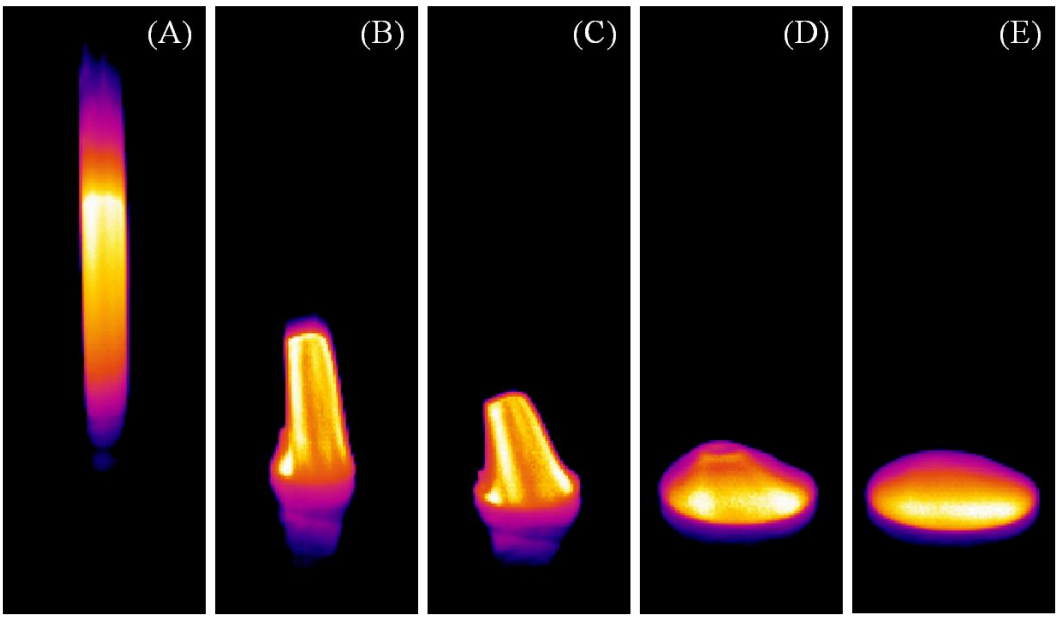

Figure 2. *Representative experimental infrared captures of the glass gob drop test. (**A**) shows the glass gob before the impact. (**B**) and (**C**) describe the initial deformation. (**D**) defines the glass flow over the plate surface until it stops in (**E**).*

As can be observed in **Figure 2**, the very same results were obtained with the infrared thermal camera from the experimental glass gob drop tests. There is a good correlation between numerical and experimental results when comparing **Figures 1** and **2**. Both results show a good agreement in the deformation of the glass gob after the impact with the cast iron plate. Additionally, from the numerical results, it can be concluded that without the use of a non-

isothermal model to describe the thermo-mechanical behavior of glass over time, glass would have continued flowing indefinitely, obtaining very different results.

Numerical simulations of the glass gob drop test were performed under different working conditions. In this sense, temperature distributions and impact velocities of the glass gobs were set to reproduce the experimental conditions measured during the drop tests at the middle and side sections of the IS machine. However, there were no relevant differences in the resulting glass geometries after the drop tests when comparing the results of the numerical simulations at the side and middle sections of the IS machine. On the other hand, **Figure 3** shows experimental samples of four drop tested gobs: on the left, there are two samples loaded in the side sections and two more loaded in IS3 are on the right. Experimental measurements showed lower values of gob velocity and surface temperature before the impact, although, the final dimensions of the glass medallion are almost the same in the four samples. Thus, it can be concluded that there is no appreciable difference in the final glass drop tested samples when the side and central sections are compared.

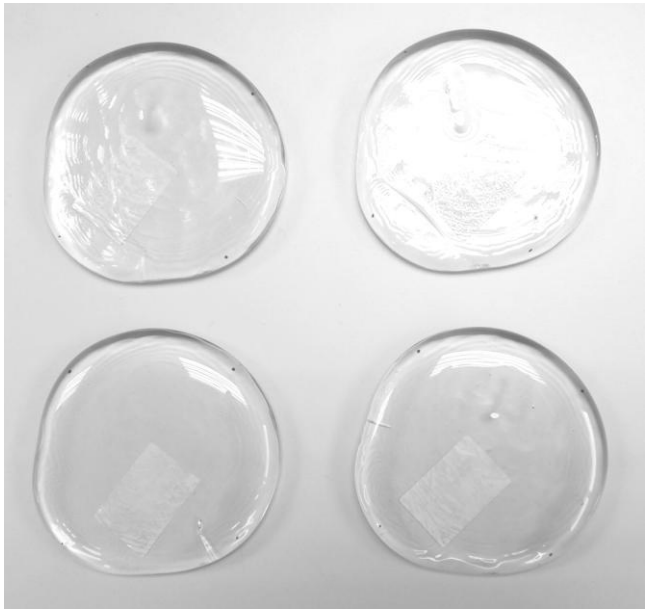

Figure 3. *Glass samples obtained from the experimental gob drop tests. Two samples loaded in the side sections on the left and two more loaded in IS3 on the right.*

Finally, the position of the deflector was adjusted to guide the loaded glass gobs and perform a normal impact against the horizontal surface of the cast iron plate. Therefore, loading of the glass gobs was completely vertical. Despite that, observing the amorphous geometry of the deformed glass samples, no circular symmetry could be found. During deformation, the gobs slightly deviated from the vertical axis. On the other hand, simulations were performed using an axisymmetric model, so symmetry axis deviations obtained in the experimental results could not be described by the numerical model.

4.3.2 MODELLING OF THE BLOW AND BLOW FORMING PROCESS

The results of the numerical and experimental glass gob drop tests were discussed in the previous section of this chapter. This test was very useful to validate the dependence of the glass viscosity on the temperature. As a result, an accurate description of the thermo-mechanical behavior of the glass flow during the deformation of the glass gob was obtained. The successful correlation of the numerical and experimental results is a very important step towards an accurate prediction of the glass thickness distribution of the manufactured containers. Therefore, the next and final step is to perform a numerical and experimental study to simulate and validate the blow and blow container forming process.

In this section, a detailed description of the mathematical formulation used to model glass behavior is presented. Using this model, the description of the glass flow was validated with the gob drop test and it will be used again in the blow and blow numerical simulations. In addition, the methodology used to define the specific initial values, material properties and boundary conditions for the numerical simulation of each glass perfume container are presented. Finally, different industrial process conditions used to manufacture several containers, together with the results predicted by the numerical simulation are also discussed.

(A) Mathematical Formulation of the Model

Governing Equations

Defining the thermo-mechanical behavior of glass under industrial manufacturing conditions involves the solution of differential equations that describe the conservation of mass, momentum and energy of the flow. Glass is assumed to be an incompressible fluid.

The conservation of mass for an incompressible fluid is reduced to

$$\nabla \cdot \mathbf{v} = 0 \tag{1}$$

where **v** is the velocity vector.

For an incompressible fluid the conservation of momentum yields

$$\rho \frac{\mathrm{D}\mathrm{v}}{\mathrm{D}t} = -\nabla p - \nabla \cdot \boldsymbol{\tau} + f \tag{2}$$

where ρ is the density, the operator $\mathrm{D}/\mathrm{D}t$ is the material time derivative, p is the pressure, $\boldsymbol{\tau}$ is the viscous stresses tensor and f is the volume force. The viscous stresses can be combined with the pressure into a total stress tensor $\boldsymbol{\pi}$ as shown below

$$\boldsymbol{\pi} = p\mathbf{I} + \boldsymbol{\tau} \tag{3}$$

where **I** is the unit tensor.

The energy equation for an incompressible fluid is given by

$$\rho C_p \frac{\mathrm{D}T}{\mathrm{D}t} = -(\nabla \cdot q) + r - (\tau : \nabla \mathrm{v}) \tag{4}$$

where C_p is the heat capacity, T is the temperature, q is the heat flux, r is the volumetric external heat source and $\tau : \nabla \mathrm{v}$ is the viscous heating rate.

As discussed in **Chapter 2**, glass non-Newtonian effects only become relevant as the glass temperatures descend near its transition temperature. Therefore, glass has been modeled as a generalized Newtonian fluid in the blow and blow forming process. The constitutive equations for the glass domain defined as a generalized Newtonian fluid are

$$\boldsymbol{\tau} = -2\mu(\dot{\gamma}, T)\mathbf{D} \tag{5}$$

where μ is the viscosity, $\dot{\gamma}$ is the shear rate and $\mathbf{D}$ is the deformation tensor, defined by

$$\mathbf{D} = \frac{1}{2}(\boldsymbol{\nabla}\mathbf{v} + \boldsymbol{\nabla}\mathbf{v}^T) \tag{6}$$

where $\boldsymbol{\nabla}\mathbf{v}$ is the dyadic product or the velocity gradient tensor and $\boldsymbol{\nabla}\mathbf{v}^T$ is its transpose. Finally, the shear rate $\dot{\gamma}$ is defined by

$$\dot{\gamma} = (2\mathbf{D} : \mathbf{D})^{1/2} \tag{7}$$

Boundary Conditions

The boundary conditions for fluid dynamics in the glass flow domain $\partial\Omega$ can be written as either velocity components (Dirichlet boundary conditions)

$$\mathbf{v} = \bar{\mathbf{v}}(\mathbf{x}, t) \qquad (\text{for } \mathrm{x} \in \partial\Omega_{\mathrm{v}}) \tag{8a}$$

or surface traction components (Newmann boundary conditions)

$$\boldsymbol{\pi} \cdot \mathbf{n} = \bar{\mathbf{t}}(\mathbf{x}, t) \qquad (\text{for } \mathrm{x} \in \partial\Omega_{\mathrm{t}}) \tag{8b}$$

where $\mathbf{n}$ is the outward vector normal to the boundary, $\bar{\mathbf{v}}$ and $\bar{\mathbf{t}}$ are specified functions.

Thermal boundary conditions at the glass-mold contact interface are the most important boundary conditions of the glass-forming problem as define heat transfer between both domains. Again, these can be defined specifying the temperature (Dirichlet boundary conditions) at the boundaries

$$\boldsymbol{T} = \bar{\boldsymbol{T}}(\mathbf{x}, t) \qquad (\text{for } \mathrm{x} \in \partial\Omega_T) \tag{9a}$$

or the heat flux (Newmann boundary conditions)

$$k(T)\frac{\mathrm{d}T}{\mathrm{d}n} = \bar{q}_n(\mathbf{x}, t) + q_c + q_r \qquad \left(\text{for } \mathrm{x} \in \partial\Omega_q\right) \tag{9b}$$

where $\mathrm{d}/\mathrm{d}n$ is the derivative normal to the boundary, $\bar{T}$ and $\bar{q}_c$ are specified functions and q_c and q_r are the convective and radiative components of the heat flux.

Free Surfaces and Contact Detection

Free surfaces are used to track the displacements of the boundaries of the glass domain during the blowing stages. Before contact with the mold cavity, dynamic and kinematic conditions define the displacement of the free surfaces.

For the dynamic condition, the normal force requires to be a prescribed value. In general, the prescribed value will be zero. However, the normal force of the free surface defined after the insertion of the plunger into the finish during the settle blow will be defined as the blowing pressure during the counter and final blow operations.

The kinematic equation for time-dependent problems is defined as

$$\mathbf{v} \cdot \mathbf{n} = \frac{\partial}{\partial t} \boldsymbol{\chi}(\mathbf{x}_0, t) \cdot \mathbf{n} \tag{10}$$

where $\mathbf{n}$ is the normal vector to the free surface and $\boldsymbol{\chi}(\mathbf{x}_0, t)$ describes the position of the free surface.

Contact detection between the moving free surfaces of the glass domain and the walls of the mold cavity is implemented through a penalty technique [28]. At each time step, each node on the glass domain is tested to determine whether it is in contact with the mold walls. Once contact is detected, the discrete momentum equation of this node is then modified by a penalty term to avoid penetrations.

In the normal direction to the contact surface the following condition is applied

$$f_{\mathrm{n}} = -k_{\mathrm{p}}(\mathbf{v} - \mathbf{v}_{\mathrm{wall}}) \cdot \mathbf{n} \tag{11}$$

where f_{n} is the normal force vector, k_p is the penalty coefficient and $\mathbf{v}$ and $\mathbf{v}_{\mathrm{wall}}$ are the velocities of the glass nodes and the mold, respectively.

Using the same principle in the tangential direction, a friction coefficient between glass and mold domains can be defined as

$$f_{\mathrm{s}} = -F_{slip}\left(\mathbf{v}_{\mathrm{s}} - \mathbf{v}_{\mathrm{s,wall}}\right) \tag{12}$$

where f_{s} is the tangential force vector and F_{slip} is the slip coefficient. As defined in the present numerical simulations, when F_{slip} is equal to k_p a sticky contact is defined between both domains. In case that F_{slip} is smaller than k_p then the glass free surface nodes in contact with the wall of the mold cavity are allowed to slip.

Numerical Solution

To solve the governing conservation and constitutive equations, along with the boundary conditions presented before, the commercial finite element method (FEM) code ANSYS Polyflow was used. The numerical simulations described the glass flow during the blow and blow glass forming process. To handle large displacements of the glass free surfaces during blowing stages a Lagrangian remeshing technique was required. Remeshing algorithms were used to correct distorted mesh elements in the glass domain after each simulation step. Volume conservation was verified so as not to modify the initial volume of the glass domain due to continuous remeshing. An implicit Euler method was used as the corrector in the time-integration procedure. The time steps were determined from conversion, precision, and contact accuracy requirements that were set for the problem. The presented penalty technique was defined for sticky contact detection of the glass free surfaces against the mold walls.

An axisymmetric and a three-dimensional model have been implemented to account for

complex shapes of glass perfume containers. Planes of symmetry have been used whenever possible to reduce the computational cost of the numerical simulations. Only one section was simulated in the axisymmetric model and ¼ of the domain was simulated in the three-dimensional model, respectively.

(B) Methodology

As presented in the previous chapters, to carry out numerical simulations of the blow and blow forming process, it is necessary beforehand to gather much information about the container specifications, IS machine operation, glass thermal conditions, etc. Once validated, the material properties, mathematical formulation and boundary conditions of the numerical model will always be the same for each new glass perfume container to be developed, manufactured and therefore simulated in the future. However, the rest of the parameters defined in the numerical model are specific for each container. Thus, to obtain the most accurate prediction of the glass thickness distribution, the mold cavity shapes, machine operation times, process conditions, glass and molds temperatures, etc. should be defined each time, based on the specific manufacturing conditions to produce a particular container.

At this point, the reader is well aware that performing experimental measurements of the glass forming process is a complex, expensive and very time-consuming task. However, numerical glass-forming models require accurate data to predict accurate results. When numerical simulations are carried out, one of the worst approaches to follow is to try to predict accurate numerical results without making sufficient effort to obtain the required input values from the modeled process. Experimental information obtained under industrial manufacturing conditions is not only very valuable for defining the initial values of the numerical simulation, but also allows the user to criticize and validate the predicted results. In short, to have confidence with the glass forming numerical model and the predicted glass thickness distributions.

Therefore, to perform the numerical simulations of the blow and blow container forming process, the following information must be specified in the numerical model: geometry of the molds and glass domains, glass material properties, boundary conditions, production process parameters and glass and mold temperatures.

- The geometric boundaries of the blank and blow molds are defined from the walls of the mold equipment cavities. As the mold cavities are designed using CAD software, these can be directly imported to ANSYS Polyflow. The initial geometry of the glass domain needs to be defined too. At the start of the numerical simulation, the glass gob is considered to be inside the blank mold and the neck ring cavity is already filled. Therefore, only the free surface at the top of the loaded gob is required. This is defined after the settle blow with the help of the infrared thermal camera. The volume of the glass domain is defined in accordance with the weight of the manufactured glass bottle. Once imported to ANSYS Polyflow, both domains are almost automatically meshed using the same parameters as defined in the remeshing algorithms.

- Material properties to describe the glass domain, including the functions or values of each

property, were described in **Chapter 2**. To summarize, glass viscosity is defined as a function of temperature using the VFT equation. Glass specific heat, density and thermal expansion coefficient are also defined using constant values. Effective thermal conductivity is defined as a function of glass temperature using a user-defined function (UDF). Dependence on thickness is not taken into account during the numerical simulation. However, different UDFs can be used based on the average thickness of the glass domain for each simulation.

- Thermal boundary conditions at the glass-mold contact interface are defined using a heat transfer coefficient. As presented in **Chapter 2**, this is described using a UDF as a function of the contact time. The previously presented penalty technique is used to detect the contact of the glass free surfaces against the mold walls. Once contact is detected, glass remains stuck to the wall of the mold cavity until the simulation ends.

- In the numerical simulation of the blow and blow forming process, dwell times between each blowing stage are taken into account to define the glass thermal conditioning. The operation times of the IS machine define the time intervals when each operation is carried out. These are described using a drum rotation system to control several pneumatic valves and movements of the IS machine. From there, the duration of the glass-forming stages can be defined (see **Table 2**). The production machine rate is specified to manufacture the glass containers in a single gob six-section IS machine. The pressures applied during the counter and final blow are also obtained from the production process. Pressure values for both blowing operations are around 2 bars.

- Thermal conditions of the glass domain are defined by performing experimental measurements of the glass under industrial manufacturing conditions. Infrared thermal measurements of the glass during the gob forming, delivery and loading operations presented in **Chapter 3** are performed to define the glass gob loading conditions and the initial temperature of the glass domain, which is assumed to be constant [29]. In addition, the flexibility of the infrared thermal camera allows obtaining thermal information from the glass surface in the few stages of the container forming process where glass is visible. These measurements will be used later to verify the predicted numerical results. In particular, temperature measurements of the parison once the blank mold is opened and until the blow mold is closed are used to follow the parison reheating. The temperature distribution of the final container along with the parison temperature measurements can be used to roughly estimate the heat transfer from the glass to the blank and blow molds, respectively. **Figure 4** shows representative infrared thermal captures of the SIERRA 60 bottle during its manufacturing process. As can be seen, the temperature in glass decreases from the initial 1,030 ºC to around 650 ºC in the less than 10 seconds required to manufacture that perfume glass container. Thermal conditions of the mold domains are described with a constant and uniform temperature. The temperature values of the blank and blow molds are defined from bibliographic data [30].

- Finally, manufactured containers are cut to obtain its cross-section profiles. This allows to measure and compare the glass thickness distribution predicted in the numerical simulations to the thickness distributions obtained when manufacturing the glass containers in the production line.

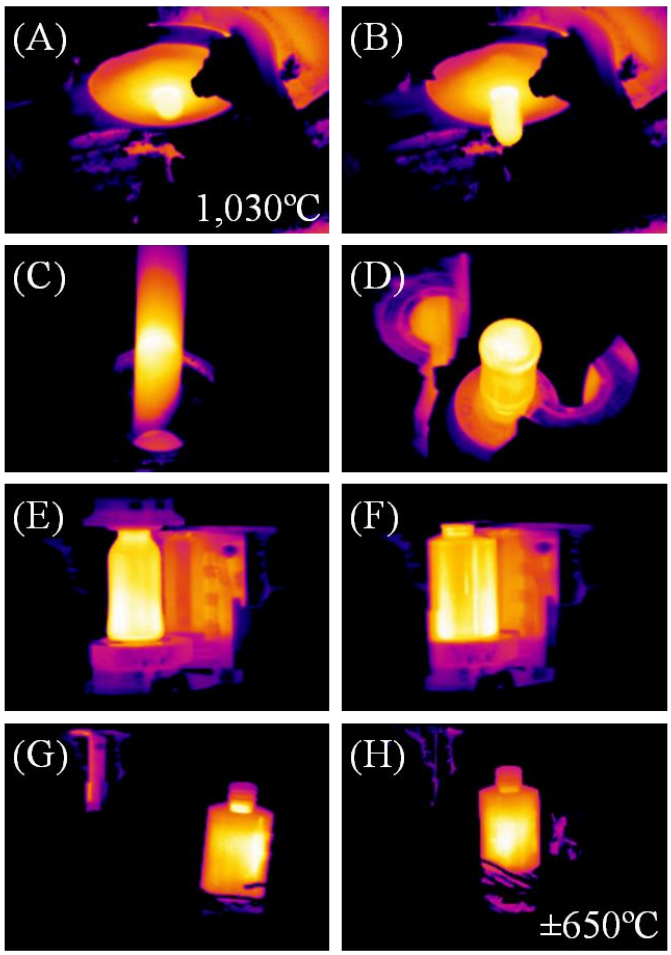

Figure 4. *Infrared thermal captures of the stages were glass can be seen during the container manufacture of SIERRA 60 bottle. (**A**) and (**B**) refer to gob forming, (**C**) to gob loading, (**D**) to blank mold opening, (**E**) to parison reheating, (**F**) to blow mold opening and (**G**) and (**H**)to take out.*

Table 2. *Relevant forming times of the numerical simulations according to the IS machine operation times defined under industrial manufacturing conditions.*

	SIERRA 60	**ALFA 200**
Gob loading (s)	0	0
Counter blow start (s)	1.7	3.0
Counter blow end (s)	2.9	5.0
Blank mold open (s)	3.1	5.7
Inversion (s)	3.9	7.7
Final blow start (s)	7.0	11.5
Final blow end (s)	9.0	17.2
Blow mold open (s)	9.6	18.0
Total simulation time (s)	7.3	12.2

(C) Description of the Numerical Simulation Results

Until now, the mathematical equations of the numerical model, which were validated with the glass gob drop test to describe the thermo-mechanical behavior of glass have been presented. In addition, the methodology followed to experimentally define all the material properties, boundary conditions and initial conditions of the container forming process has been defined too. After successfully performing these previous tasks, finally, now is the time to perform the numerical simulations of the blow and blow container forming process. Therefore, without further delay, a detailed explanation of the predicted results, describing the thermo-mechanical behavior of glass in the numerical simulations to manufacture the SIERRA 60 bottle is presented in **Figure 5**.

The numerical simulation of the blow and blow container forming process is divided into two parts. First, there is the simulation of the blank side, where the operations related to the transformation of the glass gob into a parison are taken into account. The output of that simulation, that is, the resulting geometry and temperature distribution of the glass domain, is translated as the initial values of the second simulation. There, the operations of the IS machine on the blow side are described, where the manufactured container is obtained as a result of the parison expansion. The discussed results are based on the SIERRA 60 numerical simulation using the axisymmetric and non-isothermal model, but these can be extended to any of the simulation cases that will be presented based on different container specifications and manufacturing conditions.

The gob forming, gob loading and settle blow operations are not included in the numerical model. Thus, an as initial condition, the glass gob is considered to be inside the blank mold and the neck ring cavity is already filled. The free surface at the top of the loaded gob and its volume define the initial geometry of the glass domain in accordance with the weight of the manufactured glass container (see **Figure 5A**). A constant value for the temperature distribution in the glass domain is also prescribed. When the simulation of the blank side starts, heat transfer begins immediately at the glass-mold contact interfaces at the walls of the blank mold cavity and the neck ring. Due to the contact heat transfer, a temperature distribution in the glass domain is defined before the counter blow stage (see **Figure 5B**), defining in turn a viscosity distribution that will govern the glass flow. At the specific instant of time starts the counter blow operation. Then, pressure is applied and glass expands through the blank mold cavity to create the parison (see **Figures 5C, 5D** and **5E**). Due to the large deformations of the free surfaces in the glass domain during the blowing stage, the glass domain is remeshed several times to avoid distortion of the mesh elements. After expansion, glass continues transferring heat in contact with the walls of the mold cavity (see **Figure 5F**) until the blank mold is opened. Then, the parison skin is allowed to start reheating (see **Figure 5G**) until the inversion is started. The start of the inversion stage on the real production process defines the end of the numerical simulation at the blank side.

Inversion effects are not considered. Therefore, when the parison is transferred to the blow side, the Y-axis is just inverted (see **Figure 5H**). Then, based on the previous results of the glass domain, the second numerical simulation at the blow side is started. During parison reheating, the internal temperature gradients in the glass domain redistribute the temperatures until the

parison is ready to be blown inside the blow mold (see **Figure 5I**). Parison stretching does not have a significant effect on the manufacture of perfume bottles. This is because parisons for perfume containers are relatively short, thin and light compared to parisons in other industries (e.g. beer or wine bottles). In addition, parison run distances are generally very small to hide the baffle seam at the bottom of the container. Thus, the stretching stage of the parison is not taken into account in the simulation. Therefore, at the specific instant of time, the final blow expands the parison throughout the blow mold cavity (see **Figures 5J** and **5K**) to define the glass thickness distribution of the final perfume bottle (see **Figure 5L**). The glass domain is remeshed again during the final blow and once the expansion of the glass domain is completed the simulation of the blow side ends. The remaining simulation time would keep cooling the glass domain until the blow mold is opened. However, as the thickness distribution has been already defined, these final time steps can be ignored. Deformations of the predicted geometry of the final container due to thermal contraction of the glass or to stress relaxation phenomenon are not considered either.

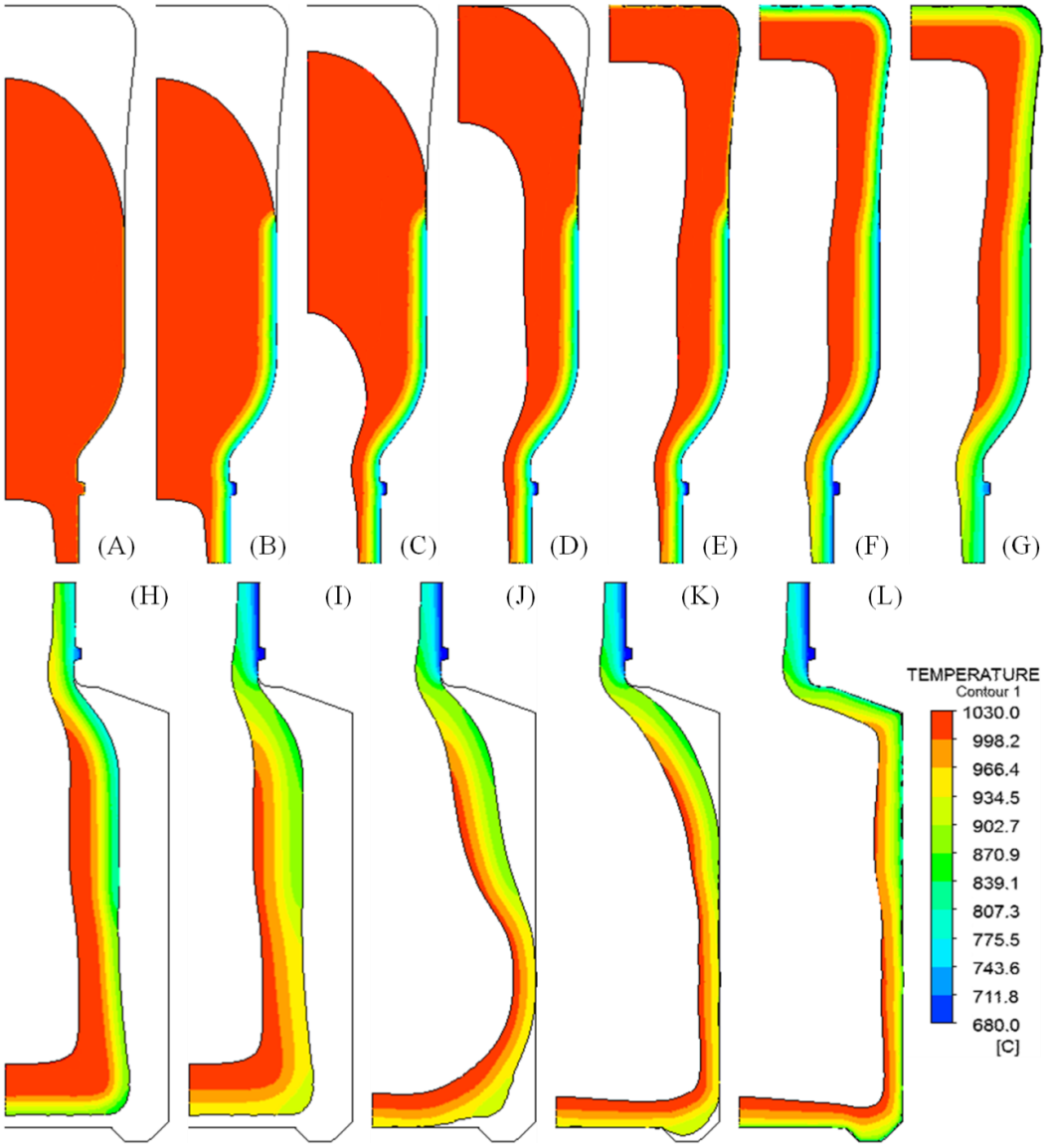

***Figure 5**. Numerical results of the glass domain and its temperature throughout the forming process of the SIERRA 60 bottle. **(A)** refers to the initial prescribed temperature and geometry.*

*(**B**) shows the temperature conditioning prior to the counter blow. (**C**) and (**D**) show the glass expansion through the counter blow. (**E**) refers to the parison geometry. (**F**) shows the temperature conditioning before the blank mold opens. (**G**) refers to the parison reheat at the blank side. (**H**) refers to the inverted parison at the blow side. (**I**) refers to the parison reheat at the blow side. (**J**) and (**K**) show the glass expansion through the final blow and (**L**) refers to the thickness distribution of the manufactured container.*

(D) Validation of the Numerical Models

In this section, numerical and experimental results of three different simulation cases are presented, including an axisymmetric simulation of the SIERRA 60 bottle; axisymmetric simulations of the ALBA 200 bottle with two different blank molds and a three-dimensional simulation of the SIERRA 60 bottle. All the simulations use the characterized glass viscosity and non-isothermal formulations previously tested with the gob drop test simulation case.

As previously defined, to validate the blow and blow container forming model, numerical results were correlated with experimental infrared measurements of the glass temperature and thickness distributions obtained sectioning manufactured containers. It was also very relevant to demonstrate the influence of the blank mold cavity design and industrial manufacturing conditions on the predicted glass thickness distributions. For this reason, to extend the validation of the blow and blow numerical model, simulations with two very different perfume bottles from Ramon Clemente and several mold designs were carried out. In this sense, material properties and boundary conditions were the same for all the simulation cases. Nevertheless, mold cavities and process parameters (e.g. machine operation times, process conditions and glass temperatures) were experimentally defined for each simulation depending on the industrial manufacturing conditions of each container. Once the presented methodology was applied, the numerical model describing the blow and blow container forming process was solved with ANSYS Polyflow.

SIERRA 60 Bottle

A numerical simulation of the blow and blow forming process of the SIERRA 60 bottle was performed using an axisymmetric and non-isothermal model. Extensive explanations of the numerical results obtained from that simulation were presented in the section above. **Figure 5** showed the geometry and temperature distribution of the glass domain throughout the forming process operations of the SIERRA 60 bottle.

Very powerful results can be obtained from numerical simulations. For instance, the heat transfer phenomena at the glass-mold contact interfaces and its effect on the temperature distribution within the glass domain are defined in every simulation step and region of the glass domain. Using the infrared thermal camera, temperatures on the surface of the glass can also be measured under industrial conditions. However, these measurements are restricted to the few stages of the forming process when the molds are open. Thus, reheating of the parison skin after the blank mold opens and until the blow mold closes can be experimentally determined. These temperature measurements show a similar trend to the numerical results of the temperature field present in the glass domain between that interval. Once the container is finished and the blow mold opens, glass temperatures can be measured again. In this sense, a comparison of

experimental measurements with numerical results showed satisfactory agreement within 15% for glass temperatures on the final container.

On the other hand, **Figure 6** focuses only on the glass thickness distribution, summarizing the main geometry changes in the glass domain during the manufacture of the SIERRA 60 bottle. The initial geometry of the glass domain is defined by the glass gob once loaded into the blank mold (see **Figure 6A**). After the counter blow, the parison is obtained (see **Figure 6B**). Then, the glass parison is inverted and introduced into the blow mold. Finally, the glass is blown again, obtaining the predicted thickness distribution of the final container (see **Figure 6C**). Moreover, manufactured SIERRA 60 bottles were also cut to obtain an experimental section profile of the glass container (see **Figure 6D**). The comparison of the thickness distribution from the manufactured glass container with the results predicted by the numerical model shows a very good agreement. The characteristic shape in the bottom of the manufactured container strongly correlates with the thickness distribution in the glass domain from the numerical model. Additionally, in Figure **6D**, it can be stated how manufactured bottles, even axisymmetric, do not always show a perfectly symmetric distribution in the glass thickness.

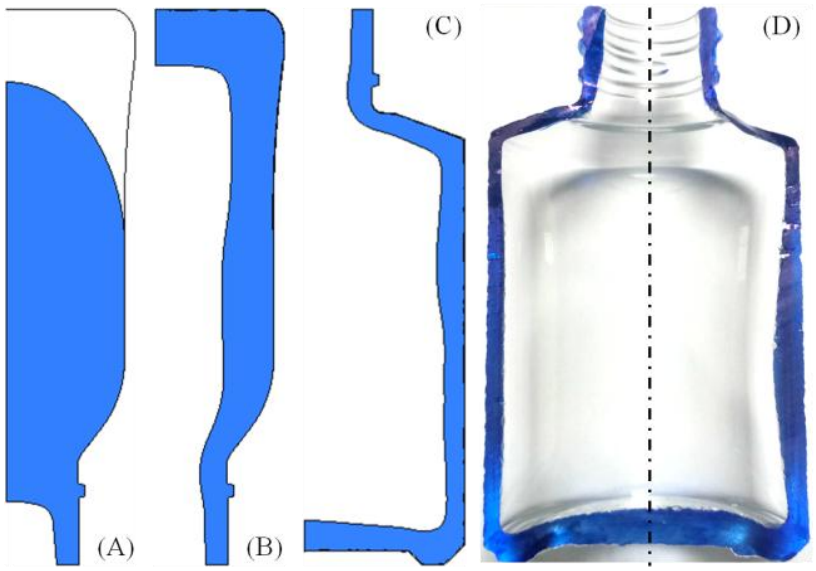

Figure 6. *Geometry of the glass domain from the numerical simulations of the SIERRA 60 bottle. (**A**) refers to the gob once loaded into the blank mold; (**B**) refers to the parison and (**C**) shows the predicted thickness distribution in the final container. These results can be compared with a section profile of the manufactured SIERRA 60 bottle in (**D**).*

To conclude, this example demonstrates the ability of the blow and blow numerical model to predict the glass thickness distribution of perfume bottles. Although temperature variations are present between numerical and experimental results, these are not introducing severe disturbances to the prediction of thickness distributions as there is a very good reliability between both results.

Influence of the Blank Mold, ALFA 200 Bottle

As defined in **Chapter 1**, the design of the mold cavities is tailor-made for each glass perfume container. For this reason, during the development of new containers a few production tests are usually required. In these manufacturing tests, the design of the mold cavities and

several production process parameters are adjusted until the desired quality in the manufactured glass bottles is achieved, including the glass thickness distribution. For this reason, the ability of the numerical model to predict the influence of the blank mold cavity on the glass thickness distributions was required. Therefore, simulations of the blow and blow forming process of the ALBA 200 bottle with two different blank molds were performed using an axisymmetric and non-isothermal model.

Two blank mold designs were required during the development of the ALFA 200 bottle, obtaining the manufacture of the same container but with different thickness distributions (see **Figure 7**). The container initially produced with blank mold cavity A showed a poor glass distribution at the base of the bottle. As previously defined, an overweighed aspect was desired for this container to enhance the aesthetic properties of the glass packaging. Therefore, more glass at the bottom of the ALFA 200 bottle was required. Then, a blank mold cavity B was defined and tested again. As can be observed in **Figure 7**, the glass thickness distribution at the bottom of the bottle was greatly improved with the design of the second blank mold, obtaining a thicker and flatter glass base and improving the aesthetics of the glass container.

Figure 7. *Comparison of the two ALFA 200 bottles manufactured with both blank molds. A lighter container was obtained with blank mold cavity A (left) and a thicker bottom resulted from blank mold cavity B (right).*

To reproduce these experimental results, two simulations of the blow and blow container forming process of the ALBA 200 bottle were performed. All the forming process conditions remained the same except for the design of the blank molds (cavity A and B), both in the production tests and in the numerical simulations.

Figure 8 summarizes the main geometry changes in the glass domain during the manufacture of the ALFA 200 bottle with both blank mold designs. Numerical results with cavity A are presented at the top (**Figures 8A**, **8B**, **8C** and **8D**) and cavity B at the bottom (**Figures 8E**, **8F**,

8G and **8E**). The initial geometry of the glass domain is defined by the glass gob once loaded into the blank mold (see **Figure 8A** and **8E**). After the counter blow the parison is obtained (see **Figures 8B** and **8F**). Then, the glass parison is inverted and introduced into the blow mold. Finally, the glass is blown again, obtaining the predicted thickness distribution of the final container (see **Figures 8C** and **8G**). Manufactured ALFA 200 bottles were cut to obtain a section profile of the glass container (see **Figures 8D** and **8H**).

The comparison of the thickness distribution from the manufactured glass containers with the predicted results of the numerical models shows a very good agreement in both cases. Modifications made to the design of the blank mold cavity B improve the aesthetics of the manufactured container. At the same time, there is a strong correlation between the glass thickness distribution in the section profiles and the predicted by the numerical results. As can be noted in the numerical results and the sectioned containers, blank mold cavity B reduces the glass thickness on the shoulder of the container while the overall thickness of the bottom is greatly improved as it is flatter and the lower corners are much more rounded.

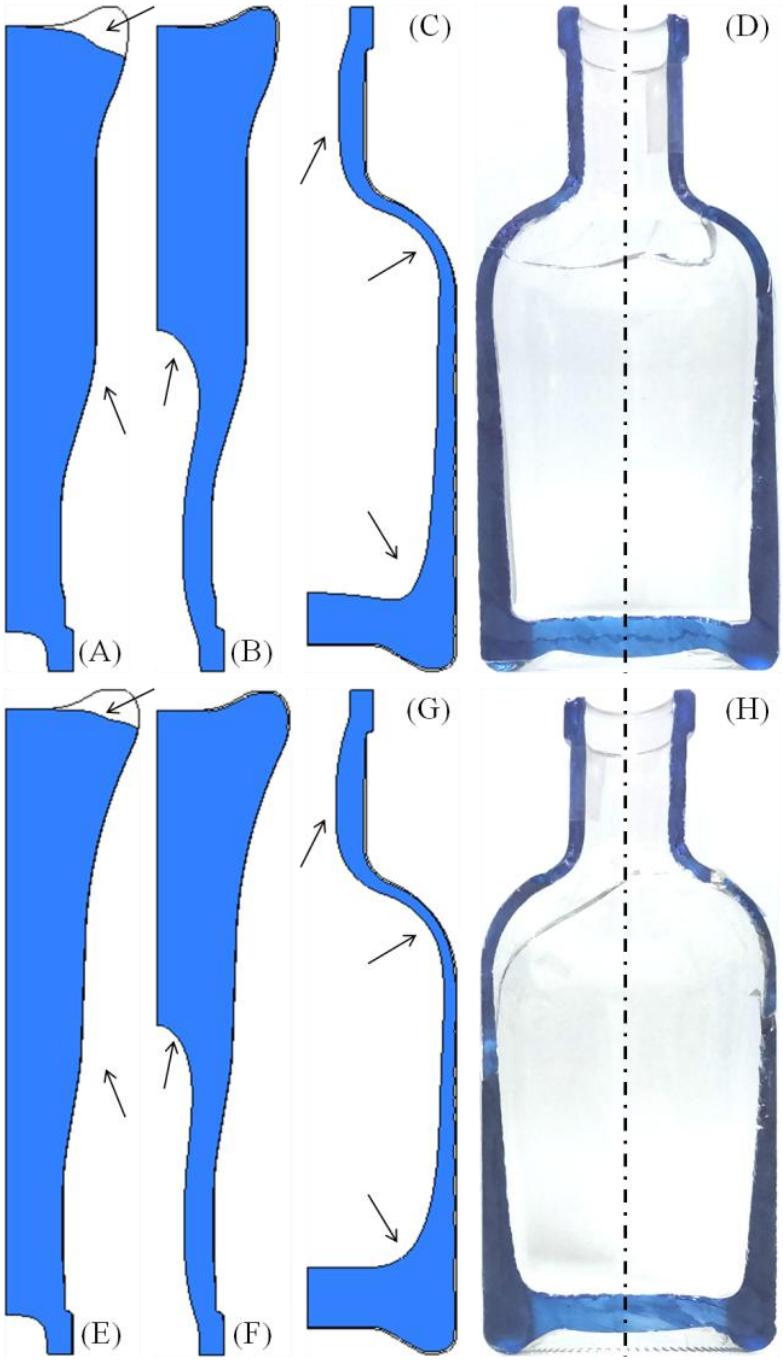

Figure 8. *Geometry of the glass domain from the numerical simulations of the ALFA 200 bottles using blank mold cavity A and B (top and bottom, respectively). (**A**) and (**E**) refer to the gob once loaded into the blank mold; (**B**) and (**F**) refer to the parison; (**C**) and (**G**) show the predicted thickness distribution in the final container. These results can be compared with section profiles of the manufactured ALFA 200 bottles in (**D**) and (**H**).*

To conclude, this example demonstrates the ability of the blow and blow numerical model to predict the influence of the blank mold cavity in the thickness distributions of glass perfume bottles. In addition, the numerical model has been validated with two containers with very different specifications, manufacturing conditions and therefore numerical parameters. Temperature variations between numerical and experimental results remain present without introducing severe disturbances.

Axisymmetric and Three-Dimensional Models Comparison

For the moment only round-base glass perfume containers were studied, so its external geometry could be defined with an axisymmetric profile. However, many glass containers in the perfumery industry tend to have difficult shapes, which are generally non-axisymmetric. In fact, many of the new Ramon Clemente perfume containers, and probably the most complex to be developed are non-axisymmetric bottles. Therefore, in addition to the axisymmetric model for the simulation of the blow and blow forming process, the implementation of a three-dimensional model capable of handling all types of container shapes would be very relevant to support the development of new perfume containers at Ramon Clemente. For this reason, the numerical simulation of the blow and blow forming process of the SIERRA 60 bottle was also performed using a new three-dimensional model.

Figure 9 summarizes the main geometry changes in the glass domain during the manufacture of the SIERRA 60 bottle using the axisymmetric and three-dimensional models. The comparison of the predicted results by the axisymmetric and the three-dimensional model shows identical results for the glass thickness distribution. This new simulation had exactly the same parameters as before, only introducing the three-dimensional model instead of the already presented axisymmetric model. Therefore, the same numerical results were expected. Nevertheless, it is important to state that as the three-dimensional model requires a larger amount of mesh elements, the computational time required to solve this simulation is greatly increased.

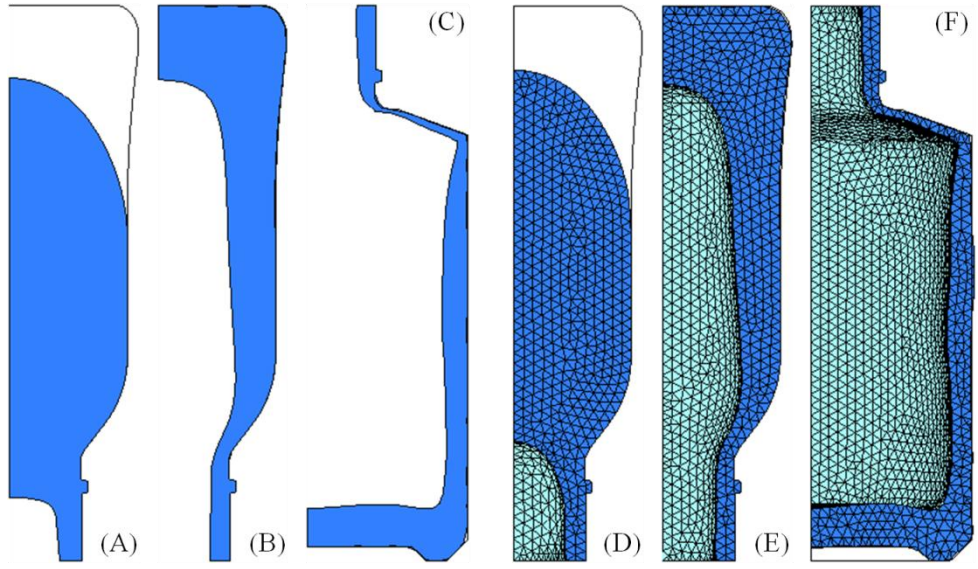

Figure 9. *Geometry of the glass domain from the numerical simulations of the SOINS 60 bottle using the axisymmetric and three-dimensional models (left and right, respectively).* ***(A)*** *and* ***(D)*** *refer to the gob once loaded into the blank mold;* ***(B)*** *and* ***(E)*** *refer to the parison;* ***(C)*** *and* ***(F)*** *show the predicted thickness distribution in the final container.*

To conclude, this example demonstrates the ability of the blow and blow container forming model to predict the thermo-mechanical behavior of glass in three-dimensional simulations. The validation of the three-dimensional model will have very strong implications for Ramon Clemente, as it paves the way to predict the glass thicknesses of complex perfume container

geometries instead of limiting to common axisymmetric bottles.

(E) Sensitivity Study

Effect of Initial Glass Temperature

As mentioned above, the comparison of glass temperatures experimentally obtained under manufacturing conditions with numerical results of the blow and blow model showed satisfactory agreement within 15% for glass temperatures on final containers. In this sense, infrared thermal measurements on glass during the gob forming, delivery and loading operations were performed to define the gob loading conditions and then prescribe the initial temperature of the glass domain in the numerical model. Additional thermal information in the few stages of the container forming process where glass is visible was also obtained. In particular, temperature measurements of the parison experimentally defined the parison reheating. Finally, the temperature distribution on manufactured containers along with parison measurements validated the thermal predictions of the numerical simulations.

Although temperature variations were present between numerical and experimental results, these did not introduce severe disturbances to the prediction of thickness distributions as there was a very good reliability between both results. Nevertheless, as glass viscosity is highly dependent on temperature, a sensitivity study of the initial glass temperatures on the numerical model was conducted. Then, simulations of the blow and blow forming process with the SIERRA 60 bottle were repeated increasing the initial temperature of the glass domain, but maintaining constant all the other parameters. This increase in temperature would take into account variations in the glass emissivity in the infrared measurements. The temperature of the glass gob experimentally determined was 1,030ºC. This value defined the initial temperature of the glass domain in the previously presented SIERRA 60 bottle simulation. In this sensitivity study, two more simulations were performed by adding 50ºC (1,080ºC) and 100ºC (1,130ºC) to the initial temperature of the glass gob.

As in previous simulations, a non-isothermal model was used, defining a temperature distribution within the glass domain as a function of heat transfer phenomena at the glass-mold contact interface. At the same time, variations in the temperature distribution resulted in different viscosities within the glass domain, modifying the thermo-mechanical behavior of glass at the counter and final blow operations. **Figures 10A** and **10D** are the numerical results of the original simulation, using 1,030ºC as the initial glass gob temperature. **Figures 10B** and **10E** show the same results but adding 50ºC to the initial temperature. In **Figures 10A** and **10D,** 100ºC were added. The numerical results of the three parisons after the counter blow can be observed in **Figures 10A**, **10B** and **10C**, respectively. Then, after the parison inversion and the final blow, the predicted thickness distribution of the final containers is obtained (see **Figures 10D**, **10E** and **10F**).

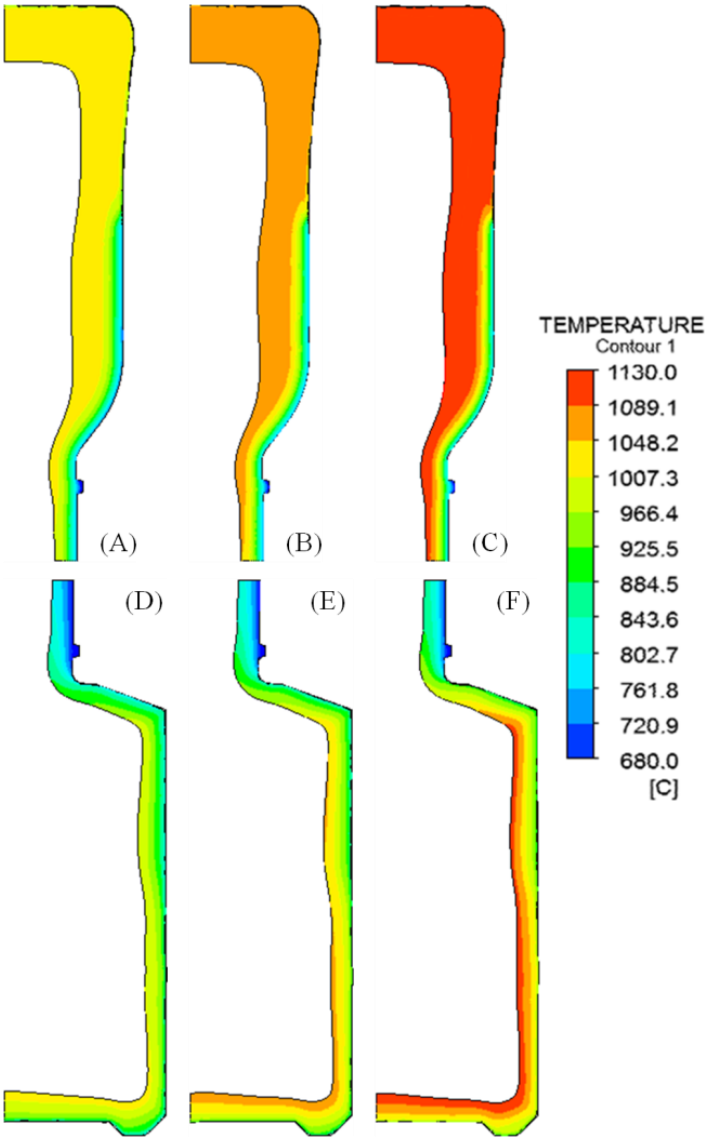

Figure 10. *Influence of the initial glass temperature on the final glass thickness distribution. (**A**) refers to the numerical result of the parison with the initial glass gob temperature obtained experimentally (1,030ºC). (**B**) and (**C**) refer to the parison results adding 50ºC and 100ºC to the initial glass gob temperature. (**D**), (**E**) and (**F**) refer to the respective numerical results of the manufactured bottles.*

As can be observed in **Figure 10**, the thickness distribution in all three simulations is almost the same. Temperatures were higher, but thermal gradients within the glass domain remained nearly identical. Therefore, in all three cases, the viscosity distribution was very similar and, as a result, any difference could be appreciated between the final containers. On the other hand, the time necessary to achieve full expansion of the glass in the mold cavity during the counter and final blow stages varies with the initial gob temperature. As expected, there was an almost uniform increase in temperature in the glass domain. Therefore, as the resistance of glass to flow is defined by its viscosity, higher temperatures in the glass domain resulted in a faster expansion during the blow stages.

As presented, a change in the initial glass temperature does not introduce relevant non-

uniformities to the temperature distribution within the glass domain. Nevertheless, numerical results might be much more sensitive if different temperature distributions are obtained in the glass domain. For example, when undesired variations in the heat flux are present in localized areas of the glass-mold contact interface, that is, temperature disturbances at the walls of the blank mold cavity due to deviations in the gob loading conditions as introduced in **Chapter 3** or due to thermal transients after swabbing the mold equipment, etc. However, these cases, although interesting, are out of scope at the moment. The conjugate heat transfer between glass and molds was successfully tested in the blow and blow numerical model but has not yet been implemented due to the lack of accurate experimental or numerical data of the temperature distribution in the mold cavities.

Effect of time step and mesh size

The influence of numerical parameters as the mesh size and time step on the accuracy of the results predicted by the numerical model was also studied. As previously introduced, to validate the numerical model of the blow and blow forming process under different conditions, two perfume bottles representative of the wide range of glass containers manufactured by Ramon Clemente were selected. Specifications in both containers were very different, including relevant variations in the brimful capacity, glass weight, production machine rate, process temperatures, glass conditions, etc. In this sense, as the two bottles had different scales of time and volume depending on the size of the glass domain and the total simulation time, different values of mesh size and time step were necessary for each simulation case.

To keep reasonable computation times without compromising the accuracy of the predicted results, it was important to study how dependent the solution of the thermal problem was on these two parameters. Heat transfer between adjacent nodes in the glass domain is defined by Fourier's law. Therefore, the temperature distribution within the glass domain depends very much on the mesh size. On the other hand, the time step in a numerical solution defines the number of time intervals used to solve the simulation, defining the accuracy of the predicted results. Several simulations were performed with different values of time step and mesh size, decreasing both parameters until obtaining the required precision. As expected, fine meshes were required to obtain an accurate calculation of the heat transfer in the glass domain and in the glass-mold contact interface, smaller time steps also lead to higher accuracy. However, the reduction of both values implied and increase in the computational cost to solve the simulation, so more computation time was required.

In relation to the mesh size and the numerical solution of large free surface deformations in the glass domain, it can also be stated that remeshing techniques should be used with caution. As the numerical solution is mesh size-dependent, the use of finer meshes is recommended. In particular, near the glass-mold contact interface, where there are huge thermal gradients and a fine mesh is required. However, as previously defined, a reduction in the mesh size results in an increase in the computation time required to solve the simulation. Temperatures in the middle of the glass domain are much more even rather than next to the boundaries, so bigger mesh elements may be used there to reduce computation time. Nevertheless, the use of remeshing techniques with different mesh sizes to reduce the element count is not recommended. In general, the use of a uniform mesh size for the entire glass domain, although more expensive, yielded more accurate results and reduced disturbances related to remeshing techniques.

4.4 CONCLUDING REMARKS

Once accomplished the many and different objectives required to describe and model the thermo-mechanical behavior of glass, it was time to introduce all these information in a numerical simulation. However, as previously defined, the solution of the blow and blow forming simulations also presented important numerical challenges. Therefore, at the beginning of this thesis, the expertise of CIMNE was considered to carry out initial simulations of the counter and final blow stages. However, the importance of describing glass viscosity as a function of temperature using non-isothermal formulations to couple the thermo-mechanical phenomena within the glass domain became evident at first glance. In this sense, difficulties with the non-isothermal PFEM model to handle heat transfer phenomena and temperature distributions at the glass-mold contact interface, as well as the lack of flexibility to simulate other experiments apart from the blow operation, led to dismiss the use of PFEM. Although these obstacles, relevant experience in numerical simulations was acquired working with CIMNE. At the same time, the shortcomings in their model made evident the steps to be taken to implement and validate a reliable numerical simulation. Thus, a robust software with a much more flexible and friendly environment as ANSYS Polyflow was chosen to model the glass flow and its thermo-mechanical behavior.

Preliminary simulations with PFEM also stated that numerical models required many experimental values sensitive to the glass forming process (i.e. material properties, initial thermal values, boundary conditions, etc.), which were extremely difficult to obtain under industrial manufacturing conditions. Therefore, it became evident how important was to measure and define accurate input values in order to obtain accurate simulation results. Otherwise, the development of the numerical model and the accuracy of its results would be limited to the possibilities of experimental validation. Many of these issues were already addressed in the previous chapters. However, the collected information was not enough to validate the numerical results of a manufacturing process as complex as the industrial blow and blow container forming. Thus, much more information was still required to successfully predict the thermo-mechanical behavior of molten glass. In particular, the inherent difficulties to perform experimental measurements inside the mold cavities were a limiting factor to define the thermal phenomena and boundary conditions defining the flow of the glass domain.

Therefore, a glass gob drop test was defined, where glass gobs impacted a cast iron plate before reaching the blank mold cavity when loaded with the delivery equipment. This experiment provided a very visual description of the glass flow over time as a function of the glass temperature and viscosity. In addition, the deformation of the gob after the impact was experimentally recorded with the infrared thermal camera. The gob drop test was also modeled using ANSYS Polyflow and numerical simulations were performed to describe the flow of the glass on the plate as a function of its temperature and viscosity.

The glass gob drop test case solved many modeling and data acquisition issues. Drop test simulations were very helpful to verify the non-isothermal model that couples the temperature evolution and the glass viscosity in the glass domain using the characterized viscosity and the VFT equation. This simulation case provided valuable experience in the use of ANSYS Polyflow and a better understanding of the numerical simulations. An initial validation of the

heat transfer, viscosity and other physical parameters was performed to be used in future simulations since all the learned knowledge in this "small scale" problem could be applied to a much more complex numerical simulation as the blow and blow glass forming process. As presented in the results, a non-isothermal model is required to describe the high dependence of glass viscosity with temperature and obtain a good correlation with the flow of glass during the impact observed in the infrared thermal recordings. Finally, variations in the loading conditions of the glass gob as a function of the loaded section of the IS machine were presented in **Chapter 3**. However, the deformation of the glass gobs obtained at the experimental and numerical results of the drop test did not show any relevant differences.

After a successful correlation of the gob drop test results, another chance was given to the numerical simulation of the blow and blow forming process. This time using the validated glass viscosity, glass thermal conditions and other material properties defined before in the gob drop test model. As an introduction of the numerical and experimental results of the blow and blow forming process, the mathematical formulation of the numerical model was presented. In addition, a methodology to define all the information required by the model was also introduced.

Finally, the results of the numerical simulations of the blow and blow forming process to predict the glass thickness distribution of manufactured containers were presented. Three different simulation cases were developed, including an axisymmetric simulation of the SIERRA 60 bottle; axisymmetric simulations of the ALBA 200 bottle with two different blank molds and a three-dimensional simulation of the SIERRA 60 bottle. To validate the blow and blow container forming model, numerical results were correlated with experimental infrared measurements of the glass temperature and thickness distributions obtained sectioning manufactured containers. The numerical model predicted consistent results of the final thickness distribution as a function of the blank mold cavities. The influence of glass thermal conditions and IS machine operation times defined in the industrial production process were also successfully tested. To obtain a more robust validation of the numerical model, the simulations of the blow and blow forming process were also performed using a three-dimensional model.

To conclude, the development of new mold equipment to manufacture the glass containers will be supported with the implementation of the presented numerical model. This will be a very useful simulation tool to guide the design of the blank mold cavities. As a result, Ramon Clemente will develop new glass perfume containers faster and of better quality, while reducing the amount of expensive experimental iterations and time to market. In addition, the numerical models presented for the glass forming simulations are also a solid foundation to continue working. More knowledge about the thermo-mechanical behavior of glass in the blow and blow container forming process can be gained using this simulation tool. Furthermore, the numerical model is undergoing continuous improvement with the study of more simulation cases based on bottles with different shapes and operation conditions. Further work will be performed to obtain more accurate experimental data of the glass thermal conditions and the heat transfer in the glass-mold contact interface.

4.5 REFERENCES

[1] M. Brown, "Computer simulation of the glass pressing process: A review," *Int. J. Mater. Prod. Technol.*, vol. 33, no. 4, pp. 335–348, 2008.

[2] M. K. Choudhary, R. Venuturumilli, and M. R. Hyre, "Mathematical Modeling of Flow and Heat Transfer Phenomena in Glass Melting , Delivery , and Forming Processes," *Int. J. Appl. Glas. Sci.*, vol. 1, no. 2, pp. 188–214, 2010.

[3] A. Cormeau, I. Cormeau, and J. Roose, "Numerical Simulation of Glass-blowing," *Numer. Anal. Form. Process.*, pp. 219–237, 1984.

[4] J. M. A. César de Sá, "Numerical modelling of glass forming processes," *Eng. Comput.*, vol. 3, no. 12, pp. 266–275, 1986.

[5] M. R. Hyre, "Numerical Simulation of Glass Forming and Conditioning," *J. Am. Ceram. Soc.*, vol. 85, no. 5, pp. 1047–1056, 2002.

[6] O. O. Den Camp, D. Hegen, G. Haagh, and M. Limpens, "TV Panel Production : Simulation of the Forming Process," in *Conference on Glass Problems*, 2003, vol. 24, no. 1, pp. 1–19.

[7] M. R. Hyre, "Modelling defect creation during the forming process," *Glass International*, no. November, pp. 55–57, 2009.

[8] M. R. Hyre, "Effect of Mold to Glass Heat Transfer on Glass Container Forming," in *Advances in Fusion and Processing of Glass III*, 2004, pp. 271–279.

[9] M. R. Hyre and B. L. Underwood, "Experimental Measurement of Glass to Mold Heat Transfer for Computational Modeling of Container Production," in *ASME International Mechanical Engineering Congress and Exposition*, 2004, pp. 319–324.

[10] P. Moreau, J. M. A. César de Sá, S. Grégoire, and D. Lochegnies, "Integration of Heat Transfer Coefficient in Glass Forming Modeling With Special Interface Element," *AIP Conf. Proc.*, vol. 908, pp. 750–764, 2007.

[11] P. Moreau, D. Lochegnies, S. Grégoire, and J. M. A. César de Sá, "Analysis of lubrication in glass blowing: Heat transfer measurements and impact on forming," *Glas. Technol.*, no. February, 2008.

[12] P. Moreau, D. Montoya, D. Lochegnies, and H. Vivier, "Friction analysis at the glass/tool interface and the lubrication influence during hot forming cycles," in *Proceedings of the Institution of Mechanical Engineers, Part J: Journal of Engineering Tribology*, 2013, vol. 277, no. 11, pp. 1253–1260.

[13] P. S. Lankeu-Ngankeu, "Improvements to Emhart Glass Vertiflow mold cooling applications in glass container production," *Conf. Glas. Probl.*, vol. 37, no. 1, pp. 185–191, 2016.

[14] A. Warude, "Analysis of glass mold to enhance rate of heat transfer," University of South Florida, 2004.

[15] M. R. Hyre, "Matching Mould Cooling Strategies to the Blank Side Forming Process," *Glass International*, no. June, pp. 76–79, 2007.

[16] T. Bewer, "Optimisation of the moulds cooling process," *Glass International*, no. September, pp. 57–59, 2007.

[17] S. Ferguson, "Stronger, lighter glass bottles; Bottero Spa is changing the way bottles are made and using simulation to do it," *Design Engineering*, 2017. [Online]. Available: https://www.design-engineering.com/stronger-lighter-glass-bottle-1004026595/.

[18] P. Grayhurst and P. J. Girling, "Packaging of Food in Glass Containers," in *Food and Beverage Packaging Technology*, 2011, pp. 137–156.

[19] C. G. Giannopapa and J. A. W. M. Groot, "Modeling the Blow-Blow Forming Process in Glass Container Manufacturing: A Comparison Between Computations and

Experiments," *J. Fluids Eng. - Trans. ASME*, vol. 133, no. 2, p. 021103, 2011.

[20] B. Martins, M. Machado, A. Reis, and J. M. A. César de Sá, "Coupled thermomechanical model for press and blow forming processes of glass containers," in *Congress on Numerical Methods in Engineering*, 2017.

[21] P. B. Ryzhakov, J. García, and E. Oñate, "Lagrangian finite element model for the 3D simulation of glass forming processes," *Comput. Struct.*, vol. 177, pp. 126–140, 2016.

[22] E. Feulvarch, N. Moulin, P. Saillard, T. Lornage, and J. M. Bergheau, "3D simulation of glass forming process," *J. Mater. Process. Technol.*, vol. 164–165, pp. 1197–1203, 2005.

[23] G. Kloosterman and V. Bouwman, "Automatic Remeshing and Rezoning for the Simulation of 3D Glass Bottle Forming with Abaqus/CAE, Abaqus/Standard and Abaqus/Explicit," *Int. J. Mater. Form.*, vol. 2, no. SUPPL. 1, pp. 105–108, 2009.

[24] D. Lochegnies, P. Moreau, and R. Guilbaut, "A reverse engineering approach to the design of the blank mould for the glass blow and blow process," *Glas. Technol.*, vol. 46, no. 2, pp. 116–120, 2005.

[25] J. A. W. M. Groot, C. G. Giannopapa, and R. M. M. Mattheij, "A Numerical Shape Optimisation Method for Blowing Glass Bottles," in *ASME Pressure Vessels and Piping Conference*, 2011, vol. 4, pp. 497–506.

[26] E. Oñate, S. R. Idelsohn, F. del Pin, and R. Aubry, "The Particle Finite Element Method. An Overview," *Int. J. Comput. Methods*, vol. 1, no. 2, pp. 267–307, 2004.

[27] P. B. Ryzhakov, "An axisymmetric PFEM formulation for bottle forming simulation," *Comput. Part. Mech.*, vol. 4, no. 1, pp. 3–12, 2017.

[28] "ANSYS Polyflow User's Guide," ANSYS, Inc., 2013, pp. 395–413.

[29] A. Biosca, S. Borrós, V. Pedret, and A.-A. García, "Glass Gob Modeling and Experimental Validation Using a Drop Test," in *MATEC Web Conf. (IC4M)*, 2018, vol. 167, pp. 1–6.

[30] D. M. Shetterly and N. T. Huff, "Mold Surface Temperatures During Glass Container Forming," *J. Non. Cryst. Solids*, vol. 38–39, pp. 867–872, 1980.

FUTURE WORK

The aim of this thesis was to implement a numerical model to describe the thermo-mechanical behavior of glass during the blow and blow forming process to numerically predict the glass thickness distribution of the manufactured containers. In several moments it seemed an impossible task, but at the end of this thesis, after many experimental measurements and numerical simulations, it can be stated that this ambitious goal was accomplished.

Not only that, but also the validation of the predicted glass thicknesses based on the blank mold cavities and machine operation parameters resulted in very strong results. Simulations with very different containers and process conditions showed a great robustness, demonstrating how material properties, boundary conditions and process parameters experimentally defined led to reproduce the manufacturing conditions in the numerical model. Therefore, in a near future the presented axisymmetric model will be implemented in Ramon Clemente. This simulation tool will be very helpful to support the design of the mold equipment to manufacture new glass perfume containers. At the same time, the simulation of more and different container geometries, blank mold designs and process conditions will be very valuable to keep testing the numerical model.

In addition, the validation of the three-dimensional model for the glass-forming simulations of non-axisymmetric containers is a solid foundation to continue working. Currently, the three-dimensional model is undergoing continuous improvement with the study of several simulation cases based on bottles with more complex shapes and different manufacturing conditions. Moreover, although not presented in this thesis, accurate glass thickness predictions of square and rectangular-base perfume containers were already obtained using the three-dimensional model. Thus, numerical simulations with even more challenging and interesting geometries will be carried out to push forward the capabilities of the numerical simulations in glassmaking.

However, further work is also needed to obtain more accurate experimental data about the glass conditions and thermal phenomena present inside the mold cavities. This research gained insight in the glass flow inside the mold cavities, but, definitely, a better definition of heat transfer at the glass-mold contact interface is one of the most notable challenges in container simulations today. In addition, by conducting new experimental measurements under manufacturing conditions, it will be possible to change the few generic bibliographic data used as input of the simulations to more specific production process data to improve the prediction of temperatures in the glass domain.

Finally, glassmaking is a very broad topic where prediction of thicknesses in the blow and blow container forming process is only a small portion. Therefore, during the development of this thesis, inevitably, some loose ends were left for further study. In any case, numerical simulations in conjunction with experimental measurements turned out to be a very powerful methodology to continue gaining more knowledge about glass. Thus, these other topics can be studied in the future following the same methodology.

CONCLUSIONS

In this thesis, a numerical model that describes the thermo-mechanical behavior of glass during the blow and blow forming process has been successfully implemented to predict the glass thickness distribution of the manufactured glass perfume containers.

First, a framework has been defined, where different topics were studied and reviewed, determining the necessary information to model the container forming process.

- A detailed description of the glass container manufacture has been presented. Defining the blow and blow container forming operations and previous processes like the glass melt delivery, gob forming, loading and delivery operations. This introduces the production process and industrial conditions that will be modeled.

- An analysis of the most relevant material properties in glassmaking has been performed. As expected, glass viscosity required special attention as it defines the thermo-mechanical behavior of glass. So viscosity of Ramon Clemente's soda-lime glass was externally characterized and modeled using the VFT (Vogel-Fulcher-Tamman) equation.

- The contribution of each heat transfer mode (conduction, convection and radiation) to the total heat flux in the container forming process has been presented and numerically approached as a single heat transfer phenomenon. Therefore, an effective thermal conductivity for the heat transfer within the glass and a contact conductance at the glass-mold interface has been defined.

- Several experimental methods to measure glass temperatures under industrial manufacturing conditions were reviewed. Due to its flexibility to perform non-contact measurements in different stages of the process (including glass gobs, parisons and manufactured containers), a FLIR A325sc infrared thermal camera has been presented as the best solution.

The conditions of the glass gobs under industrial manufacturing conditions have been defined as a result of the conducted experimental analyses at the gob forming, delivery and loading operations.

- Experimental results of thermal analyses in the gob forming process with the infrared thermal camera have been presented. Radiative heat losses and axial temperature distributions during the glass extrusion were correlated with previously published results.

- An increase in temperature during the glass extrusion through the orifice ring was experimentally defined. This phenomenon remained unnoticed in previous publications. A reasonable explanation is that higher extrusion flows result in a

reduced influence of the heat losses present at glass near the orifice ring.

- A sensitivity study has been presented measuring the dimensions of the delivery equipment and the delivery time, velocity and temperature of the loaded glass gobs. From these results, variations in the gob loading conditions were defined as a function of the individual section position where gobs were loaded.

Finally, several numerical and experimental studies to model and validate the thermo-mechanical behavior of glass in the container forming process have been successfully carried out. These numerical simulations were performed using ANSYS Polyflow.

- A numerical and experimental glass gob drop test was conducted. The deformation of the glass gob on a plate was recorded with the infrared thermal camera and compared with the results predicted by the numerical model. As a result, the non-isothermal model that couples temperature evolution and glass viscosity was verified.

- Non-isothermal simulations of the container forming process with several containers and mold designs were carried out. The numerical model was validated with the correlation of the numerical results and experimental infrared measurements of the glass temperature and thickness distributions obtained sectioning manufactured glass containers.

- Numerical results showed that the blow and blow container forming model successfully predicts the final thickness distribution of the manufactured containers as a function of the blank mold cavity and forming process conditions.

- Simulations of the blow and blow forming process were successfully conducted with a three-dimensional model. Demonstrating for the first time the feasibility to numerically predict the glass thickness distribution of perfume containers in 3D. This has strong implications for Ramon Clemente, as it paves the way to predict the thickness distributions of complex perfume containers using a numerical approach.

LIST OF PUBLICATIONS AND PRESENTATIONS

Journal Publications:

A. Biosca, S. Borrós, V. Pedret, M. R. Hyre, and A.-A. García Granada, "**Numerical and experimental study of blow and blow for perfume bottles to predict glass thickness and blank mold influence**" *International Journal of Applied Glass Science*. vol. 10, no. 4, pp. 1–15, 2019.

A. Biosca, S. Borrós, V. Pedret, and A.-A. García, "**Glass Gob Modeling and Experimental Validation Using a Drop Test**" in *MATEC Web Conf.* (IC4M), 2018, vol. 167, pp. 1–6.

Oral Contributions in Congresses or Seminars:

A. Biosca*; S. Borrós; V. Pedret; A. García, "**Numerical and Experimental Study of the Glass Blow and Blow Forming Process**" *25th International Congress on Glass (ICG 2019)*. June 2019. Boston, Massachusetts USA. Oral presentation.

A. Biosca*, S. Borrós, V. Pedret, and A.-A. García, "**Glass Gob Modeling and Experimental Validation Using a Drop Test**" *International Conference on Mechanical, Manufacturing, Modeling and Mechatronics (IC4M 2018).* February 2018. Barcelona, Spain. Oral presentation.

A. Biosca*, S. Borrós, V. Pedret, and A.-A. García, "**Polyflow Validation of Gob Drop Test**" *2017 ICG Annual Meeting*. October 2017. Istanbul, Turkey. Oral presentation.

A. Biosca*, "**Glass Characterization as a First Simulation Stage**" *Jornada sobre Simulació en Processos de Fabricació de Vidre*. May 2017. IQS, Barcelona, Spain. Oral presentation.

Competitive Research Projects:

"**VIDRESIM: Estudi Numèric-Experimental del Comportament del Vidre en el Procés de Bufat-Bufat**" (Project RD16-1-0015), Convocatòria NUCLIS 2016 from ACCIÓ, Generalitat de Catalunya.